EFFECT OF CRYOGENIC TREATMENT
ON LOW ALLOY STEELS

Thesis

Submitted in partial fulfilment of the requirements for the degree of

Doctor of Philosophy
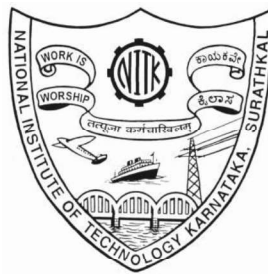
by

PAVANKUMAR R SONDAR

(MT16F05)

Under the Guidance of

Dr. SUBRAY R. HEGDE

Associate Professor

DEPARTMENT OF METALLURGICAL AND MATERIALS ENGINEERING

NATIONAL INSTITUTE OF TECHNOLOGY KARNATAKA

SURATHKAL, MANGALURU-575025

December -2022

DECLARATION

I hereby declare that the Research Thesis titled **"Effect of Cryogenic Treatment on Low Alloy Steels"** which is being submitted to the **National Institute of Technology Karnataka, Surathkal** in partial fulfillment of the requirements for the award of the **Degree of Doctor of Philosophy** in **Metallurgical and Materials Engineering,** is a bonafide report of the research work carried out by me. The material contained in this Research Thesis has not been submitted to any other Universities or Institutes for the award of any degree.

Register Number: **165064MT16F05**

Name of the Research Scholar: **Pavankumar R Sondar**

Signature of the Research Scholar:

Department of Metallurgical and Materials Engineering

Place: **NITK - Surathkal**

Date: 20/12/2022

CERTIFICATE

This is to certify that the Research Thesis titled **"Effect of Cryogenic Treatment on Low Alloy Steels"** submitted by **Mr. Pavankumar R Sondar (Register Number: 165064MT16F05)** as the record of the research work carried out by him, is accepted as the Research Thesis submission in partial fulfillment of the requirements for the award of the **Degree of Doctor of Philosophy.**

Research Guide

Dr. Subray R Hegde

Associate Professor

Department of Metallurgical & Materials Engineering
National Institute of Technology Karnataka, Surathkal
Post Srinivasnagar, Mangaluru - 575 025
Karnataka, India

Chairman-DRPC

Department of Metallurgical and

Materials Engineering

Date: 20/12/22

Chairman - DRPC
Dept. of Metallurgical and Materials Engineering
National Institute of Technology Karnataka, Surathkal
Post Srinivasnagar, Mangaluru - 575 025
Karnataka, India

ACKNOWLEDGEMENTS

ABSTRACT

Cryogenic Treatment, as an additional step to hardening and tempering heat-treatments, has proven to be beneficial in improving mechanical properties of various steel grades. To transform retained austenite into martensite in structural steels, cryogenic treatment is conventionally performed immediately after quench-hardening and prior to the tempering treatment. Contrary to this well-established conventional practice, some industrial heat-treaters often carryout the cryogenic treatment as the last step after the tempering treatment without comprehensively knowing the consequence of the same on the properties and performance of steel components. While published literature on the cryogenic treatment performed after the tempering of steels is sparse, a direct comparison of the effects of conventional and unconventional cryogenic treatments on common structural steels is almost nonexistent. This work presents a comparative analysis of deep cryogenic treatment performed on five commercial steel grades, EN8, EN18, EN47, EN24 and EN45, and highlights the effect of cryogenic exposure carried out before and after the tempering step separately. Through detailed experimentation, testing and characterization involving, several heat treatment cycles, tensile test, impact test, hardness test, wear test, fractography, metallography, and microstructural analysis, this work suggests that the cryogenic treatment carried out as an intermediate step between quenching and tempering yields much better mechanical properties than that carried out after tempering.

The results of the experimental work in this study shows that, the unconventional cryogenic treatment, that is carried out after the tempering step, has almost no influence on hardness and strength of EN8, EN18 and EN47 steels and very little influence on EN24 and EN45 steels. However, the conventional cryogenic treatment that is carried out prior to the tempering step shows significant improvements in the hardness (1-3 HRC), yield strength (4-17.4%) and tensile strength (3.9-16.8%) in the above steel grades in general. In particular, this work shows that the conventional cryogenic treatment is very effective in improving the overall mechanical properties of EN45 and EN24 grades including hardness (2-3 HRC), tensile strength (13.2- 16.8%), resilience (up to 24%), and wear resistance (36-42%). Thus, this thesis conclusively demonstrates and cautions commercial heat-treaters that the conventional cryogenic treatment that is applied as an intermediate step between hardening and tempering is much more effective than the unconventional industrial practice.

Key words: Quenching, Tempering, Cryogenic Treatment, Martensite, Tensile strength, Wear

CONTENTS

LIST OF FIGURES

LIST OF TABLES

LIST OF ABBREVIATIONS

CHT	-	Conventional Heat Treatment
SCT	-	Shallow Cryogenic Treatment
DCT	-	Deep Cryogenic Treatment
CT	-	Cryogenic Treatment
K	-	Kelvin
J	-	Joules
°C	-	Degree Celsius
MPa	-	Mega Pascal
h	-	hour
min	-	minute
HRC	-	Rockwell Hardness Number
HV	-	Vickers Hardness Number
SEM	-	Scanning Electron Microscope
TEM	-	Transmission Electron Microscope

1. INTRODUCTION

This chapter provides, a brief introduction, classification, and applications of cryogenic treatments. The chapter also highlights the problems associated with the industrial application of cryogenic treatment, and research gap that needs to be attended to address currently existing industrial problems and practices.

Arguably, steels are the most important and widely used structural materials in the industrial world. Primarily being alloys of iron and carbon, steels are blessed with a unique phase diagram. Both equilibrium and non-equilibrium phase-transformations of steels are well established through Fe-C, Time-Temperature-Transformation (TTT) and Continuous Cooling Transformation (CCT) diagrams. Thus, depending on the application requirements of the structural steel components, wide range of mechanical properties can be instilled and maneuvered rather accurately by applying suitable heat treatments, such as, spheroidizing, annealing, normalizing, hardening, tempering, etc. Apart from achieving the through-thickness or bulk properties of steel components by the standard heat-treatments, the surface properties can be enhanced by applying special treatments such as, carburizing, nitriding, nitrocarburizing, induction hardening, etc. Thus, an optimal combination of bulk and surface properties can be produced in steel components depending on the applications. However, the most commonly applied heat treatment for the property enhancement of steel components is the hardening treatment that is invariably followed by tempering.

It is now well established that the hardening treatment involves 'austenitizing' by holding the steel components above the A_{C1} temperature followed by fast-cooling in oil or water that is typically held at the room-temperature. This non-equilibrium cooling transforms stable 'austenitic phase' into metastable 'martensitic phase' in most part, and thus imparts high hardness, strength, and brittleness to the steel components. To reduce the brittleness and improve the toughness needed for the application, hardening step is always followed by the tempering treatment by reheating the as-quenched steel component typically above 300 °C for an hour or so. The components are finally cooled slowly to room temperature.

Considering that M_f (martensite finish) temperature of a typical structural steel is well below the room-temperature, a small fraction of the retained-austenite always remains embedded between martensitic colonies of as-quenched steel. Over the years, by incorporating Cryogenic Treatment (CT) as an additional step between hardening and tempering treatments, mechanical properties and performance of many structural and tool steels are enhanced significantly (Amini et al. 2012a; Cajner et al. 2012; Leskovšek and Podgornik 2013; El Mehtedi et al. 2012; Niaki and Vahdat 2015a). By introducing cryogenic treatment in between quenching and tempering steps, most of the retained austenite transforms into martensite. With the increased martensite fraction in the microstructure, provided tempering treatment is done optimally, an enhanced combination of mechanical properties including optimal hardness, good toughness and superior wear resistance can be achieved in most of the structural steels.

In general, cryogenic treatment can be classified into two types; Deep Cryogenic Treatment (DCT) where specimens are held in liquid nitrogen at -196 °C, and Shallow Cryogenic Treatment (SCT) where the holding temperature is in between -80 °C to -160 °C (Das et al. 2010a). Considering this classification, many researchers have carried out the comparative study on conventional heat treatment, shallow cryogenic heat treatment and deep cryogenic treatment and have observed that deep cryogenic treatment is most effective in enhancing the mechanical properties of steels (Das et al. 2009a, 2010b; c; Das and Ray 2012a; Senthilkumar et al. 2011). There have been many theories for the improved properties of cryotreated steels. However, most of researchers suggest that along with transformation of retained austenite to martensite, precipitation and subsequent homogenization of carbides during cryogenic treatment is responsible for increased hardness and strength of steels (Das et al. 2010b; Gill et al. 2012; Li et al. 2013c; Preciado et al. 2006; Sri Siva et al. 2012; Vahdat et al. 2013). A report suggests that low temperature exposure of as-quenched tool steels leads to deformation of virgin martensite which eventually improves the properties of tools. Similarly, many theories have been proposed on formation of carbides. One such theory states that formation of carbon-clusters takes place as a result of pinning of carbon atoms by moving dislocations. These carbon clusters

act as nucleation sites for η-carbides (Tyshchenko et al. 2010). Another study also observed η-carbide formation and claimed that this carbide precipitation is the major reason for the improved wear properties and service life of a tool steel (Stratton 2007). In contrast to the carbide precipitation theory, a separate study reported that hardness of tool steel increased after DCT. However, a TEM analysis associated with this work, could not find any secondary carbides in cryotreated tool steel (Gavriljuk et al. 2014).

Holding time plays a crucial role in improving the mechanical properties of steel grades. A study showed that extended holding at cryogenic temperatures caused increased transformation of retained austenite into martensite and that led to increased hardness and improved wear resistance of a tool steel (Akhbarizadeh et al. 2009). In another study it was reported that cryogenic treatment carried out after tempering treatment in D3 steel caused 19.6 % loss in tool life, suggesting, cryogenic treatment should not be performed after tempering. Authors claimed that stabilization of carbides and microstructural phases that occur as a result of tempering inhibits further transformation (Mohan Lal et al. 2001). Another study showed improvement in corrosion resistance of the tool subjected to cryogenic treatment along with improved hardness and wear resistance (Akhbarizadeh et al. 2012). Yet another study stated that DCT improves microstructure of high-speed steel by producing finer needle-like martensite that resulted in higher surface hardness and better tribological properties (Podgornik et al. 2012). Regarding austenitizing and tempering temperature, a report stated that combination of high austenitizing temperature and low tempering temperature helps in improving hardness and wear behavior. The report states further that a combination of low austenitizing temperature and high tempering temperature helps in increasing the bending strength and elongation at fracture (Oppenkowski et al. 2010).

Regarding the influence of cryogenic treatment, there are some contradictions. A study observed drop in impact toughness values with increased bulk hardness due to deep cryogenic treatment (Zhirafar et al. 2007). Another study stated that impact energy of cryotreated specimens improved over conventionally heat treated specimens (Dhokey and Hake 2013).

Even though significant literature is available in improving the properties of tool steels, effect of cryogenic treatment on low alloy steels is seldom reported. It is known that some industrial heat-treaters apply cryogenic treatment for low alloy steel components after tempering with the claim that such practice increases the hardness of the component by about 2 HRC that helps in improving the wear resistance. However, the effect of cryogenic treatment on tempered structural steel is not studied in depth. A direct comparison of the effect of cryogenic treatment performed before the tempering treatment with that performed after the tempering is almost nonexistent. Considering this, the present work intends to explore the influence of cryogenic treatment performed on as-quenched and as-tempered specimens separately for few key commercial low alloy steel grades. And thus, the work intends to provide a clear guideline to commercial heat-treaters about suitably applying the cryogenic treatment for realizing the full potential of the structural steels.

2. LITERATURE REVIEW

This chapter, provides an overview of heat-treatments of steels, discuses effects of alloying elements on hardening of steels, and reviews effects of cryogenic treatment on different types of steels. Further, the chapter introduces theories behind changes in the microstructural features due to cryogenic treatment, and discusses corresponding changes in the mechanical properties of various steel grades.

2.1 Heat Treatment of Steels

Structural steels can be subjected to various types of heat treatment for producing suitable microstructures and achieving required mechanical properties as demanded by different applications. Annealing, normalizing, hardening, and tempering are the most popular and well-established heat treatment processes that are generally applied to structural steel components for obtaining uniform bulk properties.

Annealing is generally carried out to reduce the hardness and increase the ductility of steels so as to produce the microstructure that is suitable for the required application or for the subsequent manufacturing process. The most common annealing heat treatment practice involves heating and isothermal-holding of steel components in a furnace at an austenitizing temperature followed by very slow cooling preferably achieved by switching-off the furnace. Thus, after annealing, the steel assumes its stable microstructure having equilibrium phases at room temperature as per the equilibrium phase diagram (Fig. 2.1). However, there are several industrial annealing practices including, spheroidization annealing, recrystallization annealing, stress-relief annealing, homogenizing annealing, etc. These annealing types are practiced by suitably controlling the exposure temperature, holding time and cooling rate.

Normalizing is generally carried out to refine coarse microstructures of plain-carbon and low-alloy steels. Normalizing is carried out by heating and holding steel components at an austenitizing temperature followed by air cooling. As a consequence of the faster cooling, normalizing brings about refinement of the microstructure. Thus, a normalized steel would

be harder, stronger and tougher than the annealed steel. Figure 2.2 shows the effect of normalizing in refining the microstructure of a medium-carbon steel.
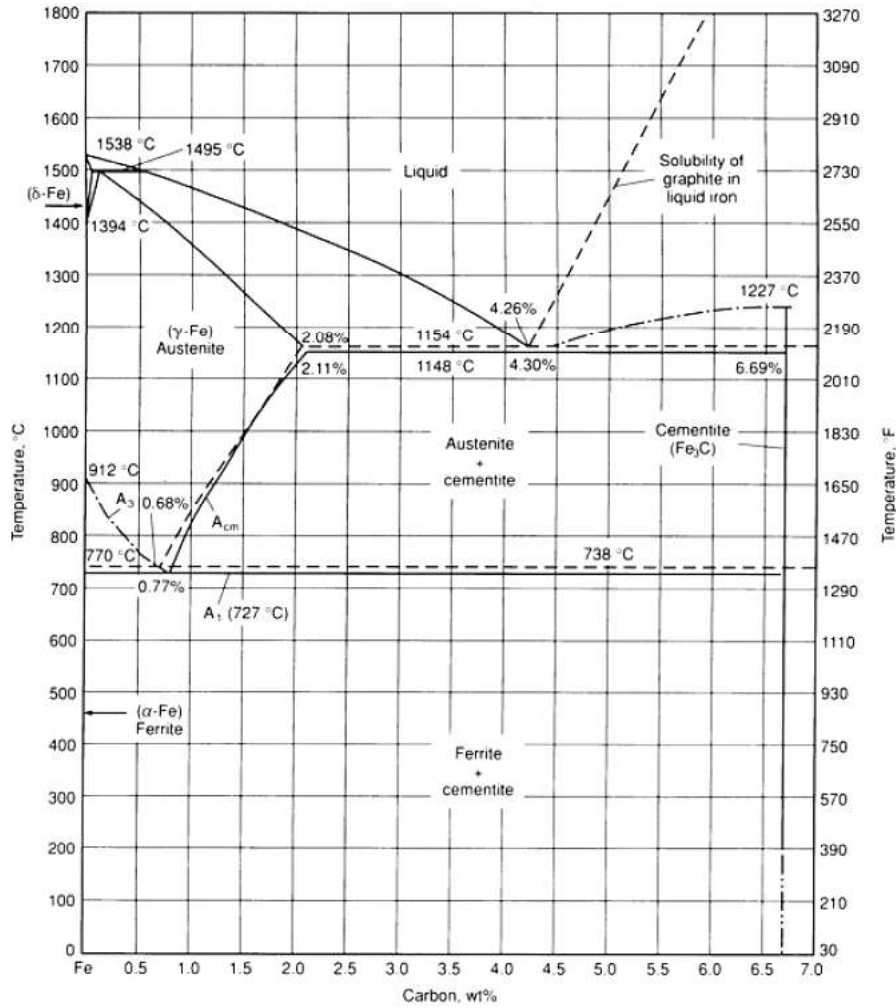
Fig. 2.1 Fe-C equilibrium phase diagram. Solid lines indicate Fe-Fe₃C diagram and dashed lines indicate iron-graphite diagram (Lyman 1973).

Hardening heat treatment involves heating and holding the steel components at an austenitizing temperature followed by rapid cooling in a suitable quenching medium such as, oil, water, salt-bath, etc. As-quenched microstructure of the steel is the pre-requisite for the subsequent tempering treatment. Thus, effective hardening is a crucial step in the heat treatment process of a structural steel. The effective hardening depends on various factors including hardenability of the steel, heating media, austenitizing temperature, holding time, cooling rate, quenching media, etc.

Tempering is the subsequent step applied invariably after quench-hardening to reduce the brittleness and impart good toughness to the steel components. Tempering is carried out by reheating and isothermally holding the as-quenched steels below the lower critical temperature followed by slow cooling. The tempering temperature is typically chosen between 300 °C and 650 °C to suit different applications. The higher the tempering temperature, the higher is the ductility, and the lower is the strength and hardness. Hence, choice of tempering temperature has to be optimal as per the hardness, strength, and toughness requirements of the application.

As dictated by the TTT diagram (Fig. 2.3), an austenitized steel must be cooled rapidly by quenching to enforce nonequilibrium phase-transformation of the soft austenite phase into the hard meta-stable martensite phase and avoid the equilibrium decomposition of austenite into ferrite and pearlite. In achieving this, composition of the steel plays a major role. Microstructures of steels obtained by hardening and tempering process are explained in the following sections.
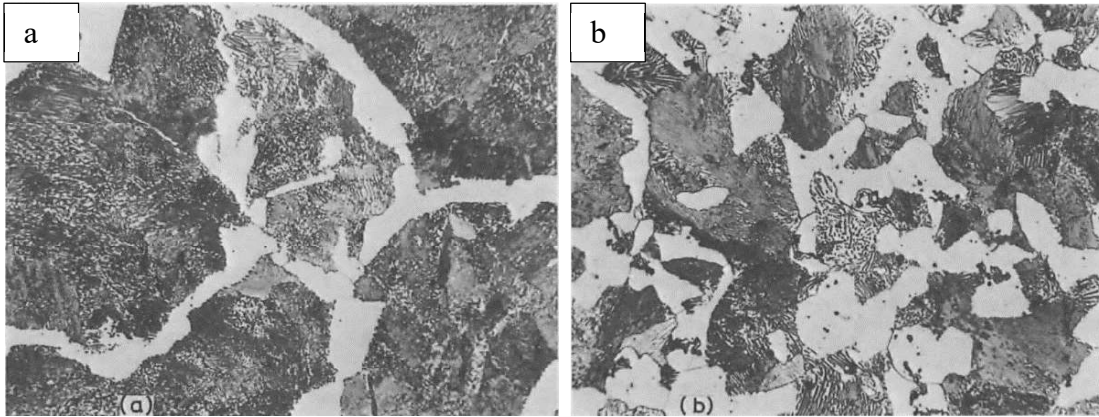
Fig. 2.2. Images showing the effects of annealing and normalizing heat treatments on 0.5% carbon steel; (a) coarse microstructure after annealing treatment, (b) fine microstructure after normalizing treatment (Thelning 1986).
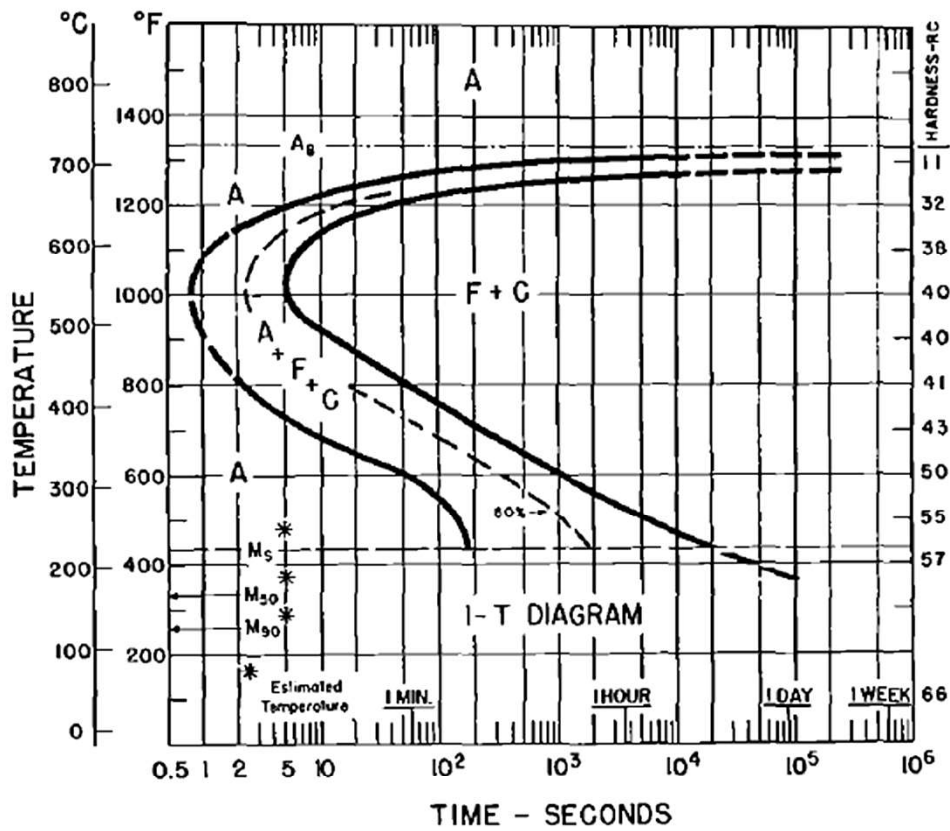
Fig. 2.3 T-T-T diagram of 1080 steel (Vander Voort 1991).

8

2.2 Martensite

When a medium carbon or alloy steel is quenched from austenitic temperature to room temperature, austenite transforms into a hard phase called martensite. Austenite to martensite transformation is a diffusionless phase-transformation that occurs by shear deformation of FCC lattice into carbon trapped BCT lattice due to rapid cooling. This transformation occurs athermally, and the fraction transformed depends on the undercooling below martensite start temperature (M_s). The extent of martensitic transformation below M_s is given by Koistens Marburgers equation,

$$1 - V_{\alpha'} = e^{[\beta\,(Ms\,-\,Tq)]} \quad \text{...............} \quad (1)$$

where, $V_{\alpha'}$ is the fraction of martensite, and T_q is the temperature below M_s to which the specimen is cooled and β is a constant whose value is about -0.011 (Bhadeshia and Honeycombe 2006). As-quenched martensite consists of colonies of fine laths or plates oriented randomly forming a unique textured microstructure as shown in Fig. 2.4a.

Cementite (Fe_3C) with orthorhombic crystal structure is the hardest phase in iron-carbon system. However, this is an intermetallic secondary phase that appears in the form of thin lamellar or fine spherical precipitates within the bulk primary phase, ferrite (α-Fe) that forms the matrix. Therefore, of various bulk phases that may be produced by the heat treatments of a given steel, the carbon supersaturated body centered tetragonal structure, martensite (α'-Fe) is the hardest, the strongest, and the most brittle phase. The FCC close-packed phase, austenite (γ-Fe) is significantly denser than martensite. Thus, during martensitic transformation upon quenching, there is a rapid volumetric expansion of the steel components. Due to consequent internal stresses, quench-cracks may be generated especially when a bulky steel component having high carbon content or carbon equivalent is subjected to hardening heat treatment.

2.3 Tempered Martensite

As-quenched martensite is so hard and brittle that it cannot be used for most applications. Therefore, ductility and toughness of as-quenched martensite is enhanced by tempering heat treatment such that the steel component can be used for intended purpose. As-quenched martensite being a metastable phase, given thermal activation, would decompose

into stable ferrite and cementite phases. The ferrite, being the soft BCC matrix phase, imparts required ductility and toughness, while the hard cementite phase dispersed within the matrix provides the required hardness and strength. Thus, tempering treatment imparts required toughness to the steel components. Tempering is accomplished by heating as-hardened steel below the critical temperature (A_1 line in the Fe-C phase diagram) for a specified time period followed by slow cooling (Thelning 1986). Normally, tempering is carried out isothermally at temperatures between 300 and 650 °C.

The microstructure of tempered martensite consists of fine and uniformly dispersed cementite particles within a continuous ferrite matrix. The hardness and strength may be explained by the large ferrite-cementite phase boundary area per unit volume that exists for the very fine and numerous cementite particles. Again, the hard cementite phase reinforces the ferrite matrix that act as barriers to dislocation motion during plastic deformation (Bhadeshia and Honeycombe 2006; Thelning 1986). Microstructure of tempered martensite resembles that of as-quenched martensite because of the reminiscence of the plate or lath colonies as shown in Fig. 2.4b. However, the sharp edges of the laths or plates are rounded-off due to the precipitation of fine cementite locally during tempering. Thus, the microstructure of tempered martensite appears hazy as compared to that of as-quenched martensite.
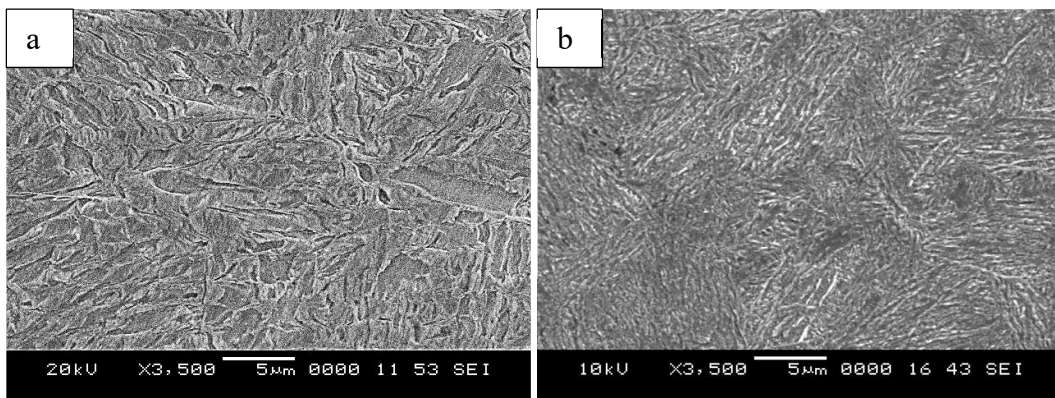
Fig. 2.4 Image showing the subtle difference in the microstructure of: (a) as-quenched martensite, and (b) tempered martensite.

2.4 Retained Austenite

From equation 1, it is clear that even when T_q is set to room temperature some amount of austenite do not transform into martensite. This untransformed austenite is termed as retained austenite. Amount of retained austenite increases as the carbon percentage of steel increases due to lowering of martensite start temperature (M_s). Presence of alloying elements also increases the percentage of retained austenite during quenching in oil or water at room temperature. This retained austenite is not a stable phase and may transform into martensite during the usage or machining of the steel component. This phenomenon may make the material brittle at that instant and ultimately leading to the failure of the component. This is where cryogenic treatment takes an edge over regular heat treatment as cryogenic exposure transforms most of the retained austenite into martensite and thus avoids embrittlement of steel structures during the application (Bhadeshia and Honeycombe 2006).

2.5 Effect of Alloying Addition to Steels

Alloying elements play a major role in defining the properties of steels. These alloys are mainly categorized into, austenite forming, ferrite forming, carbide forming, and nitride forming elements. C, Ni, and Mn are the main elements that fall under the category of austenite forming elements. Their effect is such that, sufficient amount of Ni and Mn can produce austenite phase even at room temperature. Ferrite forming elements include, Cr, Si, Mo, W and Al. Most of the ferrite forming elements also contribute in carbide forming. The affinity of these elements towards forming the carbides is as follow.

$$Zr > Ta > Nb > Ti > V > Mo > W > Cr$$
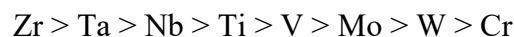
Various carbides are formed in the steel and some of them do not contain Iron. These are referred as carbide formers, e.g., Cr_7C_3, W_2C, VC, Mo_2C. There are some carbides which include both iron and carbide forming elements and are referred as double and complex carbides e.g., Fe_4W_2C. High speed and hot working steels, in general include carbides such as M_6C, $M_{23}C_6$ and MC, where M represents all the metal ions in the collective form (Thelning 1986). All the carbide formers also act as nitride formers.

Most of the alloying elements that form solid solutions in ferrite matrix help in improving the strength and hardness of the steels. As shown in Fig. 2.5, Si and Mn are the most effective elements in increasing the ferrite hardness as small addition of Si and Mn can increase the hardness to 200 – 240 HV, whereas Cr acts the least-effective element in increasing the ferrite hardness. Therefore, high Cr containing steels are generally cold-worked to increase the hardness (Thelning 1986).

Alloying elements such as Al, Ti, Nb, V inhibit the grain-growth and are added in micro constituents to form high-strength low-alloy (HSLA) steels. Austenite formers try to lower the A_1 line whereas ferrite formers help in increasing the A_1 line. All the alloying elements decrease the eutectoid point of the steels. Further, all the alloying elements except Co, lower the martensite start temperature (M_s).
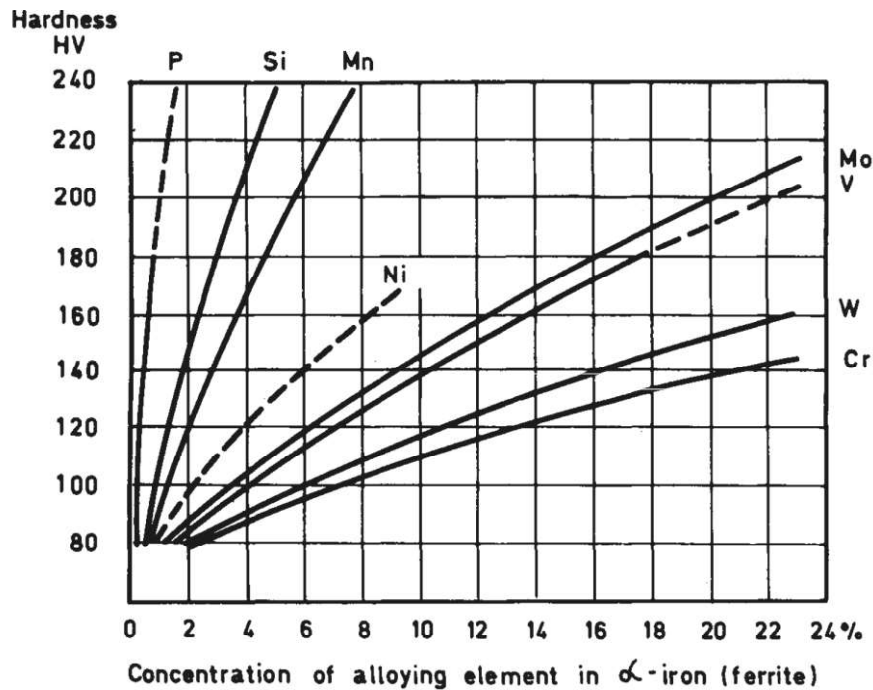
Fig. 2.5. Graph showing the effect of alloying elements on the ferrite hardness of steels (Bain and Paxton 1966).

Effect of alloying elements on M_s temperature is given by equation 2.

$$M_s \ (°C) = 539 - 423(\%C) - 30.4(\%Mn) - 17.7(\%Ni) - 12.1(\%Cr) - 7.5(\%Mo) \ \text{.......} \ (2)$$

Equation 2 clearly states that as the alloy composition increases, M_s temperature decreases accordingly (Bhadeshia and Honeycombe 2006). Nickel (Ni) is an essential alloying element in steels. Addition of nickel brings solid solution strengthening effect to steels. Addition of nickel increases hardness and hardenability along with toughness. Nickel being austenite stabilizer, does not form carbides while tempering. Chromium (Cr) is a ferrite stabilizer and addition of chromium to steel provides resistance from corrosion and high temperature oxidation. Unlike nickel, chromium forms carbide which helps in increasing wear resistance. Molybdenum (Mo) is also a ferrite-stabilizer which helps in solid solution strengthening. It increases the hardness and hardenability along with the high temperature properties including creep (Bramfitt and Benscoter 2002).

2.6 Literature on Cryogenic Treatment

2.6.1 Effect of Austenitization Temperature

Microstructure of austenite and martensite that forms after quenching is influenced by the austenitizing time and temperature. Hence, austenitizing temperature plays a major role and has to be chosen depending on the microstructural and mechanical properties required for the particular application.

A study on the effect of austenitizing temperature on PMS390MC HSS tool steel stated that at higher austenitizing temperature the volume fraction and mean diameter of carbide particles tend to reduce during tempering. This creates increased mean distance between the carbides and affects tribological properties. Further, if the austenitizing temperature is too high, positive effects of DCT cannot be achieved (Leskovšek and Podgornik 2013). Another study on high chromium steel stated that high temperature austenitizing results in complete dissolution of the carbides/carbonitrides with negligible retained austenite. Further, DCT transforms the retained austenite into martensite and affects the precipitation sequence there by increasing the hardness (El Mehtedi et al. 2012). Another researcher

carrying out sub-zero treatment on Vanadis 6 steel, stated that high temperature austenitizing temperature leads to reduced retained austenite content and further subzero treatment imparts more refined martensite as compared to conventional treatment. It also induces higher dislocation density which eventually leads to carbon rich and carbon depleted regions (Jurči et al. 2015).

Regarding austenitizing and tempering temperature, it is summarized that combination of high austenitizing temperature and low tempering temperature helps in improving hardness and wear behavior whereas combination of low austenitizing temperature and high tempering temperature helps in achieving the bending strength and elongation at fracture (Oppenkowski et al. 2010).

2.6.2   Effect of Tempering

Tempering plays a major role in removing the brittleness and relieving the internal stresses of the as-quenched martensite. During the process of tempering, carbides precipitate from the martensite. Tempering enhances the toughness at the loss of hardness and strength.

During the tempering process, the less stable austenite converts into martensite which enhances the mechanical stability and on the other hand stable austenite which does not convert into martensite provides some ductility to the materials such as tool steels (Kokosza and Pacyna 2005). However, addition of alloying elements increases the stability of the retained austenite. It is reported that in some cases, retained austenite cannot be completely decomposed even at high tempering temperatures (Zhu et al. 2008). Cryogenic treatment not only speeds up the decomposition of austenite but also decreases the temperature range required for the secondary hardening for the tool steels (Mebraki et al. 2002). Even though most of the researchers have incorporated cryogenic treatment as an intermediate step between quenching and tempering, there are some reports where researchers have carried out cryogenic treatment after tempering.

2.6.3 Soaking Temperature and Time

Table 2.1 provides cryogenic temperature and soaking time of the cryogenic treatment carried out for various steel grades. Liquid nitrogen is commonly used as the cryogenic medium for the Deep Cryogenic Treatment at -196 °C as the soaking temperature. Many authors have carried out cryogenic treatment with soaking period varying from 4 h to 60 h for various steel grades. However, most of the steel grades are subjected to cryogenic exposure for 24 h as the preferred soaking time.

Table 2.1. Temperature and soaking period for cryogenic treatment.

Material	Temperature (°C)	Holding time (h)	Reference
AISI 4140	-196	24	(Senthilkumar et al. 2011)
815M7 (carburized steel)	-196	24	(Bensely et al. 2007)
TiCN, TiN	-176	24	(SreeramaReddy et al. 2009)
H13A	-180	24	(Thornton et al. 2014)
M2 HSS	-196	24	(Firouzdor et al. 2008a)
W18Cr4V, W6Mo5Cr4V2	-196	24, 48	(Yun et al. 2008)
AISI D2	-196	36	(Das and Ray 2015)
AISI 52100	-145	12, 24, 36, 48, 60	(Gunes et al. 2014)
AISI H13	-145	24	(Çiçek et al. 2015)
EN31	-183	24	(Vimal et al. 2008)

High-vanadium Steel	-196	12, 24, 48	(Li et al. 2016)
HY-TUF Steel	-196	48	(Zare et al. 2015)
SAE 8620	-185	4, 8, 12, 16, 20	(Ghosh and Dhokey 2017)
AISI H13	-196	12	(Pérez and Belzunce 2015)
AISI D2	-196	4	(Ghasemi-Nanesa and Jahazi 2014)
1.2080 tool steel	-196	36	(Amini et al. 2013)
AISI S1 steel	-196	24, 36, 48	(Niaki and Vahdat 2015b)
AISI T42	-185	4, 8, 12, 16, 20, 24, 28, 32	(Dhokey and Hake 2013)
DIN 1.2380	-150, -196	24, 36, 48	(Tyshchenko et al. 2010)
AISI A2, D6, M2	-180	24	(Thornton et al. 2013)
X153CrMoV12 tool steel	-150	24	(Gavriljuk et al. 2014)
45WCrV7	-196	24, 36, 48	(Vahdat et al. 2013)
D3, M2	-180	24	(Mohan Lal et al. 2001)
AISI M2	-110, -196	18, 38	(Gill et al. 2012)
AISI D2	-196	48	(Amini et al. 2012a)
1.2080 tool steel	-196	24, 48	(Akhbarizadeh et al. 2012)

S390MC steel	-196	25, 40	(Leskovšek and Podgornik 2012a)
AISI M2	-196	24	(Firouzdor et al. 2008b)
18NiCrMo5	-185	24	(Baldissera 2009)
815M17	-196	24	(Bensely et al. 2007)
Low carbon tool steel High carbon tool steel High speed steel	-196	25	(Podgornik et al. 2016)
AISI D2	-196	1, 5, 24	(Oppenkowski et al. 2010)
AISI H13	-196	24	(Xu et al. 2010)
CR7V Tool Steel	-196	3, 6, 12	(Liu et al. 2018)
DIN 1.2344	-196	24	(Mokarian et al. 2019)
M35	-185	4, 8, 12, 16, 20, 24, 28, 32	(Dhokey and Lalge 2018)

2.6.4 Comparison of Deep cryogenic treatment with conventional and sub-zero heat treatment

In general, cryogenic treatment can be classified into two types, one being Deep Cryogenic Treatment (DCT) where specimens are held in liquid nitrogen at -196 °C and another one is Shallow Cryogenic Treatment (SCT) where the holding temperature is in between -80 °C to -160 °C (Das et al. 2010a). There have been many studies in the past that have compared deep cryogenic treatment with conventional and subzero treatments. Following

are the reports, focusing on the comparison of different heat treatments with respect to deep cryogenic treatment.

A recent work on AISI 4140 steel reported that the material following CHT, SCT, and DCT attained hardness values of about 55, 57, and 60 HRC respectively. This demonstrates that DCT is more effective than SCT in increasing the hardness of as-quenched steels (Senthilkumar et al. 2011). In another comparison study of AISI D2 steel, involving conventional heat treatment, cold treatment, shallow cryogenic treatment and deep cryogenic treatment, deep cryogenic treatment significantly increased the hardness values as compared to the other treatments. It was observed that the retained austenite content was found to be 9.8 % and 4.8 % in conventionally treated and cold treated samples respectively whereas the retained austenite content was below the detection limit for both shallow cryogenic treated and deep cryogenic treated samples. The authors claimed that incorporation of shallow or deep cryogenic treatment reduces the amount of retained austenite either significantly or completely which is reflected in improving the hardness. Volume of large size and small size secondary carbides was increased to 47% and 39% respectively in DCT as compared to the cold treatment. This was claimed as the main reason for the improvement of hardness in AISI D2 steel (Das et al. 2010b). Similar results were found in another study involving AISI D2 steel. They claimed that reduction in retained austenite and increase in secondary carbides in deep cryogenic treatment as the main cause for increase in mechanical properties (Das and Ray 2012a). Another study carried out on D6 tool steel showed that effect DCT is better than SCT in improving wear resistance and hardness. The work also highlighted that by increasing the soaking time in DCT, more retained austenite was transformed into martensite, there by further increasing the hardness and wear resistance (Akhbarizadeh et al. 2009).

A study involving comparison of cold treatment and DCT of AISI D2 steel stated that, along with more retained austenite transformation, DCT also increases secondary carbides which further enhances the tribological properties (Das et al. 2009a). Comparing the wear behavior of AISI D2 tool steel with various sub-zero heat treatments, it was found that cold treatment produces highest wear rate whereas wear rate is lowest for DCT. The authors

claim that reduction in retained austenite and increase in amount of hard secondary carbides are the main reasons for the substantial improvement of tribological behavior in DCT (Das et al. 2010c).

A study involving DCT and SCT on AISI M2 high speed steel stated that deep cryogenic treatment promotes uniform distribution of carbides by accelerating the precipitation of small secondary carbides and thereby increasing their volume fraction which improves mechanical properties of the deep cryogenic treated specimens significantly as compared to SCT and CHT (Gill et al. 2012). However, in contrast, a study indicated a reduction in tensile strength for SCT and DCT samples over conventional heat treatment by 1.5 % and 9.34 %, respectively (Bensely et al. 2007).

2.6.5 Carbide Precipitation Study

There have been many reports that have highlighted secondary carbide formation and uniform distribution of carbides as the main reason behind the improvement of mechanical properties. Following are some of the key reports that have highlighted the carbide formation during the deep cryogenic treatment.

A study of DCT on D2 steel stated that, apart from elimination the retained austenite, increase in carbide content and homogeneous carbide distribution also takes place in DCT thereby increasing the hardness and wear resistance of the material (Amini et al. 2012a). Similar observation was observed in 1.2080 tool steel. Improvement in hardness and wear resistance because of secondary carbide formation is proved by applying magnetic field during deep cryogenic treatment. The magnetized samples showed lesser wear resistance as compared to the deep cryogenic treated samples as carbide precipitation was hindered by magnetization (Akhbarizadeh et al. 2012).

In a study where holding duration of DCT was conducted on 1.2080 tool steel, researchers found out that carbide percentage increased up to 36 hours and there after started decreasing. The carbide percentage increased by 5 % (from 18 % to 23 %) after 24 hours and reached to 26 % at 36 h and then dropped to 24% beyond 36 hours soaking period. It was also observed that carbide percentage did not change after 48 hours and remained the

same in the period of 48 to 120 hours. The authors claimed that deep cryogenic treatment influences homogeneous carbide distribution along with uniform particle size and newly formed nano carbides. Wear resistance and hardness dropped beyond 36 hours owing to the fact that bigger carbides formed beyond 36 hours and affected the formation of fine precipitation of carbides (Amini et al. 2012b).

A study on high speed steel with prolonged holding in DCT observed improvement in microstructure by producing needle like martensitic structure. Improved microstructure was corelated with higher surface hardness, increased abrasive and galling resistance. However, the improvement in tribological properties observed was minimal (Leskovšek and Podgornik 2012b). Another study stated that, decreased thermodynamical potential for dissolution as the main reason for formation of precipitation of fine carbides which along with transformation of retained austenite to martensite leads to increase in hardness and wear resistance (Firouzdor et al. 2008b).

One of the studies involving Vanadis 6 steel stated that, increase in the small globular carbide density is directly proportional to the soaking time of sub-zero treatment. Further, sub-zero treatment accelerates decomposition of retained austenite with the increase in soaking period. It was also observed that tempering process decreases the population density of small globular carbides, with the increase in the tempering temperature (Jurči et al. 2017). One of the authors stated that segregation of carbon atoms near dislocations during DCT and their precipitation from the matrix during tempering leads to improvement in the mechanical properties. The authors claimed that carbon atoms near the dislocations either act as or grow into nuclei to form carbides which helps in enhancing the wear resistance (Li et al. 2011).

2.6.6 Wear study

A study was conducted using taguchi method for the optimization of deep cryogenic treatment process on 100Cr6 bearing steel considering the parameters such as cooling rate, soaking temperature, soaking time, and tempering temperature, in order to enhance hardness and wear resistance. It was concluded that soaking period was the most crucial

factor in improving the wear resistance of that particular steel. Soaking period of 36 h, at -185 °C and tempering temperature of 200 °C were considered as the optimum parameters which improved the wear resistance by 49 % and hardness by 19 %. Further, the microstructural study carried out claimed that conversion of retained austenite to martensite and fine carbides precipitation as the main reasons for enhanced the hardness and wear resistance (Sri Siva et al. 2012). A similar study of DCT carried out on high-speed steel showed improvement in the microstructure by producing finer needle-like martensitic structure and thereby improving the hardness and wear behavior (Podgornik et al. 2012).

One of the researchers stated that improvement in wear resistance is due to favorable distribution of carbides rather than reduced retained austenite (Meng et al. 1994). Another study on improving the wear resistance of D2 steel attributed to elimination of retained austenite, refinement of carbide particles, and their homogeneous distribution for the attainment of better wear resistance after deep cryogenic treatment (Das et al. 2007).

A study involving AISI D2 steel, correlated wear resistance with microstructures and stated that improvement in wear resistance is caused by elimination of soft retained austenite and increase in hard secondary carbides along with uniform tempered martensite (Das et al. 2009b). Same author in another article mentioned that microstructural changes modified during DCT, increased the resistance of tool steels to plastic deformation and thermal softening during wear test and thereby improving the wear behavior of D2 steel (Das and Ray 2012b).

2.6.7 Deep cryogenic treatment carried out before and after tempering

In a study that compared DCT applied before and after tempering of EN31 steel revealed that DCT applied immediately after quenching and before tempering offers much better wear resistance than DCT applied after tempering (Vimal et al. 2008). In another study of T1, M2 and D2 steels where cryogenic treatment was compared with coatings, it was found out that cryogenic treatment of tool steels showed better tool life than the tool steels with coating. Further, combination of cryogenic treatment and coatings resulted in better wear resistance and tool life. The work also showed that cryogenic treatment carried out at -140 °C after tempering showed negative results in terms tool life. However, the results were

favourable when cryogenic treatment was carried out at -180 °C. During the tempering process, stabilization of the carbides and the microstructural phases takes place and this inhibits further transformation during cryogenic treatment. Hence, higher degree of undercooling is required to transform the tough or stabilized microstructural phases (Mohan Lal et al. 2001). In one of the studies, it was shown that hardness and wear resistance were increased by incorporating DCT in between quenching and tempering. However cryogenic treatment carried out after tempering had negligible effects in increasing both hardness and wear resistance (Molinari et al. 2001).

In one of the DCT studies involving case carburized steels, it was reported that segregation of carbides and transformation of retained austenite to strain induced martensite leads to increased hardness when DCT was carried out after tempering (Preciado et al. 2006). Performing DCT after tempering showed no side effects and instead improved the fatigue behavior by increasing the fatigue limit up to 25 % (Baldissera 2009). In numerous recent studies involving DCT, it has been clearly demonstrated that key mechanical properties such as, hardness, tensile strength, toughness, and bending strength of structural steels can be significantly improved by suitably adding a DCT step in the heat treatment cycle (Cajner et al. 2012; Çiçek et al. 2015; Ghasemi-Nanesa and Jahazi 2014; Khun et al. 2015; Niaki and Vahdat 2015a; Zare and Hosseini 2016; Zhang et al. 2014).

Apart from the study of DCT after quenching and before tempering, researchers have also studied the effects of DCT on annealing also. DCT carried out after annealing improved hardness and wear resistance and it was attributed to reduction in interlamellar spacing of uniform pearlitic microstructure (Thornton et al. 2013).

2.6.8 Deep cryogenic treatment on various steel grades

Most of the literature that is available for DCT is mainly focused on improving the mechanical properties of tool steels. There are very few reports that have attempted to study the behavior of low/medium carbon steels upon implanting cryogenic treatment. Following are some of the reports that have focused on cryogenic treatment on various steel grades.

A study showed that both hardness and wear resistance of M2 tool steel increased by DCT due to the conversion of retained austenite into martensite (Mahmudi et al. 2008). Another study on DCT of tool steels revealed increased impact-toughness by 58 % and 43 % for T1 and M2 steels respectively (Yun et al. 2008). In one of the studies of AISI D2 tool steel, volumetric fraction of nano sized carbides was larger and more homogeneous after DCT and it was attributed to higher volumetric fraction of martensite (Farina et al. 2013). Similar study on deep cryogenic treatment of a high vanadium steel revealed that amount of carbides formed increased and that the carbides were even more homogeneously distributed due to deep cryogenic treatment followed by optimal tempering (Li et al. 2016). It was even suggested that fine η-carbide precipitation takes place during DCT of S156 steel which subsequently improves both toughness and wear resistance of the material (Oila et al. 2014). Using internal friction measurements, one of the researchers suggested that shrinkage in strain energy during DCT leads to segregation of interstitial carbon atoms to nearby dislocations and formation of η carbides will take place as a result of tempering in cold worked die steel (Li et al. 2013c). From the perspective of phase transformation and associated microstructural changes, it is understandable that increased martensite fraction during DCT and consequent improvement in the distribution of cementite during tempering is the key reason for the overall improvement in the bulk mechanical properties of steels as quantitatively demonstrated by recently reported studies (Ghosh and Dhokey 2017; Gunes et al. 2014; Wierszyllowski et al. 2008).

One of the studies relating to DCT of tool steel confirmed the transformation of retained austenite to martensite through internal friction method as the quenched sample was cooled down to -160 °C and heated back to room temperature (Li et al. 2013b). Another study involving T-42 steel showed maximum carbide density for a cryosoaking period of 8 h as a result of the low residual compressive stress. The stress then increased the surface energy of carbides which led to the nucleation and of growth of new carbides in order to reduce the surface energy. Hardness values vary linearly in accordance with carbide density of the matrix, producing uniform microstructure. In this work, impact energy of DCT specimens was improved as compared to the conventionally treated specimens (Dhokey and Hake

2013). Another theory suggested transformation of martensite at low temperature leads to deformation of virgin martensite which eventually improves the properties of tool steels. Formation of carbon clusters takes place as a result of capture of carbon atoms by moving dislocations. These carbon clusters act as nucleation sites for η-carbides (Tyshchenko et al. 2010). Similarly, another study stated η-carbides formation as the major reason for improving the wear properties of tool steels and thereby improving the tool life (Stratton 2007). In contrary to carbide precipitation theories, one of the studies stated that hardness of tool steel increased after DCT but there were no secondary carbides observed in TEM study (Gavriljuk et al. 2014).

A study showed that precipitation of fine carbides during DCT helped in achieving the enhanced strength and exhibiting the same even at elevated temperatures for EN52 and 21-4N valve steels. For EN52, the tensile tests were conducted at room temperature and at an elevated temperature of 400 °C while 21-4N was subjected to 650 °C and were compared with room temperature tensile tests. DCT samples of both the materials showed 11 % improvement in tensile strength compared to CHT samples at the room temperature. When tests were conducted at elevated temperatures, DCT samples of EN52 showed improvement of 7.87 % over CHT samples while DCT samples of 21-4N steel showed the improvement of 7.1 % over CHT samples. It was stated that fine secondary carbides that precipitate during the DCT exhibit better strength at elevated temperature (Jaswin and Lal 2011).

Though it is believed that complete transformation of unstable retained austenite to martensite takes place after DCT, researchers have shown that even after DCT, there will be a small amount of retained austenite that remains untransformed in die steel (Li et al. 2013a). High population density and higher volume fraction of secondary carbides are two effective parameters in improving the toughness of tool steels. By simultaneously increasing the soaking time in DCT and tempering temperature, toughness of the tool steels can be enhanced (Vahdat et al. 2013). Also, quench severity is the another important factor that influences conversion of retained austenite to martensite (Amini et al. 2013).

One of the studies stated that formation of dislocation networks occurs because of interaction of dislocations at cryogenic temperature. Further, upon implementing aging treatment, density of dislocations increases and leads to twin formation in the microstructure of Ti–6Al–4V alloy (Gu et al. 2013). Another study on cold-worked tool steel revealed that DCT improved fracture toughness without compromising on hardness through finer needle like martensitic microstructure in addition to plastic deformation of primary martensite (Podgornik et al. 2016). One of the researchers provided a theory for tool steels that plastic deformation at low temperature leads to martensitic transformation. A separate study revealed that maximum transformation of retained austenite takes place around -150 °C due to the optimal driving force of the transformation and the thermal activation. The work states that, during isothermal cryogenic holding, as-quenched martensite deforms and the new or virgin martensite appears from the retained austenite and thus increasing the martensite fraction (Gavriljuk et al. 2013).

One of the researchers observed maximum hardness and compressive strength for alloyed Bainitic Ductile Iron after carrying out DCT for 6 h. The attributed factors were plate like martensite and carbide precipitation. However, mechanical properties dropped after tempering process due to Ostwald ripening of precipitated carbides (Cui and Chen 2017). A study on AISI H13 hot work steel stated that shrinkage of martensite unit cell takes place during tempering and the carbon atoms trapped in the supersaturated martensite diffuse out and precipitate to form carbides during tempering. The shrinkage will be more for DCT indicating more carbide precipitation. Shrinkage is defined by low tetragonality martensite in the DCT samples and this low tetragonality is the main reason for martensite to become more homogeneous after tempering thereby increasing wear resistance and durability of the tool steel (Xu et al. 2010). Another study stated that DCT followed by tempering induces higher thermal stresses and structural defects and thereby producing dispersed network of fine carbides which improves fracture toughness of the AISI H13 tool steel (Pérez and Belzunce 2015).

From the above literature review, it can be summarized that the cryogenic treatment applied prior to the tempering treatment ensures superior mechanical and microstructural

properties for steel components. However, some commercial heat-treaters apply cryogenic treatment after tempering step for certain steel components claiming that this practice increases the hardness by 2 HRC and thus greatly helps in improving the wear-resistance of the components. This unusual industrial practice is not well studied with keen scientific intent and that the implication of this practice on the properties, service life, and performance of the steel components is not well understood. There are no clear guidelines formulated for commercial heat-treaters regarding the influence of cryogenic treatment applied after the tempering step. Therefore, present work intends to explore the influence of cryogenic treatment performed on as-quenched and as-tempered steels that are commonly used as structural materials.

3. CASE-STUDY AND MOTIVATION

This chapter presents a case-study that investigates the failure of a hydraulic lathe chuck assembly whose parts were subjected to sub-zero treatment after tempering. Using standard failure analysis and FEA based numerical stress analysis the investigation reveals the mechanism and the root-cause of the failure. Through heat-treatment experiments the chapter highlights the effects of regular and unusual cryogenic treatments and presents the motivation behind this thesis.

3.1 Introduction

Successful precision machining dictates the ability to manufacture reliable products, complying to design intent with close dimensional tolerances which has put an impetus to rely on high–speed Computerized Numerical Control (CNC) machines. However, to address the surging demand for the fast production rate, high-speed spindle rotation is preferred that poses a significant threat for the operator during the unforeseeable events, such as, loss of gripping force, compromised clamping systems, tribological issues, etc. Modern numerical control lathes are now equipped with power-operated holding devices such as, pneumatic, hydraulic, and electromagnetic chucks which help in reducing the clamping time. Generally, jaw-chucks are the most preferred clamping systems, especially in turning operations. However, the clamping force may induce deformation, lateral bend and displacement at clamping position (Feng et al. 2008). Machining industry often encounters the failure of jaw-carriers and plungers of CNC chucks during operation. Most of the failures are attributed to centrifugal force acting on jaws which are prone to slip (Zhou et al. 2011). With a minimum actuating force, the chuck achieves a very high clamping pressure ensuring firm gripping of the specimens (Kosmowski 1985). In one of the reports, finite element analysis of three-jaw chuck reported that larger holding diameter and higher rotational speed led to higher gripping losses (Karthik et al. 2020). A similar study reported that centrifugal force which acts in the opposite direction of the gripping force, decreases the gripping force with an increase in the rotational speed. Furthermore,

the study reported that the chuck materials having higher densities impose reduced gripping force during the operation (Basavaraja and Mujawar 2014).

In general, all the sliding surfaces are hardened for precision operation, reduced wear and tear, and extended service life. Carburizing is the most common method of increasing the surface hardness of the chuck parts. Case-carburizing produces a carbon-rich surface and sub-surface in steel components. After quenching followed by tempering, the carburized components are strengthened with high hardness at the surface and high toughness at the core. This is the perfect combination for a long run (Cameron et al. 1983). Though carburizing improves surface hardness by increasing the carbon percentage, formation of retained austenite during quenching will affect the material during the operation. Commercial heat-treaters apply many techniques and methods in controlling the retained austenite including: sub-zero treatment, cryogenic treatment, hardening with reheating, and quenching from different temperatures (Zinchenko et al. 1987). A study showed improved fatigue properties by reducing the retained austenite when the cryogenic treatment was carried out on carburized steels followed by tempering (Bensely et al. 2008). Another study showed improvement in fatigue resistance by reheating (to 850 °C) and quenching the previously carburized samples (Pacheco and Krauss 1989). Even though, proper care and strict guidelines are followed in processing, many carburized materials fail because of poor mechanical design and other external parameters. One such study observed that overloading during the operation caused contact-fatigue that led to the failure of a case-carburized gear (Boniardi et al. 2006). A similar study claimed that contact fatigue is a common phenomenon that leads to reduced load-bearing capacity of carburized gear materials eventually leading to fracture of gear teeth (Widmark and Melander 1999).

In a separate study where square edged carburized specimens and round edged carburized specimens were subjected to the bending test, it was reported that square edged specimens had lower fatigue limit than the round edged specimens. The lower fatigue limit in the square-edged samples was attributed to the presence of high-volume fraction of retained austenite in the sample corners and a lower surface residual compressive stress (Cohen et al. 1992). In another study involving failure of carburized helical gear, it was observed that

several teeth were cracked as a result of coarse grinding. Cracks propagated from the flank towards the gear end. The flanks at the acute angle side were unable to fully support the grinding stress leading to cracking of the flanks. The thick carburized case and weak inter-crystalline bonding of the carburized layer attributed to the initiation and propagation of crack. In addition, unsuitable grinding operations aggravated the cracking of the flanks. It was recommended to chamfer the edges of the flanks that intersect with the gear end, to support the grinding stress and to prevent cracking of the flanks (Xu and Yu 2012). Yet another study reported failure of carburized splined shafts used in a diesel engine that fractured after 7–8 hours of service. Fracture occurred at the root fillet between the tooth and cylinder portion. Intergranular fracture was observed as a result of intergranular internal oxidation. However, the authors claimed that high stress concentration at the fracture location resulting from over-short axial free length between the tooth and cylinder portion along with intergranular internal oxidation caused premature failure of spindled shaft (Yu et al. 2012). An experimental investigation in which specimens were carburized in hydrogen atmosphere revealed that the components usually do not display brittle fracture by hydrogen embrittlement. However, they do so when high tensile stresses combined with a high stress concentration and a martensitic microstructure are present (Straffelini and Versari 2009). Another study reported failure of a carburized secondary driving helical gear used in an electric vehicle due to improper heat treatment and high stress concentration. The fracture surface revealed that the crack originated from the tooth-root and displayed intergranular fracture. The study concludes that a combination of improper heat treatment and presence of high stress concentration led to the failure of the helical gear (Feng et al. 2020).

Present work investigates the failure of a jaw-carrier and plunger assembly of a CNC hydraulic lathe chuck. The chuck assembly failed after five weeks of installation as reported by the lathe operator. The plunger consists of three T-slots to house three jaw-carriers. The T-slots have varying profile matching the wedge-shaped projections in the jaw-carriers. This wedge design of the assembly has a self-locking feature that restricts any loss in the gripping-power of the chuck and is suitable for CNC machines (Fig. 3.1). The

jaw-carriers hold the jaws that are secured via T-nut. This arrangement ensures proper gripping of the job during machining. All these components have holes/slots for the hydraulic circuitry and are activated by rear mounted hydraulic cylinders (Fig. 3.2). The chuck assembly under the hydraulic pressure articulates by sliding of the jaw-carriers within the chuck body. The gripping or the loosening of the job is achieved by synchronized radial motion or simultaneous convergence or divergence of the jaws that are fastened to the jaw-carriers. Though the assembly is well lubricated during the operation, there is always wear and tear issue during the service due to the sliding action of the mating parts. The surface roughness and dimensional tolerance in these precision hydraulic components are typically maintained within a few micrometres. Excessive wear may cause slack in the chuck-assembly leading to: jerky operation, vibration, noise, oil spillage, reduced plunging force, loss of gripping, etc.
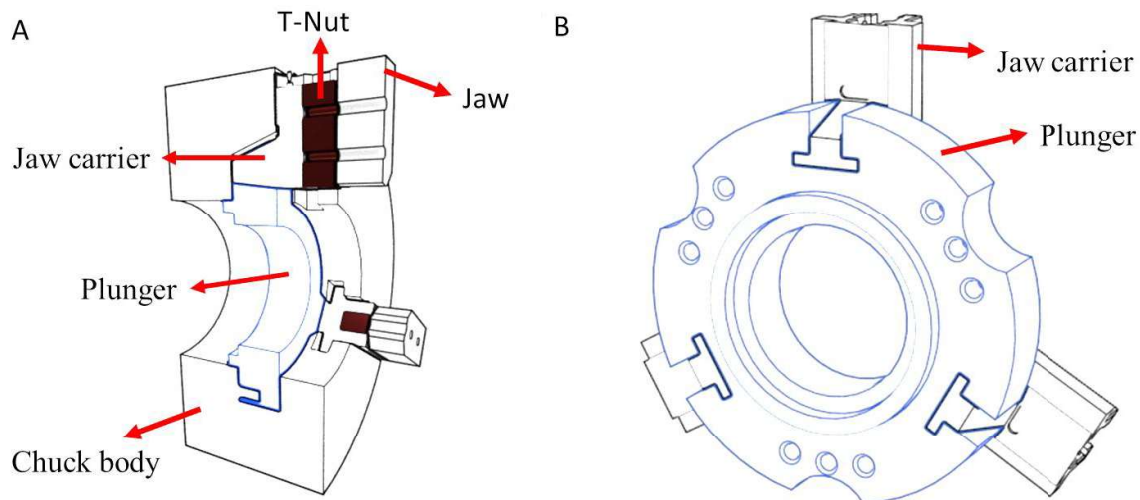
Fig. 3.1. Schematics showing: (a) sectional view the hydraulic lathe chuck, (b) isometric view of jaw-carrier and plunger assembly.
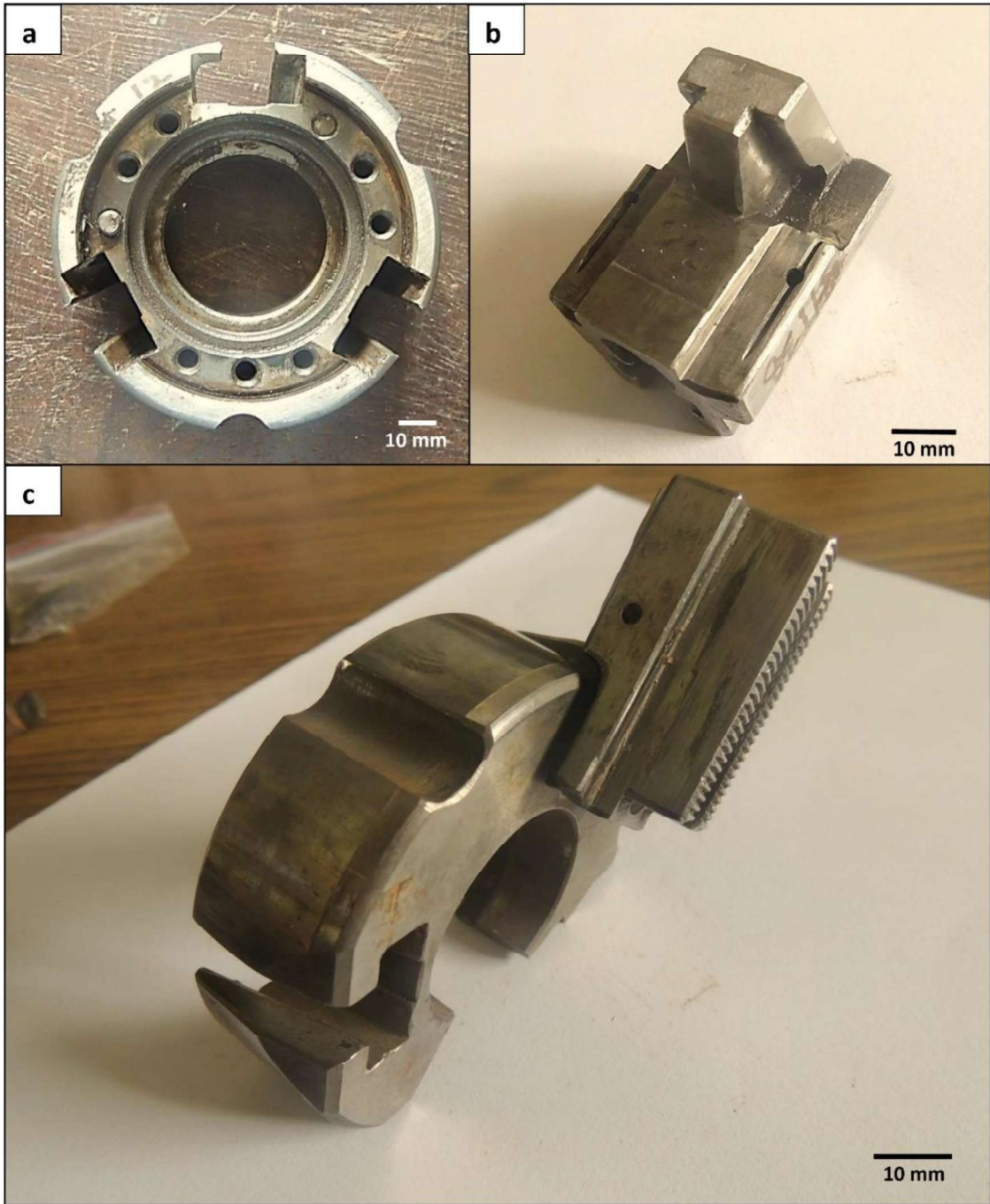
Fig. 3.2. Images showing critical components of a hydraulic lathe chuck; (a) rear-side view of the plunger showing several steps, holes and three T-slots, (2) oblique view of a jaw-carrier showing the T-shaped projection, and (3) the jaw-carrier assembled in a T-slot of the plunger from the front-side.

The standard fabrication process of the jaw carrier and plunger starts with forging the steel billets to the required sizes. Intricate shapes, sliding surfaces, and slots are machined in the billets while maintaining close dimensional tolerances. The components are then subjected to carburizing heat-treatment followed by low temperature tempering as the desired surface hardness is 58-60 HRC and the case-depth is about 1.5 mm. However, some customers demand the surface hardness of 60 HRC to minimize the wear and facilitate the smooth sliding between the plunger and the jaw-carrier. To reduce the wear and increase the service life, the sliding components, including the plunger and the jaw carriers, are case-hardened by carburizing. The surface hardness and the case-depth in excess of 60 HRC and 200 μm respectively are always desirous for the long life and smooth functioning of the hydraulic chuck assembly. The required case-depth of the steel components can be achieved by suitably adjusting, carbon potential, austenitizing temperature, and the diffusion time during the carburizing treatment. However, it is extremely difficult to achieve the surface hardness of more than 60 HRC in the components that are generally made of forged billets of low-alloy structural steels. As the carburized and oil-quenched components are always tempered, the surface hardness generally drops to below 60 HRC. To retain a high surface hardness (close to 60 HRC), the industry often resorts to low temperature (150-200 °C) tempering and thereby compromising on the toughness of the steel components. Thus, the heat-treatment of hydraulic steel components is always challenging.

Therefore, along with the component design and machining quality, appropriate heat treatment process is essential for the smooth functioning and a long service life of the hydraulic chuck assembly. The objective of this work is to study the mechanism of the failure and then to suggest solutions to mitigate such failures in the future.

3.2 Materials and Methods

As confirmed by the chuck manufacturer, the plunger and the jaw carrier are made of EN36C, a case hardenable low-carbon alloy steel, whose nominal composition is shown in Table 3.1. Both the plunger and the jaw-carriers were subjected to gas-carburizing in different batches at 930 °C for 6 h followed by quenching in an oil bath. After the quenching, tempering was carried out at 200 °C for 1 h in a muffle furnace. Further, to

increase the surface-hardness and to meet the customer/designer requirement of 58-60 HRC, the tempered components were then subjected to sub-zero treatment at about -15 °C for 24 h in a freezing mixture of ice and salt. This is an unusual practice, as the sub-zero and cryogenic treatments are generally performed on as-quenched steel components to transform retained austenite into martensite so that on tempering, the steel component would achieve optimal hardness, toughness and microstructural uniformity. In numerous recent studies involving Deep Cryogenic Treatment (DCT) of steels, it has been clearly demonstrated that key mechanical properties such as, hardness, tensile strength, toughness, and bending strength of structural steels can be significantly improved by suitably adding a DCT step in the heat treatment cycle (Cajner et al. 2012; Çiçek et al. 2015; Ghasemi-Nanesa and Jahazi 2014; Khun et al. 2015; Niaki and Vahdat 2015a; Zare and Hosseini 2016; Zhang et al. 2014).

Table 3.1. Measured chemical compositions (wt. %) of the Jaw-Carrier and the Plunger against the EN36C steel grade specification.

	C	Mn	Si	Ni	Cr	Mo	S	P	Fe
EN36C Spec.	0.12-0.18	0.30-0.6	0.10-0.35	3.00-3.75	0.60-1.10	0.10-0.25	0.05 max	0.05 max	Balance
Jaw-Carrier	0.16	0.45	0.22	3.32	0.85	0.10	0.04	0.04	Balance
Plunger	0.15	0.37	0.23	3.38	0.91	0.13	0.03	0.04	Balance

However, the chuck manufacturer of the current study claims that the hardness of a tempered steel component increases by about 2 HRC after the sub-zero treatment and that this increased hardness helps in reducing the surface wear and meeting the customer requirement. It is important to confirm this claim and compare the effectiveness of the regular sub-zero treatment with that of the unusual sub-zero treatment. Considering that the construction and the performance of the lathe chuck components involve mechanical design part and materials processing part, the failure analysis and the heat treatment experiments were conducted separately as described in the following sections.

3.2.1 Failure Analysis

For the failure investigation of the lathe chuck assembly, the standard failure analysis procedure involving, visual inspection, fractography, microstructural analysis, and hardness testing, was carried out. As-received lathe chuck components were cleaned, washed and dried to reveal the various signs of destress and the fracture surface features. For the microstructural analysis, the lathe chuck components were sectioned using an abrasive-disc slicer to obtain coupon size specimens. The specimens were ground using a series of abrasive papers, and polished using a velvet cloth and 1 μm silica suspension on a disc-polisher as per the standard metallographic procedure. 2 % Nital was used as an etchant to reveal the microstructure. A Zeiss AXIO optical microscope was used for studying the microstructures. A JEOL JSM-6380LA Scanning Electron Microscope (SEM) was used in secondary electron mode for the fractography. Hardness tests were carried out on the test coupons using a standard Rockwell hardness tester fitted with a cone indenter and 150 kg as the major load. The hardness measurements were carried out on the carburized-case as well as at the specimen core. Five reliable readings with a variation of $\pm$ 1 HRC were taken at the critical regions on each component and the average hardness values were tabulated. To know the depth of carburizing and effective case depth, Vickers hardness test was carried out using Shimadzu HMV-G 20 ST tester with 1 kg load.

3.2.2 Numerical Stress Analysis

The objective of the numerical stress analysis is to simulate the operational stress contours by considering the realistic dimensions of the plunger, room temperature mechanical properties of the plunger material, and suitable boundary conditions. The simulated stress contours can show the stress concentration at the fracture critical location. However, it is important to note that by suitably considering, the gripping force, the machining force applied by the cutting tool, and the centrifugal force arising out of the rotation, the stress contours of the plunger may be generated. But, the stresses due to real-life incidents such as, improper gripping, eccentricity due to misaligned centering of the job, accidental bumping during the setting or removal of the job, jerky operation, abrupt shutdown and start-up cycles due to power outages, etc., cannot be easily generated. Thus, the stress

analysis is limited to generating realistic stress profile of the critical component under ideal operating condition.

For the optimal use of computational time and resources, only the plunger was considered for finite element analysis as shown in Fig. 3.3. By considering the measured dimensions, 3D CAD model of the plunger was built using the commercial software package, SOLDIWORKS. Unwanted features including holes, fillets and chamfers especially at non-critical locations were ignored in the 3D model. The CAD model was imported to ANSYS workbench to perform static structural analysis. For more accurate results, the plunger was meshed with hexahedral brick elements in most part. Due to geometric constraints a few tetrahedral elements were also included. Care was taken for the mesh connectivity at the critical regions to capture the reliable magnitude of the stress.
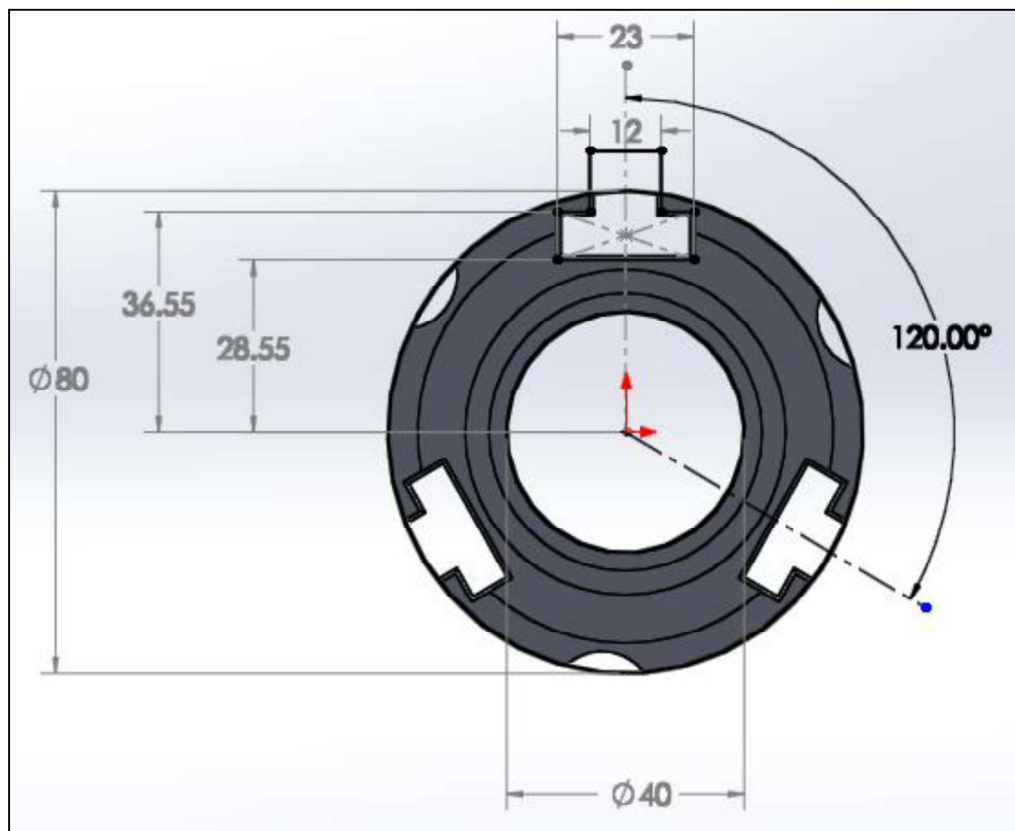
Fig. 3.3 3D CAD model of the plunger.
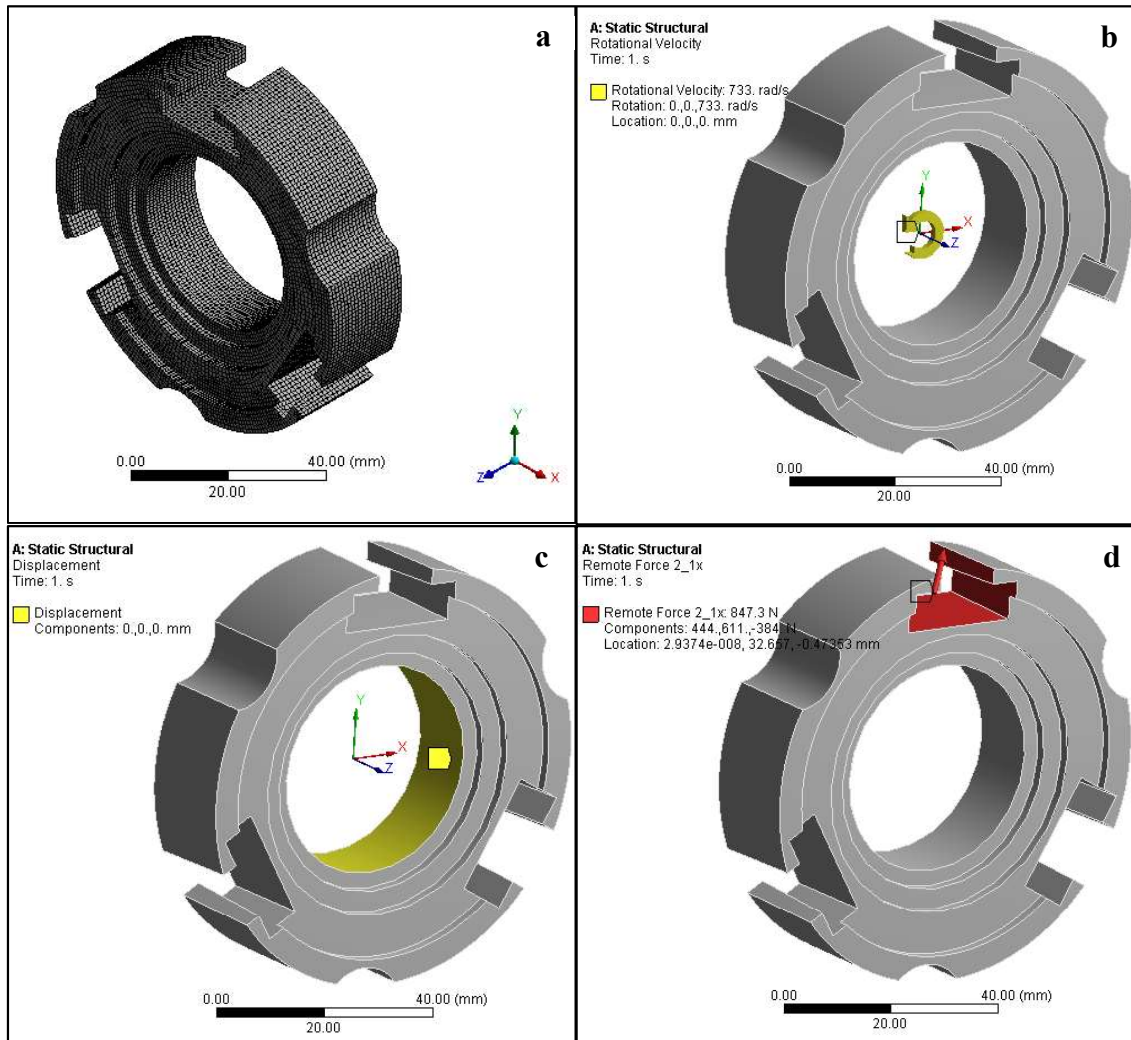
Fig. 3.4 Images showing: a) meshed plunger model, (b) rotational velocity in the anti-clockwise direction along the Z –axis, c) arrested translational motion in X, Y and Z directions (d) cutting force applied to the surface of the wedge slot.

Boundary Conditions

The plunger material is assumed to be a structural steel and corresponding room-temperature materials properties were considered in the finite element model. The meshed model and the boundary conditions applied on the model are shown in Fig. 3.4. The inner face of plunger was constrained from any translation motions in X, Y and Z directions. The axis of plunger was given a rotational motion in the Z axis with a rotational velocity of 733 rad/s (7000RPM). The magnitude of force components associated during the cutting

36

operations (Shunmugam and Kanthababu 2018) in X, Y and Z directions was applied to the wedge slot face by creating a remote point and applying a remote force over the wedge-surface representing the cutting force during the machining operation. Linear elastic stress analysis was performed to simulate operational stresses in the plunger. Equivalent von misses stress criteria was used to obtained stress contours from the simulation.

3.2.3 Heat Treatment Experiments

A set of heat-treatment experiments involving cryogenic treatment of EN36 steel were designed to simulate the real-life industrial practice and compare the same with a scientifically proven and well-established practice. To study the effectiveness of the cryogenic step in the heat-treatment cycle of carburized EN36, following heat treatment experiments were carried out.

16 mm diameter EN36C grade steel bars were procured and sliced to obtain the experimental specimens of 20 mm length. The specimens were then subjected to carburizing and quenching treatment followed by, 1) conventional hardening and tempering treatment, 2) cryogenic treatment (CT) carried out after tempering, and 3) cryogenic treatment carried out as an intermediate step between quenching and tempering. The austenitizing temperature/duration, quenching medium/temperature, tempering temperature/duration, and cryogenic medium/temperature/duration, were all kept constant for the heat-treatment cycles.

A box-type furnace was used for the heat-treatment of the specimens. Considering that the actual chuck components were carburized before quenching, in order to simulate the real-life industrial heat-treatment, pack-carburizing method was adopted for the experimental specimens. A carburizing mixture of barium carbonate, calcium carbonate and charcoal in the ratio 7:3:90 was prepared and the specimens were properly packed using the carburizing mixture in a mild steel box. The box was closed with a lid and then sealed using bentonite clay paste to avoid decarburization. The specimens were then austenitized to 930 °C for 6 h to achieve the required case-depth. The carburizing pack was broken and the specimens were then quenched in an oil bath. Tempering was carried out by holding the

specimens at 200 °C for 1 h. For cryogenic treatment, the specimens were immersed in liquid nitrogen for 24 h. After various heat treatment steps, the specimens were sectioned, ground, and etched as per the standard metallographic procedure to study the hardness variation and the microstructural changes occurring at the surface and the core of the specimens.

3.3 Results and Discussion

3.3.1 Visual Inspection

The fractured jaw-carrier and the plunger in as-received condition are shown in Fig. 3.5. The plunger fractured at a T-slot and the jaw-carrier fractured at the T-shaped projection. This suggests that plunger and jaw-carrier assembly failed at the mating slot. It is important to consider that these two mating parts carry the hydraulic plunging force for gripping the job. During the lathe operation, the contact stresses caused by the gripping of the job would be superimposed by the additional stresses caused by the lateral force imposed by the cutting tool. Thus, the failure of any one component during operation should cause immediate damage to the mating part. Thus, it is likely that both the plunger and the jaw-carrier failed in one event as a cause and the effect during the lathe operation. However, it is important to figure out which component failed first and then caused the failure of the other component.

Images of the jaw-carrier after cleaning, washing and drying are shown in Fig. 3.6. Considering the complex geometry of the jaw-carrier, the fracture surface is quite undulated. Close-up views of the fracture surface observed from either side of the jaw-carrier, in most part, suggests the rough brittle fracture features indicative of sudden snapping. The rough features on the fracture surface coupled with the absence of any gross deformation or bending suggests that the jaw-carrier snapped and fractured suddenly likely due to instant over-stressing during the lathe operation.
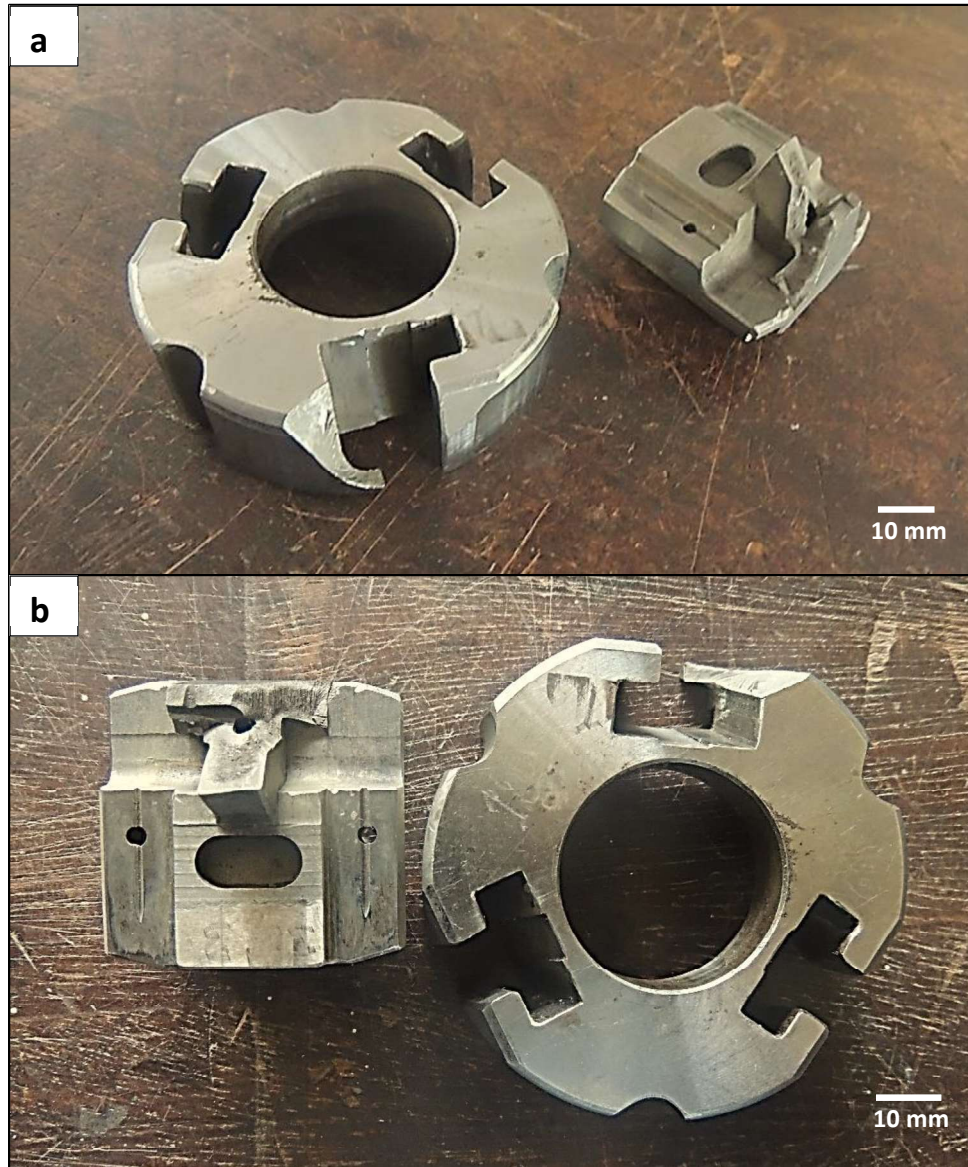
Fig. 3.5. Image showing as-received plunger and jaw-carrier; (a) oblique view, (b) top view.
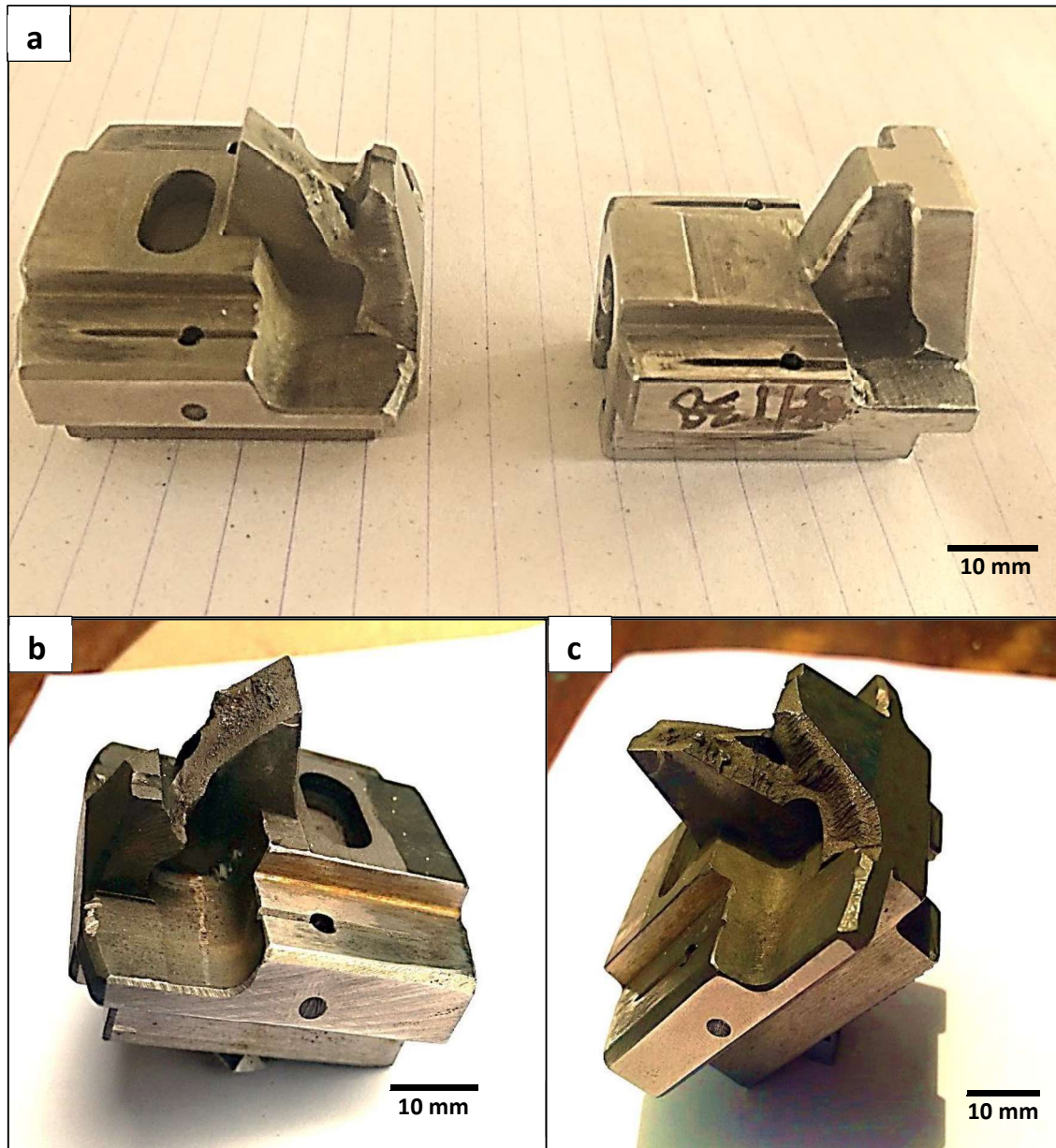
Fig. 3.6. Different views of failed jaw-carrier showing the fracture-location and surface features; (a) side-view of the failed jaw-carrier in comparison with a good jaw-carrier showing the location of the fracture, (b, c) oblique views from either side indicating the brittle fracture features.

Images of the failed plunger and close-up views of the fracture surface are presented in Fig. 3.7. Two key points can be noted from visual inspection of the failed plunger; the fracture surface reveals circumferential thumbnail propagation features identified as beach marks that indicate the direction of propagation of the fracture. The epicenter of the circumferential marks is a sharp corner in the T-slot suggesting that the fracture originated from this location of the plunger and that the crack propagated progressively during the lathe operation. Any sharp corner without a fillet or suitable radius of curvature can act as the stress raiser and hence becomes a fracture critical location during the service. These critical observations suggest that the plunger failed by fatigue fracture. The lifting or bending forces exerted by the mating jaw-carrier must have imposed highly concentrated and variable tensile stresses at the sharp-corner in the plunger while gripping the job during the lathe operation. This implies that a crack generated in the T-slot corner of the plunger and propagated slowly during the service before the final fracture. As the contact stress distribution in the mating parts changed suddenly, the jaw carrier fractured immediately likely due to instant over-stressing during the service. The visual inspection suggests that the plunger suffered a progressive fatigue failure and as an effect, the jaw-carrier failed by sudden snapping. Thus, it can be stated that the primary failure is the fatigue fracture of the plunger and that the sudden fracture of the jaw-carrier is the secondary failure of the chuck-assembly.
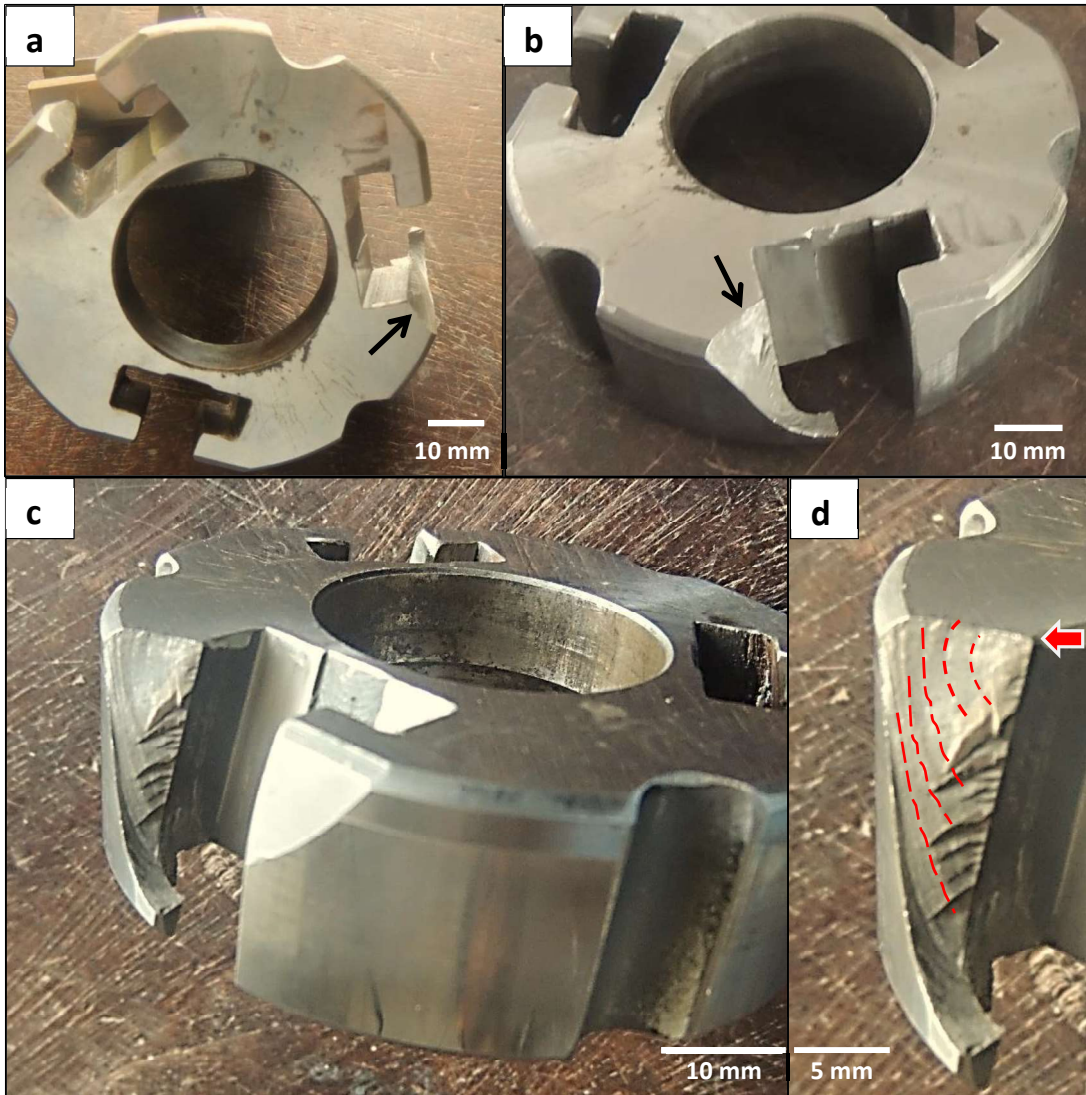
Fig. 3.7. Different views of the failed plunger showing the fracture-location and surface features; (a, b) oblique views showing that the plunger fractured at one corner of a T-slot, (c, d) close-up views of the fracture surface showing fatigue beach-marks suggesting that the fracture initiated from the top corner of the T-slot as illustrated by the arrow and the dotted-lines.

3.3.2 Fractography

A fractographic image and SEM fractographs of the plunger are presented in Fig. 3.8. The photographic image (Fig. 3.8a) shows crack initiation site and propagation pattern. The low-magnification SEM fractograph (Fig 3.8b) captured at the termination site clearly shows the fatigue beach marks. Further, high-magnification fractographs (Fig. 3.8c, Fig. 3.8d) indicate intergranular fracture and fatigue-striations on the grains. Thus, the fractography confirms that the plunger failed in a progressive fatigue fracture.

Figure 3.9 provides the typical fractographic features of the jaw-carrier. The fractograph shown in Fig. 3.9a shows the contrasting fracture features of the core and the carburized case. The core shows the ductile fracture features with highly undulated fracture surface due to plastic deformation while the carburized sub-surface shows a flat-granular fracture surface that is indicative of the brittle fracture. The faceted intergranular fracture features shown in Fig. 3.9b confirms that the carburized case of the jaw-carrier suffered brittle fracture. The fractographs of the failed jaw-carrier captured at a critical region shows typical ripped features with signs of compression/pinch points adjacent to the ripped region comprising skewed dimples as shown in Fig. 3.10. This is the indication of the failure due to overstressing of the component. The localized pinching/pressing suggests that the loading during the fracture was localized likely due to misalignment or non-uniform contact of the mating surfaces. The fractographic analysis endorses the findings of the visual inspection that the jaw-carrier failed catastrophically in a single event while the plunger failed progressively by fatigue fracture. This further affirms that the fracture of the plunger is the primary failure and the fracture of the jaw-carrier is the secondary failure.
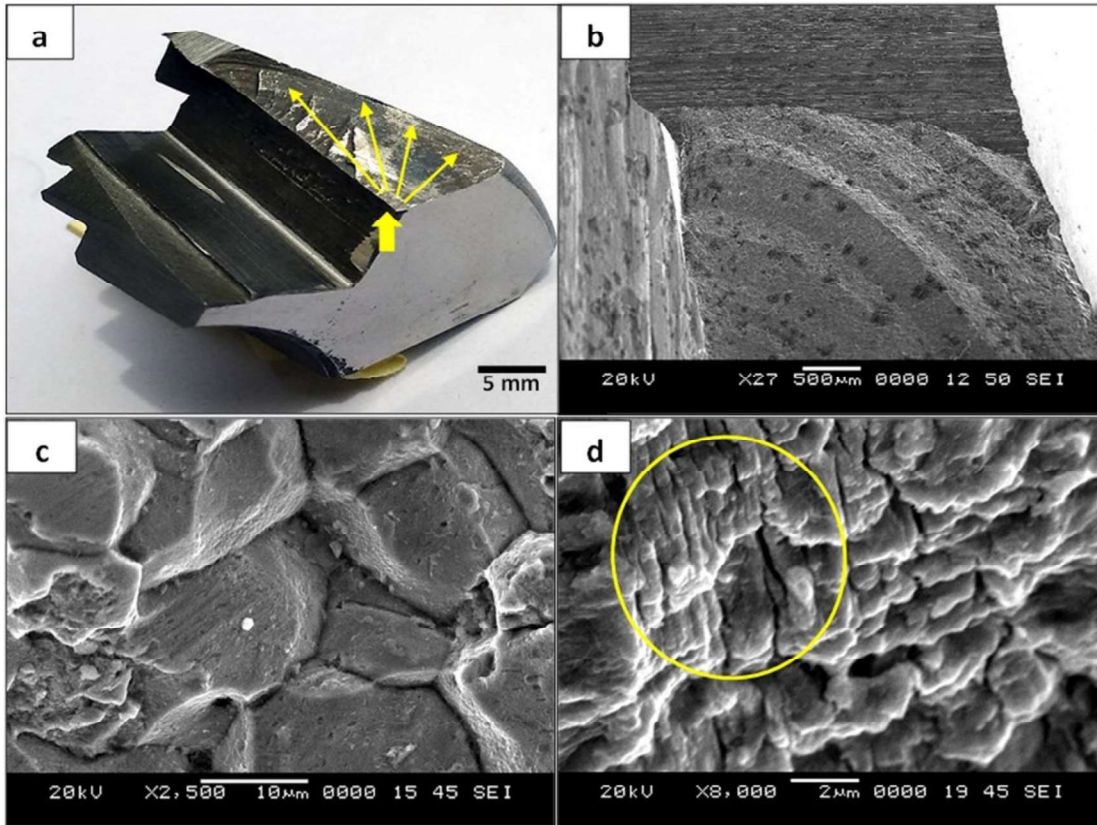
Fig. 3.8. Images showing fracture surface features of the failed plunger: (a) photographic image of the fracture specimen with the arrow showing crack initiation site, (b) low magnification SEM image showing fatigue beach marks with banded thumb-nail propagation features on the fracture surface, (c) high magnification SEM image showing granular fracture surface that confirms intergranular crack propagation, and (d) high magnification SEM image revealing the diffused fatigue striations in the fracture surface as highlighted in the circle.
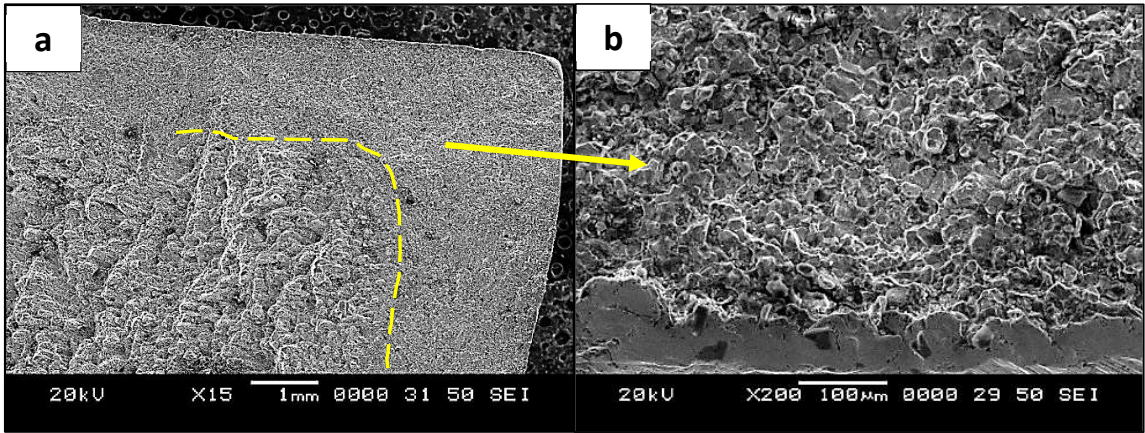
Fig. 3.9. SEM fractographs of the failed jaw carrier showing: (a) two distinct fracture patterns at the carburized-case and the core, (b) brittle intergranular fracture feature at the case.
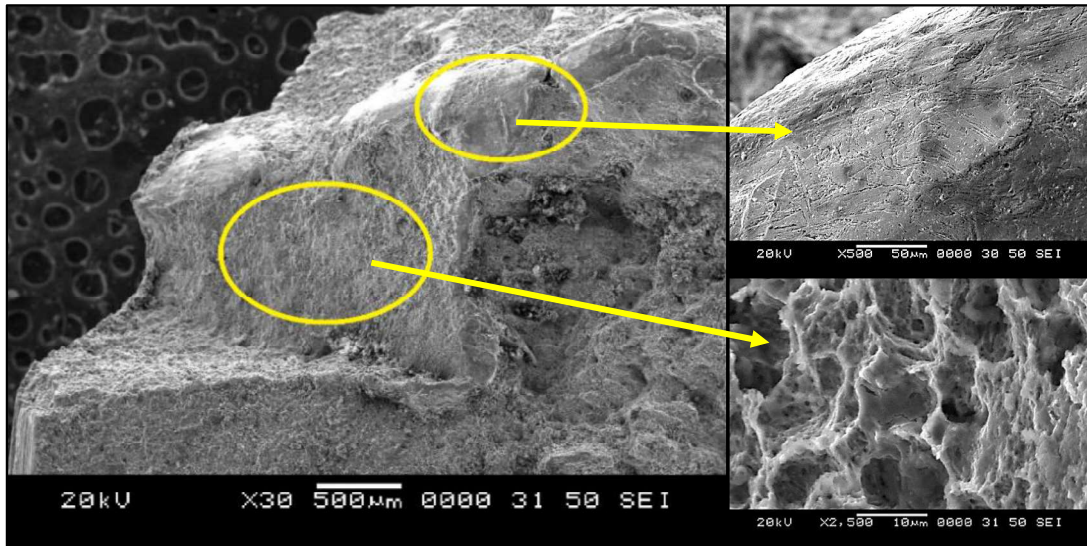
Fig. 3.10. SEM fractographs focused at an edge of the jaw-carrier showing the compression point adjacent to the ripped region suggesting failure due to overstressing; inset images showing the crushed lateral flow pattern at the compression point and skewed dimples at the ripped region.

3.3.3   Numerical Stress Analysis

The fractographic analysis suggests that the fatigue fracture of the plunger is the primary failure or the cause and the fracture of the jaw-carrier is the secondary failure. Thus, it is important to know why the plunger failed. Considering that the plunger failed progressively by fatigue failure, fracture critical location in the plunger must have been under high tensile stress during the operation or setting-up of the chuck. Technically, the peak stress at the fracture critical location should exceed the endurance limit of the material. However, only the operational stress as per the plunger design is considered for the FEA simulation. The stress profile of the plunger is shown Fig. 3.11.

As expected, the stress concentration is at the slot-corner. As shown in Fig. 3.12 Max von-misses stress is found to be 47 MPa and is acting at the slot-corner where the actual plunger failed during service. The magnitude of cutting forces and rotational velocity at the time of failure could be even higher. However, FEA simulation corroborates that the jaw carrier which fits into the slots of the wedge plunger transmit the aforesaid forces during the operation and the wedge slot region is prone to crack initiation. Thus, the numerical stress analysis identifies the fracture-critical location and the result matches well with the observations made in the visual inspection and fractography.

It is understandable that the stress concentration in the critical region may be minimized by providing suitable fillet in the slot and corresponding rounding-off of the mating jaw-carrier projection. Thus, much better stress-distribution can be achieved during the gripping and operation of the chuck.
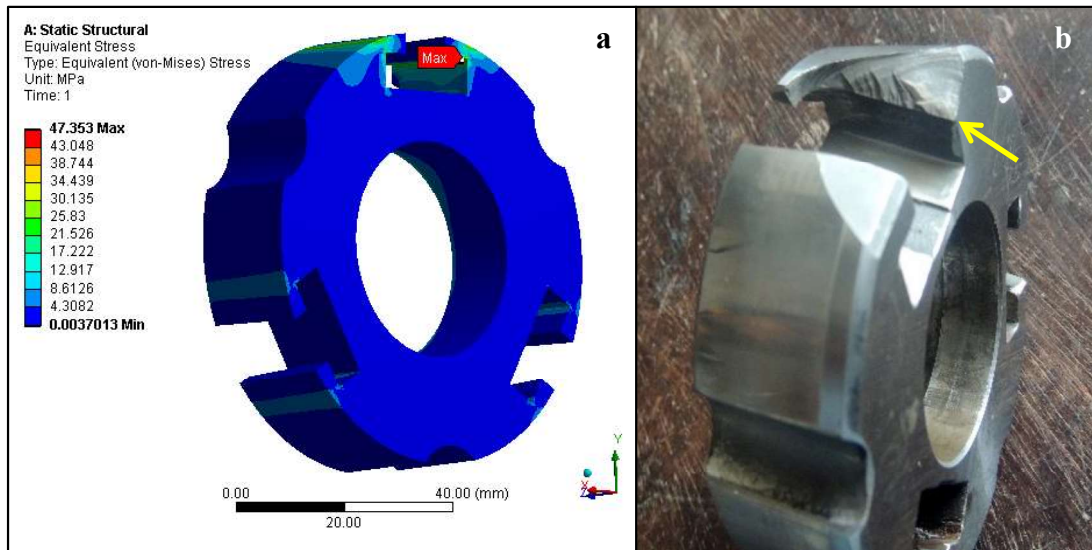
Fig. 3.11. Image comparing, (a) the FEA simulated stress distribution in the plunger, with (b) the actual fractured plunger showing the fatigue crack initiation site.
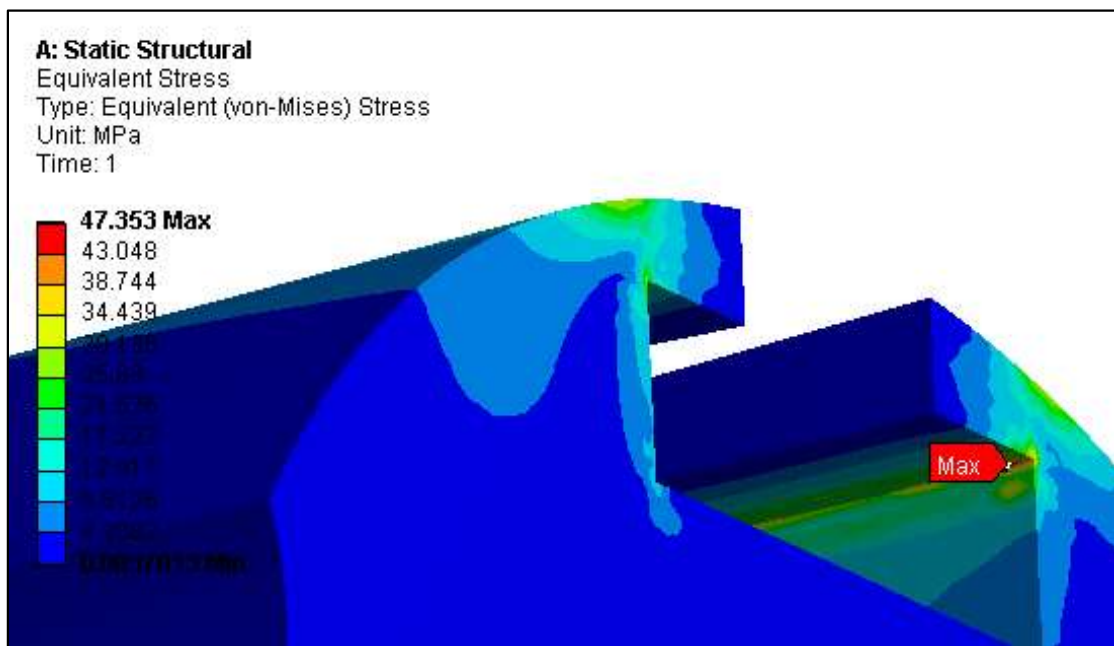
Fig 3.12. Images showing Close-up view of the FEA simulated stress contours in the plunger showing the stress concentration at the sharp edge of the T-slot where the in-service fatigue fracture initiated.

3.3.4 Microstructural Analysis

Optical micrographs of transversely sectioned jaw-carrier and plunger are shown in Fig. 3.13 and Fig. 3.14. Figure 3.13a and 3.13b show the microstructures of the jaw carrier observed at surface and core respectively. As the jaw carrier is case carburized the surface displays sharp needle like martensitic microstructure while the core shows more diffused tempered martensite. Figure 3.14a and 3.14b show the microstructures of the plunger observed at surface and core respectively. Similar observation can be made in the cross-sectional microstructure of plunger as the case shows sharp martensitic microstructure and core displays diffused lathe shaped tempered martensitic microstructure. This shows that both the failed components were case-hardened by carburizing treatment.
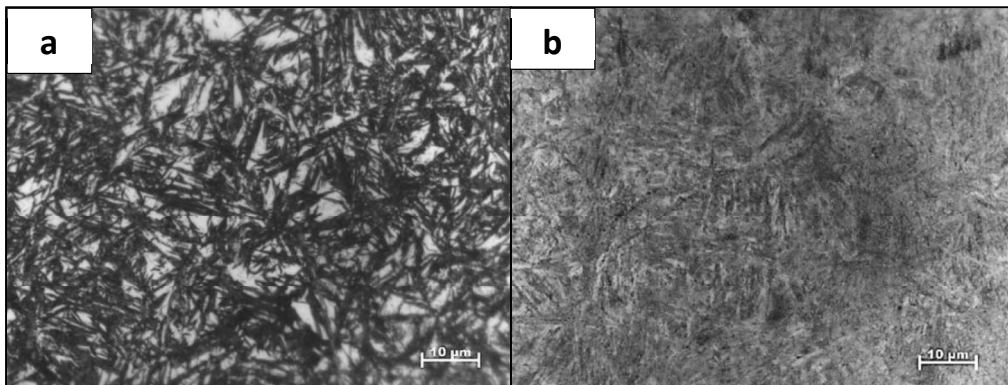
Fig. 3.13. Cross-sectional micrographs of failed jaw carrier: (a) carburized case, (b) core.
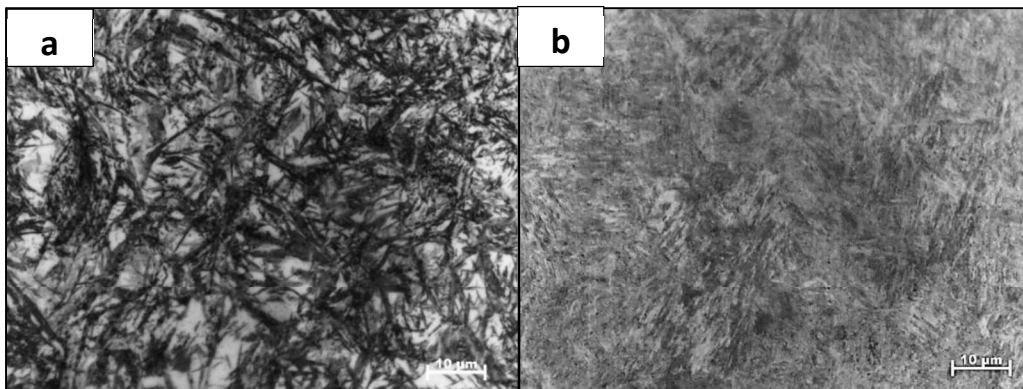
Fig. 3.14. Cross-sectional micrographs of failed plunger: (a) carburized case, (b) core.

3.3.5 Hardness Measurements

Table 3.2 presents the hardness values of the chuck components measured on the surface as well as at the interior. The table compares the hardness values of: the failed plunger, the fractured jaw-carrier and a jaw-carrier that performed very well in service. The hardness of the core is quite consistent at 42-43 HRC in all the specimens. Similarly, the surface hardness of the plunger and the good jaw-carrier is also consistent at 57-58 HRC. However, the jaw carrier that suffered brittle fracture possessed significantly higher hardness (60 HRC) at the surface. This suggests that the heat-treatment process of these components was not consistent and the process parameters varied from batch to batch. The component with a high case-hardness suffered brittle fracture during the service likely due to poor toughness of the hardened case. The hardness tests performed on the service-exposed components suggest that high surface-hardness and good toughness of the hardened-case would be necessary for the extended service life of the chuck-components.

Table 3.2. Hardness Measurements.

Component	Location	Hardness (HRC)
Failed Plunger	Surface	57
	Interior	43
Failed Jaw-Carrier	Surface	60
	Interior	43
Good Jaw-Carrier	Surface	58
	Interior	42
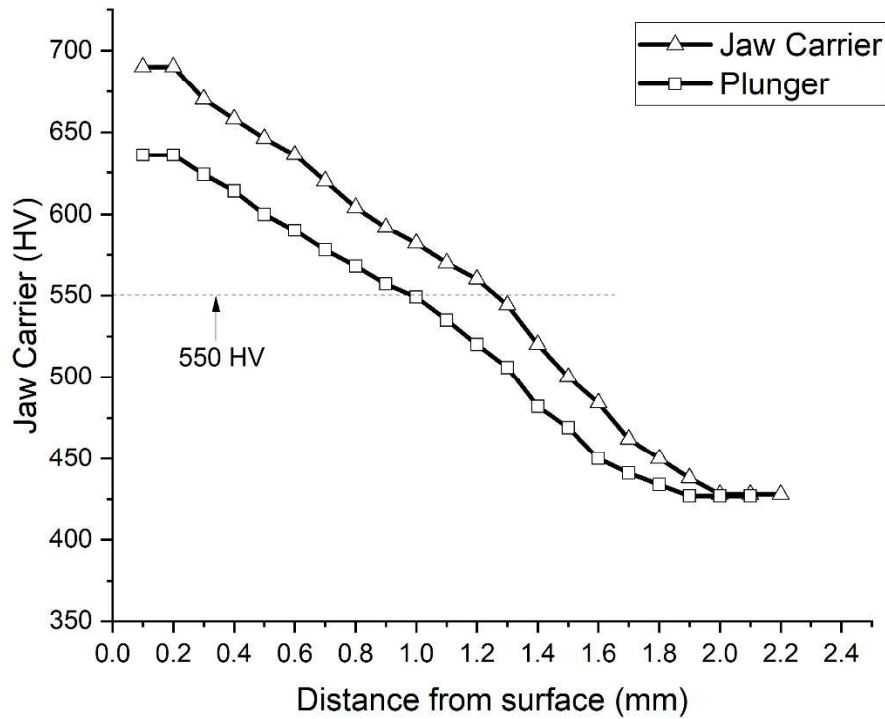
Fig. 3.15. Hardness profile of jaw carrier and plunger depicting the depth of case and effective case depth.

Figure 3.15 presents the hardness profile of the failed jaw carrier and the plunger depicting the depth of case and effective case depth. It is observed that the required case depth of 1.5 mm has been achieved in both the failed components with the effective case depth of about 1.3 mm corresponding to 550 VHN.

3.3.6 Heat Treatment Experiments

Table 3.3 shows the hardness variations in case-carburized EN36 steel specimens after various heat treatment steps and Fig. 3.16-3.18 illustrate the corresponding microstructural variations in the hardened-case and the core. A significant difference in the as-quenched hardness values of the case (60 HRC) and the core (44 HRC) and corresponding microstructures confirm that the pack-carburization experiment performed on EN36 specimens is quite successful. It is obvious that the tempering treatment on carburized and quenched specimen caused reduction in the hardness of both the case and the core by 2

50

HRC. It is important to note that the cryogenic treatment performed after tempering caused an increase in the hardness at the surface as well as at the core by 1-2 HRC as claimed by the industrial heat-treaters. However, it is quite impressive that the cryogenic treatment carried out immediately after hardening is quite effective as the hardness of both the surface and the core increased significantly. The hardness increased from 60 HRC to 65 HRC in the surface while the core showed an increase in the hardness from 44 HRC to 47 HRC. Even after tempering, the quenched and cryogenic treated specimen retained a high hardness of 61 HRC at the surface and 44 HRC at the core. This result suggests that the regular cryogenic treatment performed as an intermediate step between the hardening and the tempering is more effective than the unusual industrial practice of the cryogenic or sub-zero treatment applied as the final step after tempering. This result is in agreement with the reported result of a carburized 18NiCrMo5 steel, in which cryogenic treatment carried out in-between quenching and tempering showed an increase in the hardness by 2.4 HRC. The specimens for which cryogenic treatment was carried out after the tempering step showed an increment of only 0.6 HRC (Baldissera and Delprete 2009).

Table 3.3. Notation, description, and hardness variations of heat-treatment steps.

Notation	Description	Hardness (HRC)	
		Surface	Core
Q	Quenched	60	44
Q+T200	Quenched + Tempered at 200 °C	58	42
Q+T200+CT	Quenched + Tempered at 200 °C +Cryogenic Treated	60	43
Q+CT	Quenched + Cryogenic Treated	65	47
Q+CT+T200	Quenched + Cryogenic Treated +Tempered at 200 °C	61	44
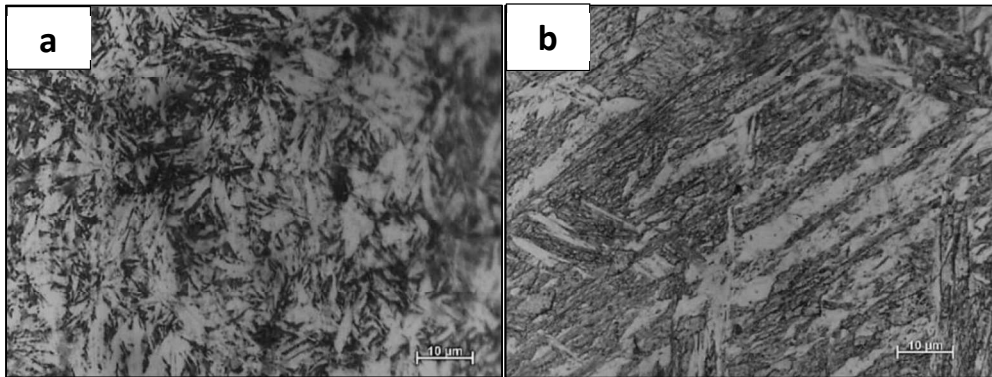
Fig. 3.16. As-quenched microstructure of carburized EN36 showing: (a) densely populated fine martensite phase at the hardened case, and (b) coarse martensite at the core.
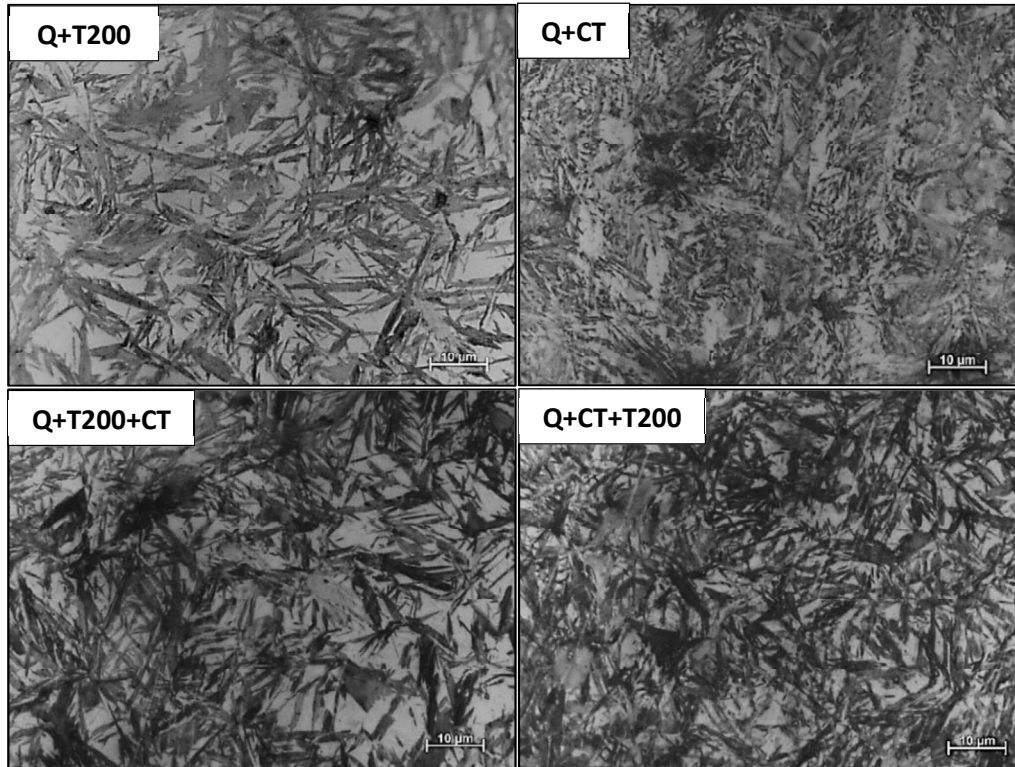
Fig. 3.17. Microstructural variation in the hardened-case of EN36 following various heat treatment steps; (Q+T200) quenched and tempered specimen showing martensitic needles embedded within large fraction of retained austenite, (Q+CT) quenched and cryogenic treated specimen showing an increased martensitic fraction and reduced retained-austenite, (Q+T200+CT) quenched, tempered and cryogenic treated specimen showing slightly refined microstructure; (Q+CT+T200) quenched, cryogenic treated and tempered specimen showing highly refined microstructure.
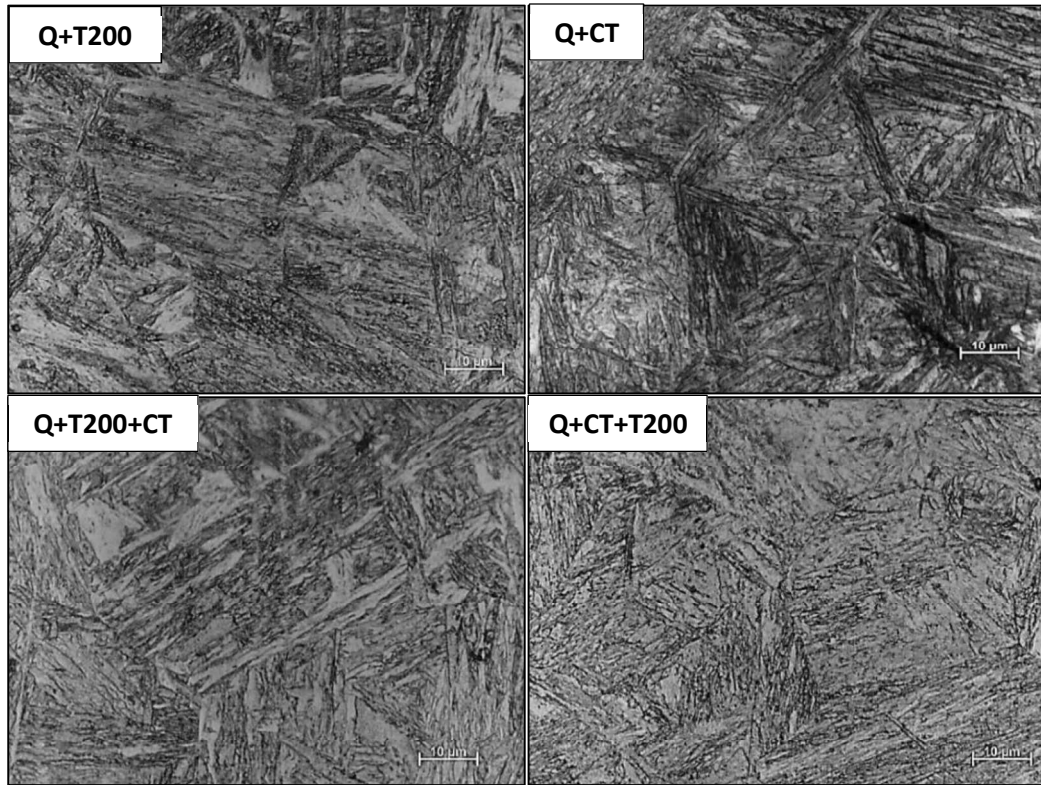
Fig. 3.18. Image showing the microstructural variation of the EN36 core following various heat treatment steps.

The microstructure of quenched and tempered (Q+T200) specimen shows sharp martensite phase embedded within the retained austenite matrix. The fraction of retained austenite is significantly high. The quenched, tempered and cryogenic treated (Q+T200+CT) specimen shows a subtle increase in the martensitic fraction suggesting that martensitic transformation occurred during the cryogenic exposure. However, the as-quenched specimen when subjected to the cryogenic treatment (Q+CT) developed much finer and denser martensite. This effect is very clear in the quenched, cryogenic treated and tempered (Q+CT+T200) specimen that shows highly refined microstructure with fine and dense martensitic colonies with minimal retained austenite in the microstructure. By comparing the figures in the second row (Q+T200+CT and Q+CT+T200), it is clear that the cryogenic treatment when applied as an intermediate step between the quenching and tempering is more effective than when applied after the tempering treatment. The hardness measurement done on the specimen surfaces clearly reflects this observation.

The above observation is consistent even in the specimen cores as presented in the Fig. 3.18. The microstructural variations in the core are similar to that of the case except that the martensitic colonies are coarser in the specimen cores. The most refined and uniform microstructure is observed in the quenched, cryogenic treated and tempered (Q+CT+T200) specimen. The hardness measurements performed on the specimen cores also endorse that the cryogenic treatment is highly effective when applied immediately after the quenching. Thus, the results of the heat-treatment experiments suggest that, though the specimens subjected to cryogenic treatment after tempering show dense and uniform microstructure, the specimens subjected to cryogenic treatment as an intermediate step show much denser and more uniform martensitic microstructure in the hardened-case as well as in the core. This microstructure should make the component much harder, stronger and tougher.

During tempering, stabilization of the carbides and the microstructural phases takes place and this inhibits further transformation during cryogenic treatment. Hence, higher degree of undercooling is required to transform the tough or stabilized microstructural phases (Mohan Lal et al. 2001). Therefore, it can be stated that cryogenic treatment carried out as an intermediate step between quenching and tempering transforms most of the retained austenite into martensite. This helps in achieving more refined microstructure with a uniformly distributed tempered martensite and carbides within the matrix. However, cryogenic treatment carried out after the tempering treatment is not very effective as it becomes difficult to break the stable microstructure achieved by conventional tempering. This may also lead to the adverse effects as the material would be in a state of stress after the cryogenic treatment and that, without any stress relieving/tempering process, the fatigue and impact resistance of the components would be compromised.

It is important to recognize that the microstructure of these heat-treated specimens especially in the hardened-case do not show well-tempered martensitic structure. The sharp and dense martensitic colonies embedded within the matrix suggest that the tempering temperature (200 °C) is too low. To achieve the optimal combination of hardness, strength and the toughness, the tempering temperature should be increased. Since the required

surface hardness for the EN36 components is 58-60 HRC, the quenched and cryogenic-treated components may be tempered at a higher temperature (300 °C) for achieving good impact and fatigue resistance. Since, the surface-hardness of the quenched and cryogenic treated specimen is quite high (65 HRC), a higher temperature tempering may be applied to the chuck components. This way, the service life of the components may be increased with a good combination of impact-fatigue-wear resistance.

3.4 Summary

The failure investigation and numerical stress analysis of the chuck assembly concludes that, the cracks initiated in the mating parts as a result of high stress concentration at the fracture critical locations and eventually caused catastrophic failure. The visual observation and the fractography suggest that the plunger failed first by fatigue fracture initiated at the sharp corner of a T-slot. As an effect, the T-projection of the jaw-carrier misaligned and snapped instantaneously by misalignment and overstressing. Thus, the presence of stress-raisers in the form of sharp corners in the mating components, which is a design flaw, is the root-cause for this failure. Modifying the existing design by providing fillets and rounding-off the sharp corners should minimize such failures in the future.

The microstructural analysis and the hardness measurements suggest that sub-zero treatment was carried out after tempering the components to achieve the required hardness. However, lack of stress relieving/tempering after the sub-zero treatment led to brittleness of the material especially at the hardened-case. The heat-treatment experiments conducted in this work suggest that, to increase the surface-hardness and the strength without compromising on the toughness of the steel components, sub-zero or cryogenic treatment has to be carried out before the tempering process. This way, catastrophic failure of the hydraulic chuck components can be minimized.

3.5 Motivation

The case-study presented here demonstrates the disconnection between the industrial practice and the scientific understanding of the cryogenic treatment. The heat treatment experiments conducted on EN36 material show the potential of the regular cryogenic

treatment against the unusual industrial practice. However, several structural steel grades, especially low-alloy steels are used for manufacturing industrial components. A direct comparison of cryogenic treatment applied before and after tempering of key structural steel is not reported yet. Thus, this thesis is motivated to make such attempts such that industrial heat treaters are provided clear guidelines to realize the full potential of deep cryogenic treatment applied to general structural steels.

4. PROPOSED WORK

Based on the case-study and the motivation, this chapter proposes the objective, experimental materials chosen, and tasks involved in the research work. The chapter provides a list of experimental materials, their nominal composition, and rational behind choosing them for achieving the desired objective.

Most of the studies on cryogenic treatment have been carried out on high alloy steels, high carbon steels, and carburized steels typically for improving the surface hardness and wear resistance. However, it is to be noted that unlike carburizing and nitriding treatments which improve the surface properties, cryogenic treatment improves bulk properties of the materials. For example, cryogenic treatment as an additional step to the conventional heat treatment is known to improve the bulk mechanical properties of tool steels such as, AISI D2, T1, M2, etc. However, effects of cryogenic treatment on the bulk mechanical properties of low-alloy steels are not widely studied.

The case-study presented in the previous chapter highlights the issues related to the unusual 'sub-zero' treatment practiced in the industry. The case-study demonstrates the advantages of isothermal cryogenic exposure prior to tempering over the post-tempering cryogenic exposure of a low-alloy steel, EN36. The effects of usual 'sub-zero' treatment and unusual industrial practice were compared and evaluated for the same material. Thus, commercial heat treaters can be convinced about designing the appropriate heat-treatment cycles that may involve an additional sub-zero or cryogenic treatment depending on the application. However, it is to be noted that EN36 is a Ni-bearing low-alloy steel. There are other structural steel grades containing low fractions of alloying elements such as, Cr, Mn, Si, Mo, etc., and are used as the materials of construction for various industrial components. It is not clear yet as to how these steel grades respond to the cryogenic treatment. Therefore, this research work focuses on studying the influence of cryogenic exposure, prior to, and after the tempering of few important low alloy steel grades that are widely used for constructing industrial components and structures. Considering that the cryogenic

treatment influences both bulk and surface properties, its true potential can be realized in both static and dynamic structures made out of low-alloy structural steels.

The main objective of the present work is to demonstrate the influence of deep cryogenic treatment on low-alloy structural steels and to provide a clear indication as to isothermal cryogenic exposure is to be carried out 'prior to' or 'after' the tempering step. Thus, the current work aims at providing clear guidelines to industrial heat treaters for fully realizing the potential advantages of the deep cryogenic treatment if included in the heat treatment cycles of common structural steels. For achieving this objective, the steel grades chosen as the experimental materials are: EN8, EN18, EN47, EN45, and EN24 whose nominal compositions are shown in Table 4.1.

Table 4.1 Nominal compositions of the selected experimental materials in wt. %.

Material	C	Si	Mn	Cr	Mo	Ni	Fe
EN8	0.4	0.3	0.8	-	-	-	Bal.
EN18	0.4	0.27	0.8	1.0	-	-	Bal.
EN47	0.5	0.27	0.65	1.0	-	-	Bal.
EN45	0.6	1.75	0.85	-	-	-	Bal.
EN24	0.4	0.27	0.57	1.2	0.27	1.5	Bal.

4.1 Materials and Application

1. EN8 is a widely used medium carbon steel that does not contain any special alloying additions. Typical applications of EN8 include, forgings, heavy power transmission shafts, crank-shafts, bolts, connecting rods, flanges, axels, couplings, etc. EN8 is a heat-treatable grade due to the optimal carbon content (~ 0.4%) and is generally used in through hardened and tempered condition. However, EN8 can be subjected to case-hardening treatment including carburizing, induction-hardening, nitriding etc. Being a plain-carbon steel mechanical properties of EN8 almost entirely dependent on the

carbon content. Thus, this steel grade serves as a reference material and hence EN8 is chosen for the study. Equivalent of EN8 grade is AISI 1040.

2. EN18 is a medium-carbon low-alloy steel whose carbon content (~ 0.4 % C) is same as that of EN8. However, the carbon equivalent of EN18 is slightly higher than that of EN8 due to the addition of chromium (1%). Thus, EN18 is superior to EN8 in terms of mechanical properties, hardenability, and corrosion resistance. Therefore, EN18 is used in slightly challenging environments and applications including, studs, bolts, shafts, gears, steering levers, axels, and crank-shafts, etc. The effects of cryogenic treatment on EN18 can be directly compared with that of EN8 and thus the influence of the key alloying element, Cr, can be easily validated. Therefore, EN18 is chosen as an experimental material for this research work. Equivalent of EN18 grade is AISI 6140.

3. EN47 is also a medium-carbon low-alloy steel whose carbon content (~ 0.5 %) is slightly higher than that of EN18. However, the key alloying addition and the chromium content (~ 1 %) of this grade is same as EN18. Therefore, the carbon equivalent of EN47 is higher than that of both EN8 and EN18. Thus, EN47 is superior to EN18 in terms of the heat-treatability and mechanical properties. Thus, EN47 is largely used for automobile axles, springs, spindles, power transmission shafts, crank-shafts, gears, etc. EN47 is chosen as an experimental material considering that the carbon equivalent and the hardenability of this material is progressively higher than that of EN8 and EN18, and the influence of the Cr can be confirmed and the role of carbon equivalent can be validated. Equivalent of EN47 grade is AISI 6150.

4. EN45 is a high-carbon low-alloy steel having a higher carbon content (~ 0.6 %) than EN47 along with Si as the key alloying addition (~ 2 %). Because of its high strength, hardness, toughness, resilience, and hardenability, EN45 is commonly referred to as spring steel and used predominantly in automotive industries in manufacturing leaf springs. EN45 is chosen as an experimental material of this thesis as the progressive

effect of carbon equivalent on the cryogenic treatment can be compared with the other experimental materials and the possibility of applying cryogenic treatment to other Si bearing spring steels can be proposed. Equivalent of EN45 grade is AISI 9255.

5. EN24 is a medium-carbon low-alloy steel whose carbon content (~ 0.4 %) and chromium content (~ 1%) are same as that of EN18 steel. However, EN24 has the additional alloying elements, Ni (~ 1.5 %) and Mo (~ 0.2 %). This material has the highest number of alloying elements and corresponding carbon equivalent. Thus, EN24 has the best combination of mechanical properties, and pitting corrosion resistance. EN24 is normally used in heavy machineries for constructing high performance shafts, gears, crankshafts, etc. EN24 is chosen as an experimental material to validate the effects of alloying additions and high carbon-equivalent to the cryogenic treatment. Equivalent of EN24 grade is AISI 4340.

4.2 Objectives of Research Work

Based on the experimental materials selected, objectives of the research work are stated as follows.

1. Study the effect of cryogenic treatment on the mechanical properties of a plain-medium-carbon steel.
2. Study the effect of cryogenic treatment on Cr, Ni, Si containing medium-carbon low-alloy steels.
3. Compare the effect of cryogenic treatment on as-hardened and as-tempered steels.
4. Generalize the effect of cryogenic treatment for low-alloy structural steels and provide clear guidelines to industrial heat-treaters.

5. EXPERIMENTAL METHODS

This chapter provides the methodology and experimental details in achieving the research objectives stated in the proposed work. The chapter describes, the heat-treatment cycles designed, cryogenic exposure applied, equipment employed, and the specimen preparation method/standard followed for carrying out experiments, testing and characterization.

5.1   Methodology

As stated in the previous chapter, the main objective of this research work is to compare the effects of regular cryogenic treatment that is applied prior to the tempering step with that of the unusual cryogenic treatment that is applied after the tempering step in the heat treatment cycles of few commercially important structural steels. The effects of regular and unusual cryogenic treatments can be directly compared and evaluated by following, testing, characterization, and performance of the heat treated specimens. Thus, commercial heat-treaters would develop a clear understanding of the influence and full potential of the cryogenic treatment if applied to key structural steel grades that are used in large quantities. Therefore, the methodology adopted here is to perform conventional hardening and tempering treatments on selected experimental materials first. Thus, the limitation of the conventional heat treatment cycles should be established which acts as the reference. Once the reference level is established, benefits of applying cryogenic treatments can be measured by direct comparison. Thus, effects of regular and unusual cryogenic treatments can be evaluated for each experimental material. Once the results of heat-treatment experiments are analyzed for all experimental materials, effects of cryogenic treatment as a function of alloying additions and carbon equivalent can be assessed. The experimental methodology of this research work is shown Fig. 5.1 in the form of a flow chart. General flow of the experimental work would be: Procurement, Annealing, Austenitizing, and Quenching of the experimental materials followed by, a) Tempering, b) Cryogenic Exposure prior to Tempering, and b) Cryogenic Exposure after Tempering. The experimental specimens would be subjected to testing and characterization.

Considering that tempering temperature for commercial alloys may typically vary from 300 °C to 450 °C, these two extreme temperatures are included in the experiments. Thus, a general understanding of the effects of cryogenic treatment for a bunch of commercial steel grades can be obtained for typical applications.
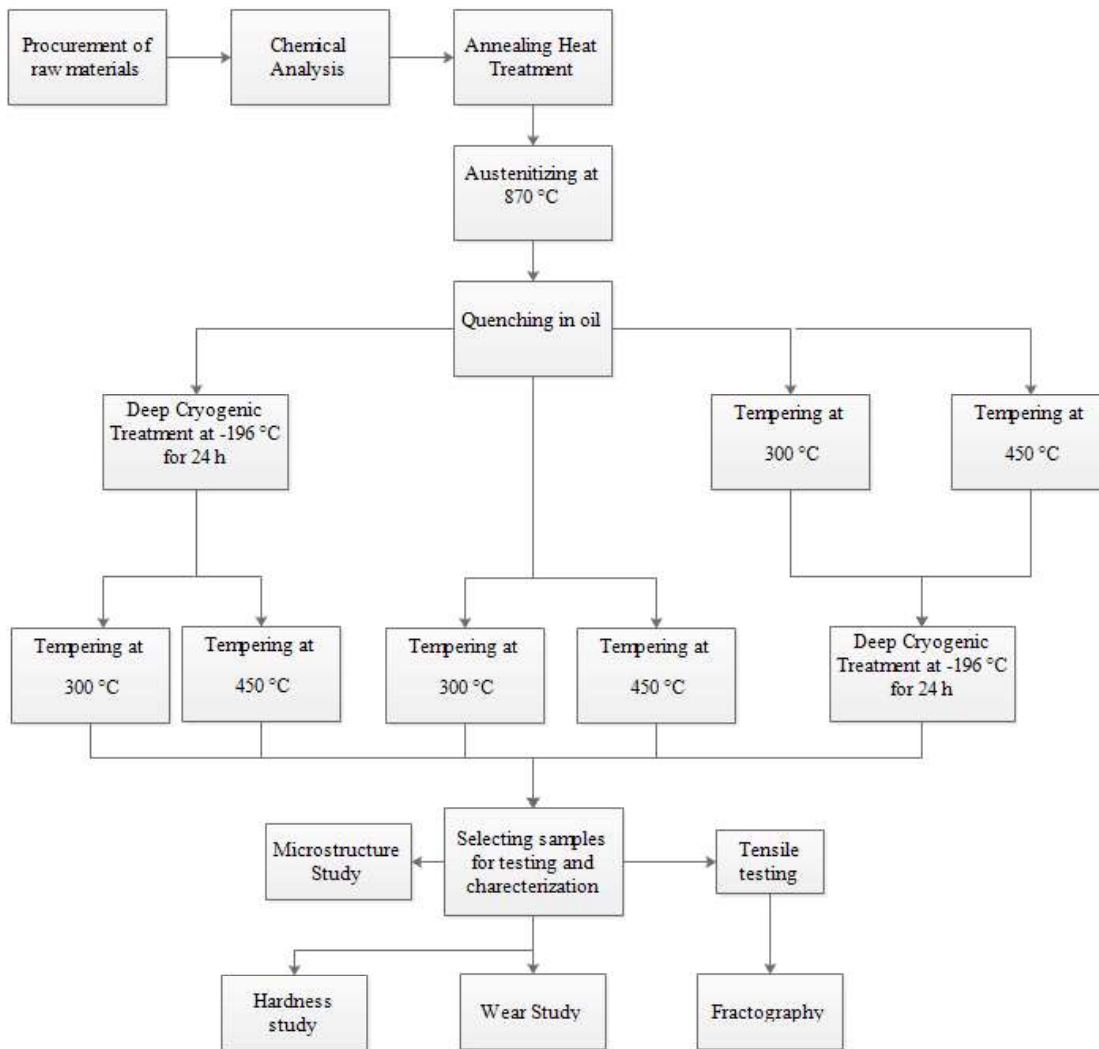
Fig. 5.1 Flow chart showing the experimental methodology of the research work.

5.2 Experimental Details

Sufficient quantities of experimental materials were procured from a local vendor and received in the form 16 mm diameter circular bars. These bars were sliced transversely to obtain experimental specimens for, compositional analysis, heat treatment experiments, metallography, hardness measurements, tensile tests, and wear tests.

Considering that the vendor received the materials stock from various sources, to erase any thermomechanical history and homogenize the procured bars, all the experimental specimens were annealed at 900 °C for 1 h in a box type furnace. The specimens were then austenitized and quenched in oil. Depending on the requirement, a few specimens were just tempered, a few as-quenched were immersed in liquid nitrogen and then tempered, and a few specimens were tempered and then immersed in liquid nitrogen. Irrespective of the sequence of the heat treatment cycles, austenitizing temperature/duration (870 °C/1 h), quenching medium/temperature (oil bath/room temperature), tempering-temperature/duration, (300 °C/1 h or 450 °C/1 h) and cryogenic medium/temperature/duration (liquid nitrogen/-196 °C/24 h), were all kept constant.

Cryogenic treatment was carried out by immersing the specimens in a liquid nitrogen tank of 5 liters for 24 hours. Liquid nitrogen was procured from the locally available industry, Mangalore Chemicals and Fertilizers Limited (MCF). The specimens that were subjected to quenching were thoroughly cleaned before immersing in liquid nitrogen and the specimens that were subjected to tempering were allowed to cool to room temperature before immersing in liquid nitrogen.

5.2.1 Metallography and Microstructural Analysis

Heat treated specimens were sectioned transversely and standard metallographic specimen preparation procedure involving, grinding using SiC abrasive papers, fine polishing using Al_2O_3 suspension, and etching with 2 % Nital solution was followed before mounting the specimen in a metallurgical microscope or a scanning electron microscope. For the microstructural analysis Zeiss AXIO optical was used in bright-field imaging mode at various magnifications up to 1000X to analyze low magnification microstructure. JEOL

JSM-6380LA Scanning Electron Microscope and JEOL FESEM 7610FPLUS were used for higher magnification imaging and analysis.

5.2.2 Tension Test

A 100 kN Shimadzu AG-X Plus Universal Testing Machine was used for performing tensile tests as per ASTM standard E8. Standard tensile test specimens shown in Fig. 5.2 were machined from the heat treated experimental specimens. By setting the initial gauge length and cross-sectional area, engineering stress-strain curves were generated. After processing the raw-data and plotting the curves, required information including yield strength, ultimate tensile strength, ductility, percentage elongation and reduction in area were obtained for each specimen.
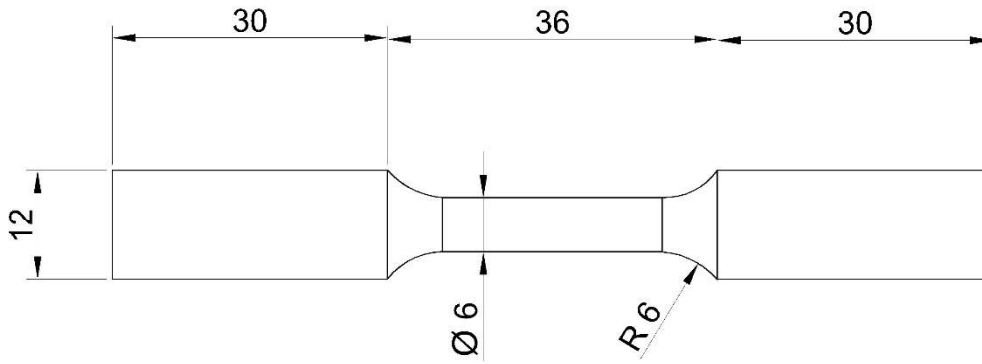
Fig. 5.2. Standard tensile test specimen (dimensions are in mm).

5.2.3 Hardness Test

Experimental specimens were sectioned transversely and ground using 100 grit SiC paper. A calibrated Rockwell hardness tester was used for measuring the indentation hardness in C scale whose details are shown in Table 5.1. Five concordant readings were obtained for each specimen before expressing the average hardness value in HRC.

Table 5.1 Specifications of the hardness test used in the experiments.

Test	Rockwell
Scale	HRC
Indenter	Diamond cone 120°
Minor load	10 kg
Major load	150 kg

5.2.4 Wear Test

Wear test was carried out according to ASTM G99 standard using a pin-on-disc apparatus as shown in Fig. 5.3. Three specimens were used for each test condition. In the pin-on-wear test, the pin specimen is made to press against the rotating disk at a specified load by means of lever arm with attached weights. The rotating disc is made of EN31 with hardness of 65 HRC. Figure 5.4 shows the dimensions of standard specimen used for the wear test. All the specimens were subjected to standard metallographic polishing procedure to obtain the mirror surface before subjecting to wear test. The disc was cleaned with emery paper after every test. The worn-out surfaces were observed using JSM-6380LA SEM to study the morphology and mode of wear.
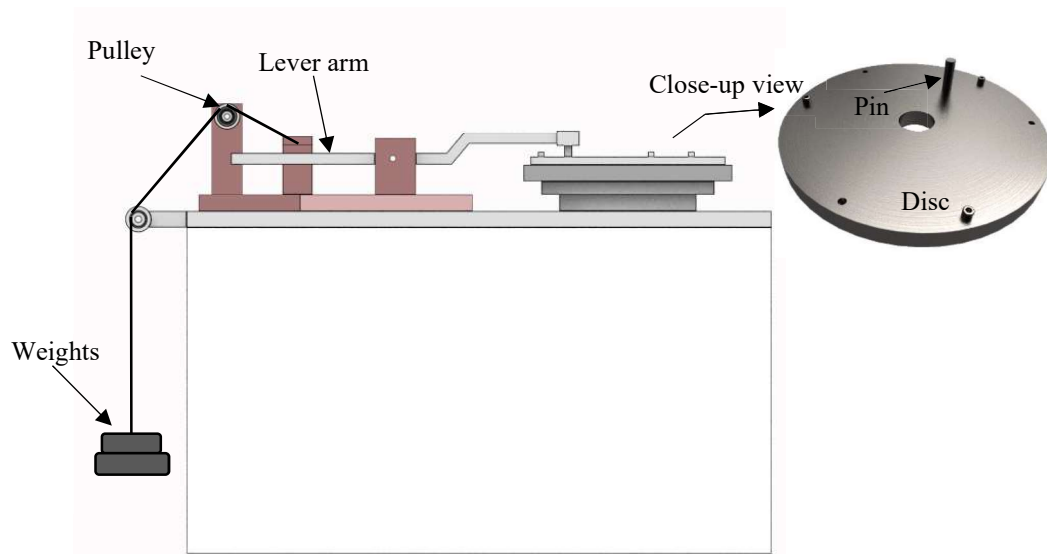
Fig. 5.3 Schematic showing wear test setup.
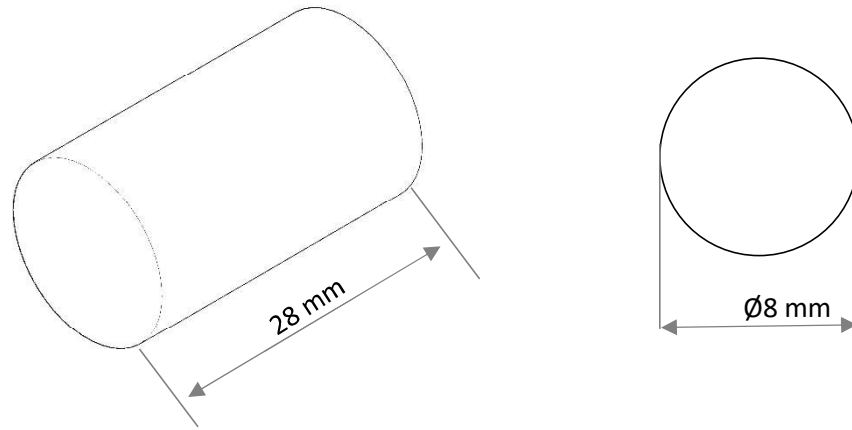
Fig. 5.4 Standard wear test specimen.

Table 5.2 Wear test parameters.

Parameters	Values
Load	58.81 N, 39.94 N
Sliding distance	4000 m, 8000 m
Wear track diameter	120 mm
Revolution speed	1000 RPM

Table 5.2 shows the parameters used for the wear test. The weight loss observed before and after the test is converted into the volume loss and is used to measure the wear rate of the specimen.

Determination of wear rate

The specimen subjected to wear test will be weighed using standard weighing machine both before and after the test and the difference will be taken as the weight loss.

Weight loss in grams Δw = Initial weight (w_i) – Final weight (w_f) ....(1)

The measured weight loss will be converted into volume loss

$$\text{Volume loss (mm}^3\text{) } \Delta V = \Delta w/\rho \dots\dots\dots\dots\dots\dots\text{(2)}$$

where, ρ is density of the material in g/mm^3

sliding speed and sliding distance are calculated using following formulae

$$\text{Sliding speed (m/min), } v = \pi \text{ x D x N}\dots\dots\dots\dots\dots\text{(3)}$$

Where, D is the wear track diameter in mm and N is the disc speed in revolutions/minute

$$\text{Sliding distance in meters, } d = v \text{ x } t\dots\dots\dots\dots\dots\text{(4)}$$

After obtaining volume loss, sliding distance wear rate and specific wear rate can be calculated using the following formulae

$$\text{Wear rate m}^3\text{/min} = \Delta V/d\dots\dots\dots\dots\dots\dots\text{(5)}$$

$$\text{Specific wear rate} = \Delta V/(\text{L x d})\dots\dots\dots\dots\dots\text{(6)}$$

where, L is the load applied in N

Wear resistance is the reciprocal of wear rate and is given by

$$\text{Wear resistance} = d/\Delta V\dots\dots\dots\dots\dots\dots\text{(7)}$$

6. RESULTS AND DISCUSSION

The chapter presents the results of hardness test, tensile test, microstructural analysis, fractography, and wear test in separate sections for all the experimental materials. Thus, the chapter tracks the variation in the microstructure and corresponding changes in the mechanical properties after every step in the heat treatment cycle for each material. In the end, chapter compares and discusses the effects of conventional quench-hardening and tempering treatment, cryogenic treatment added as an intermediate step between quenching and tempering, and cryogenic treatment applied as the final step after tempering.

The experimental work is designed to track the microstructure and properties of every experimental material as a function of heat treatment steps. Thus, for every experimental material, 8-10 specimens were used for the hardness tests and microstructural analysis, 4-8 specimens were used for the tensile tests, and 24 specimens were used for the wear tests. Total number of test specimens used for this study is more than 125. Thus, it is important to designate and identify these specimens as a function of the thermal history or the heat-treatment step for every experimental material. Therefore, a simple notation system is followed to identify and denote each specimen as a function of thermal history. Table 6.1 describes the notations used for identifying individual specimens consistently for all the experimental materials.

Table 6.1. Notations and description of heat-treated specimens.

Specimen No.	Notation	Description
1	A	Annealed
2	Q	Quenched
3	Q+T300	Quenched + Tempered at 300 °C
4	Q+T450	Quenched + Tempered at 450 °C
5	Q + CT	Quenched + Cryogenic Treated
6	Q + CT + T300	Quenched + Cryogenic Treated + Tempered at 300 °C
7	Q + CT + T450	Quenched + Cryogenic Treated + Tempered at 450 °C
8	Q + T300 + CT	Quenched + Tempered at 300 °C + Cryogenic Treated
9	Q + T450 + CT	Quenched + Tempered at 450 °C + Cryogenic Treated

6.1   Results of EN8 Steel

6.1.1   Chemical composition

Spark emission spectroscopy is employed to determine the chemical composition of the steel bars received from the vendor. The result of the spark emission spectroscopy for EN8 bars is shown in Table 6.2 against the materials specification. The measured composition of the steel bars conforms to the standard specification confirming that the experimental material used for the heat -treatment experiments are indeed medium carbon steel, EN8.

Table 6.2. Measured chemical composition (wt. %) of steel bars against EN8 specification.

	C	Mn	Si	Ni	Cr	Mo	S	P	Fe
EN8 Spec.	0.36-0.44	0.6-1.0	0.10-0.40	-	-	-	0.04 max	0.04 max	Balance
Measured	0.36	0.65	0.19	-	-	-	0.04	0.04	Balance

6.1.2 Hardness Measurement

Figure 6.1 presents hardness variations in EN8 steel following various heat treatment steps. The hardness test results show that the hardness of the as-quenched specimen is 45 HRC and that cryogenic treatment applied right after quenching increases the hardness from 45 to 48 HRC. This suggests that a medium-carbon steel responds positively for the cryogenic treatment when applied immediately after quenching. However, cryogenic treatment carried out after tempering does not show any measurable increase in the hardness.

When the hardness values of the tempered specimens are compared with that of as-quenched specimens, it is clear that EN8 being a plain-carbon steel greatly loses its hardness. However, by implementing the cryogenic treatment in-between quenching and tempering helps in avoiding a massive drop in the hardness of tempered specimens. This suggests that regular cryogenic treatment has enough leverage in retaining the hardness in the tempered condition. Thus, hardness results confirm the advantage of regular cryogenic treatment for EN8.
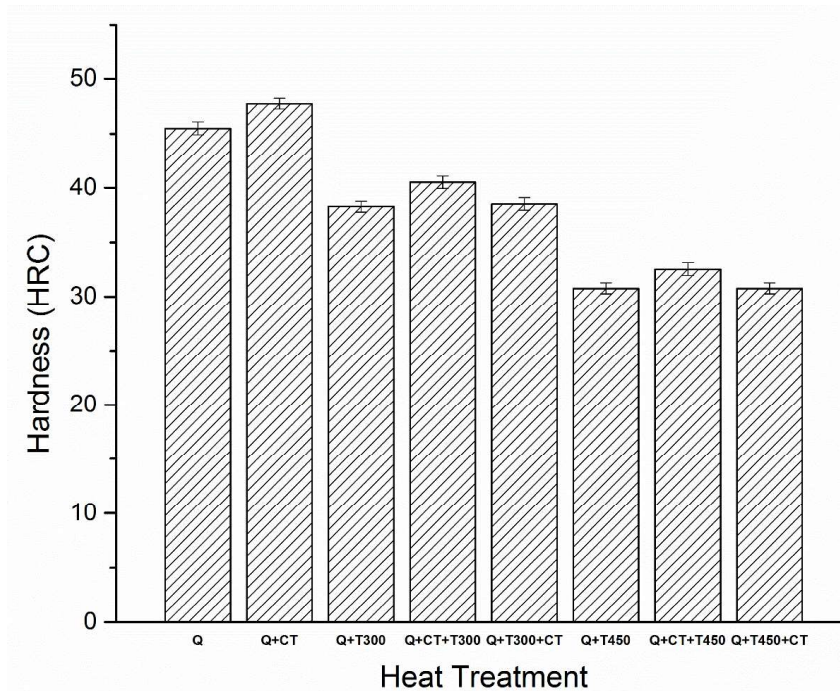
Fig. 6.1 Bar-Chart showing hardness variations of EN8 after various heat treatment steps.

6.1.3 Tensile Test

Engineering Stress-Strain curves of EN8 after key heat treatment steps are presented in Fig. 6.2 and vital quantitative data obtained from the tensile tests is summarized in Table 6.3.

As expected, annealed specimens show the lowest strength and highest ductility among the heat-treated specimens. The elongation recorded for annealed EN8 is 23% suggesting the ductile nature of EN8 in the annealed condition. The yield ratio (yield strength/ultimate tensile strength) observed for annealed specimens is 0.58. However, yield ratio obtained for all other specimens is above 0.9. This confirms that both annealing and tempering treatments are carried out properly (Bannister et al. 2000).

Tensile behavior of tempered EN8 steel is comparatively presented in Fig. 6.3. This clearly indicates that cryogenic treatment performed in-between quenching and tempering (Q+CT+T450) shows significantly increased strength and ductility as compared to both conventional heat treatment (Q+T450) and unusual cryogenic treatment carried out after tempering (Q+T450+CT). It is important to note that there is a considerable increase in both the strength and the ductility, the toughness should also improve when EN8 is subjected to regular cryogenic treatment.
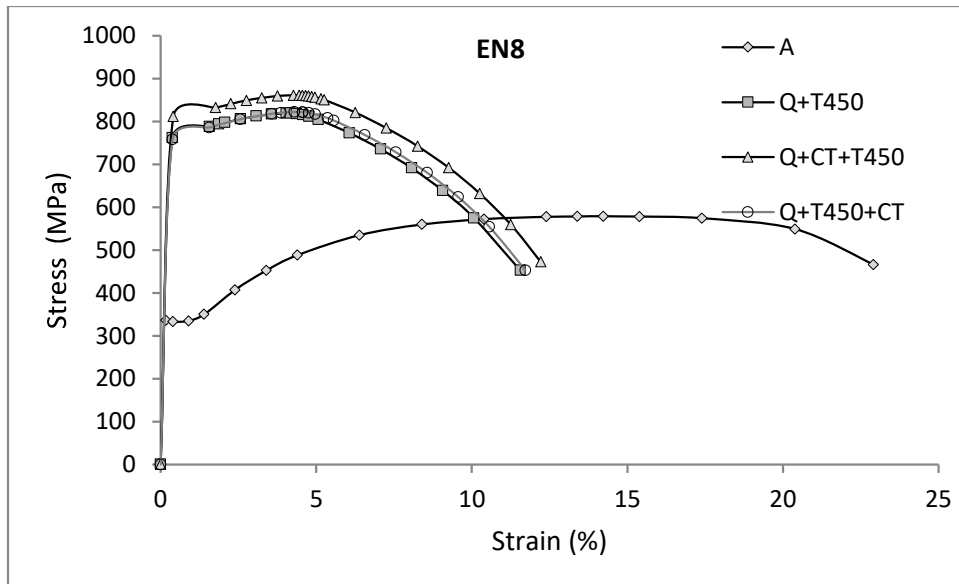
Fig. 6.2. Engineering Stress-Strain curves of EN8 for key heat-treatment cycles.

Table 6.3. Tensile properties of EN8.

Heat treatment	YS (MPa)	UTS (MPa)	Elongation (%)	Reduction (%)	Yield Ratio	Toughness (MJ/m^3)
A	335	578	23	18.7	0.58	132.94
Q+T450	761	818	11.56	10.36	0.93	94.56
Q + CT + T450	811	865	12.22	10.89	0.94	105.70
Q +T450 + CT	760	822	11.73	10.5	0.92	96.42
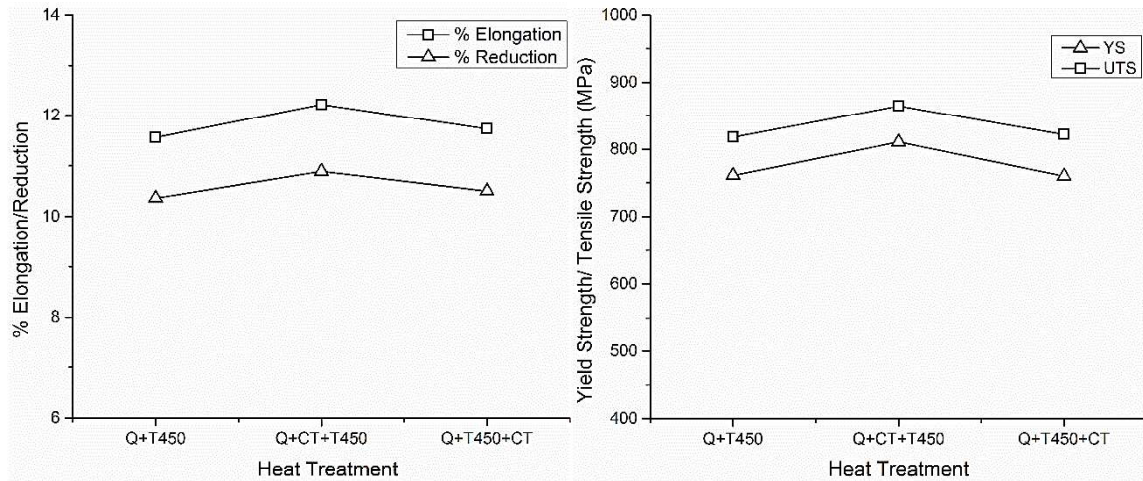
Fig. 6.3. Variation in the key tensile properties of tempered EN8 as a function of heat treatment cycles.

6.1.4 Microstructural Analysis

Microstructure of EN8 in annealed condition is shown in Fig. 6.4. The carbon equivalent of EN8 being 0.4%, as expected, the microstructure shows pearlitic and ferritic grains in almost equal fractions. Thus, the microstructure of the experimental specimen conforms to EN8 grade.

Microstructures of as-quenched, and quenched and cryogenic treated EN8 specimens are presented comparatively in Fig. 6.5. Visual comparison indicates that as-quenched coarse martensitic microstructure is transformed into fine and uniformly distributed martensite in the cryogenic treated specimen. This suggests that at least a fraction of the retained austenite in the as-quenched specimen is transformed into fine martensite during the cryogenic exposure.
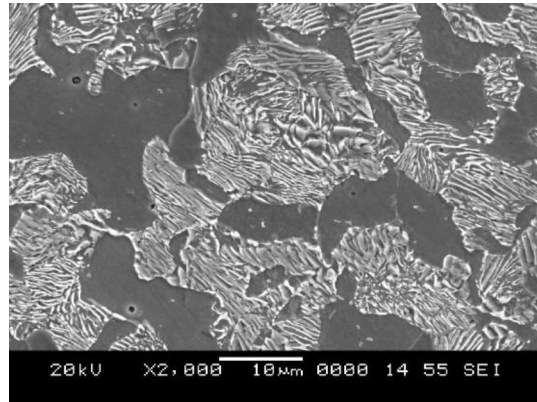
Fig. 6.4. Microstructure of the annealed EN8 specimen.
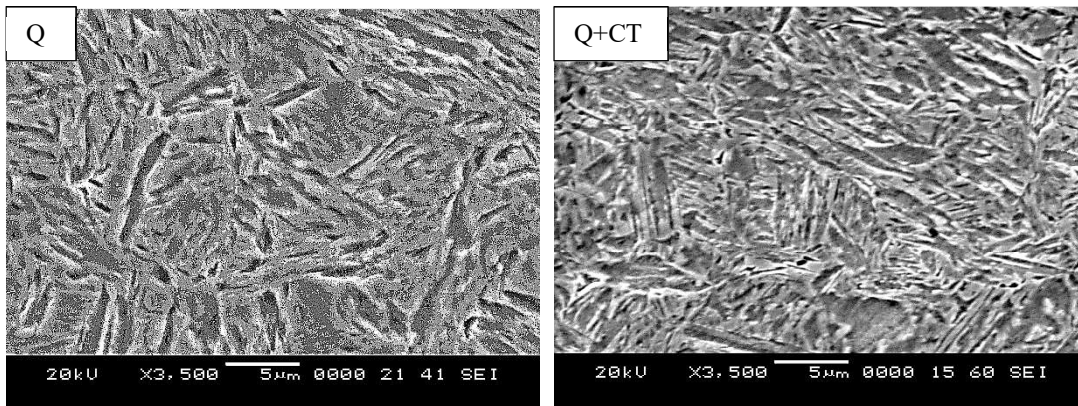
Fig. 6.5. SEM images of as-quenched and cryogenic treated microstructures of EN8.
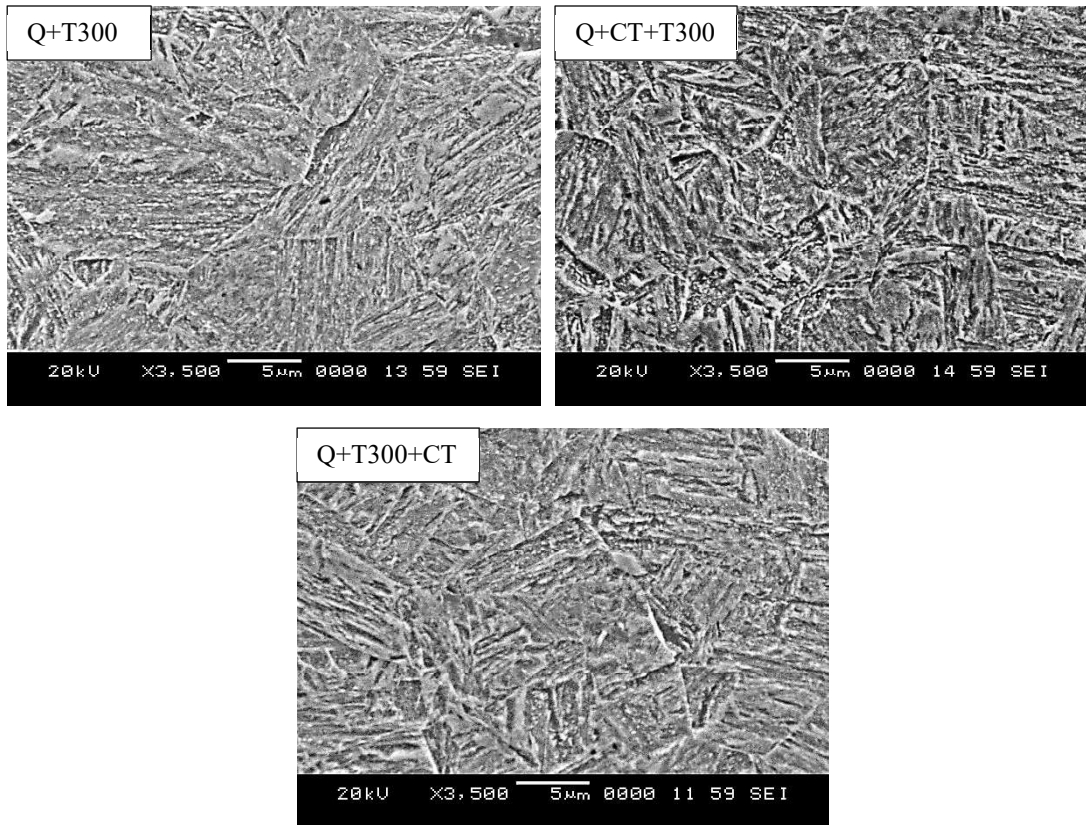
Fig. 6.6. SEM images of EN8 after different heat treatment cycles with tempering temperature of 300 °C, involving cryogenic treatment at different stages.
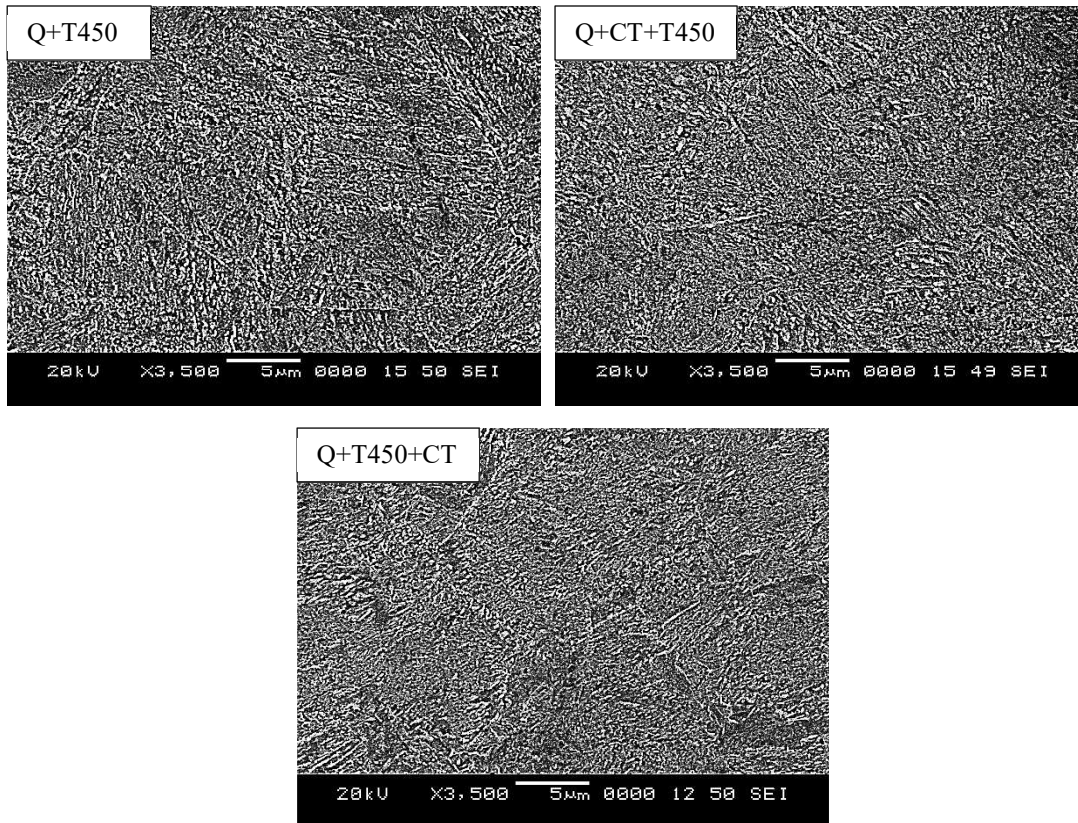
Fig. 6.7. SEM images of EN8 after different heat treatment cycles with tempering temperature of 450 °C, involving cryogenic treatment at different stages.

Microstructures of 300 °C and 450 °C tempered specimens are shown in Fig. 6.6 and 6.7 respectively. As shown in Fig. 6.6 microstructural difference between these tempered specimens is subtle as the 300°C-tempered specimens show reminiscence of coarse martensitic colonies. However, by visual comparison, cryogenic treatment carried out in-between quenching and tempering (Q+CT+T300) shows slightly finer and more uniformly distributed tempered martensitic structure as compared to other two specimens.

This microstructure refinement is more pronounced in 450 °C-tempered specimens as they show completely tempered features with fine carbides distributed uniformly in ferritic matrix. As shown comparatively in Fig. 6.7, tempering carried out after cryogenic treatment (Q+CT+T450) gives rise to the finest and the most uniform microstructure.

6.1.5 Fractography

Fractographic features of key tensile test specimens as studied using an SEM are presented in Fig 6.8. All these specimens show dimples indicating ductile mode of fracture. However, Q+CT+T450 specimen shows finer and more uniformly distributed dimples as compared to the other two specimens. Fine and uniformly distributed dimples in Q+CT+T450 specimen suggest that regular cryogenic treatment improves the ductility of EN8 as indicated by the tensile test data.

6.1.6 Summary of Results

Results of hardness test, tensile test, microstructural analysis and fractography as presented in this section suggest that pre-tempering cryogenic treatment is quite effective in improving the mechanical properties of EN8. However, post-tempering cryogenic treatment is not effective.
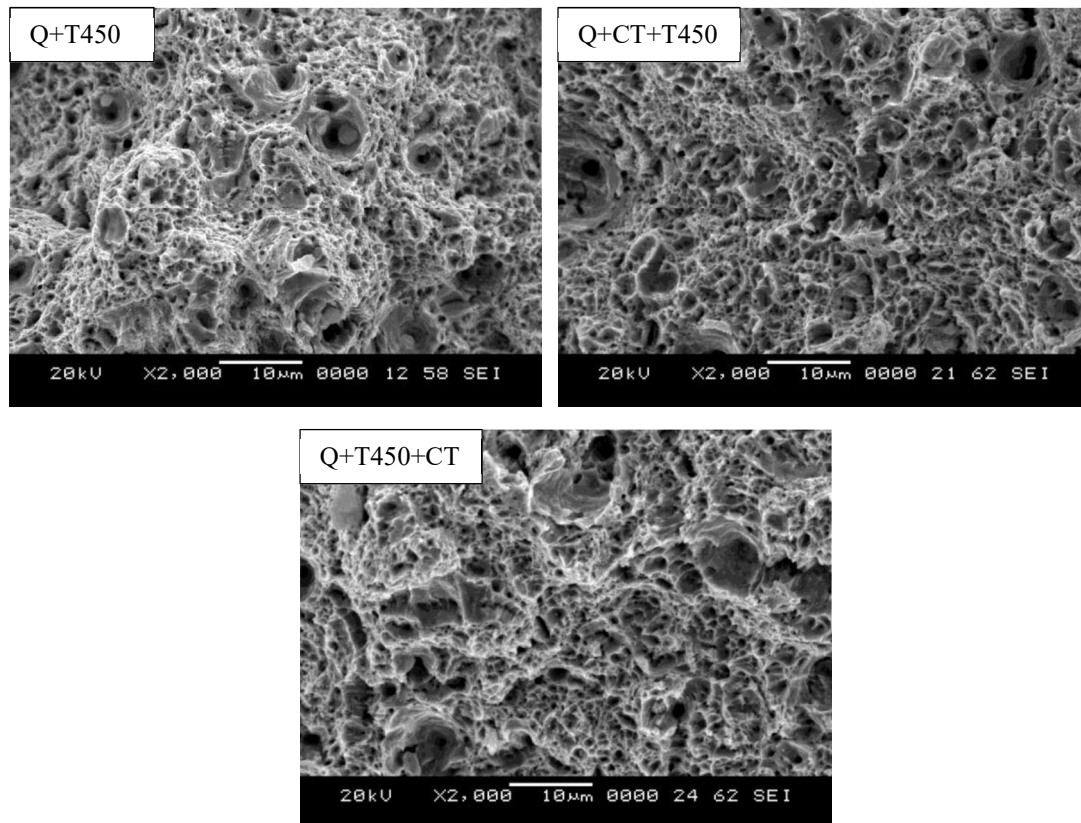
Fig. 6.8. Fractographic images of 450 °C tempered EN8 tensile specimens.

6.2 Results of EN18 Steel

6.2.1 Chemical composition

Table 6.4 shows the chemical composition of the EN18 steel bars against the materials specification obtained through spark emission spectroscopy. The measured composition of the steel bars agrees well with the standard specification confirming that the experimental material used for the heat -treatment experiments is a medium carbon steel, EN18.

Table 6.4. Measured chemical composition (wt. %) of steel bars against EN18 specification.

	C	Mn	Si	Ni	Cr	Mo	S	P	Fe
EN18 Spec.	0.35-0.45	0.6-1.0	0.10-0.35	-	0.85-1.15	-	0.04 max	0.04 max	Balance
Measured	0.39	0.75	0.27	-	1.10	-	0.03	0.04	Balance

6.2.2 Hardness Measurement

Figure 6.9 provides the hardness variations in EN18 steel following various heat treatment steps. Upon quenching, EN18 attains the hardness of 50 HRC. However, the hardness increases to 53 HRC when the as-quenched samples are subjected to cryogenic treatment, indicating that EN18 grade responds well to the cryogenic treatment. Similar to EN8, cryogenic treatment carried out after tempering does not show any measurable increase in the hardness of EN18.

When tempering is followed after the conventional hardening step, the hardness drops with the increase in tempering temperature. The hardness observed for tempering at 300 °C is 46 HRC and further drops to 42 HRC for the tempering temperature of 450 °C. However, it is observed that by implementing cryogenic treatment as an intermediate step between quenching and tempering, the hardness increases at about 1 HRC for both the tempering temperatures. Even though EN18 has 1 % chromium, addition of chromium, being ferrite stabilizer has very less capability in producing retained austenite in the as-quenched condition. Hence, the improvements observed after implementing cryogenic treatment are marginal.
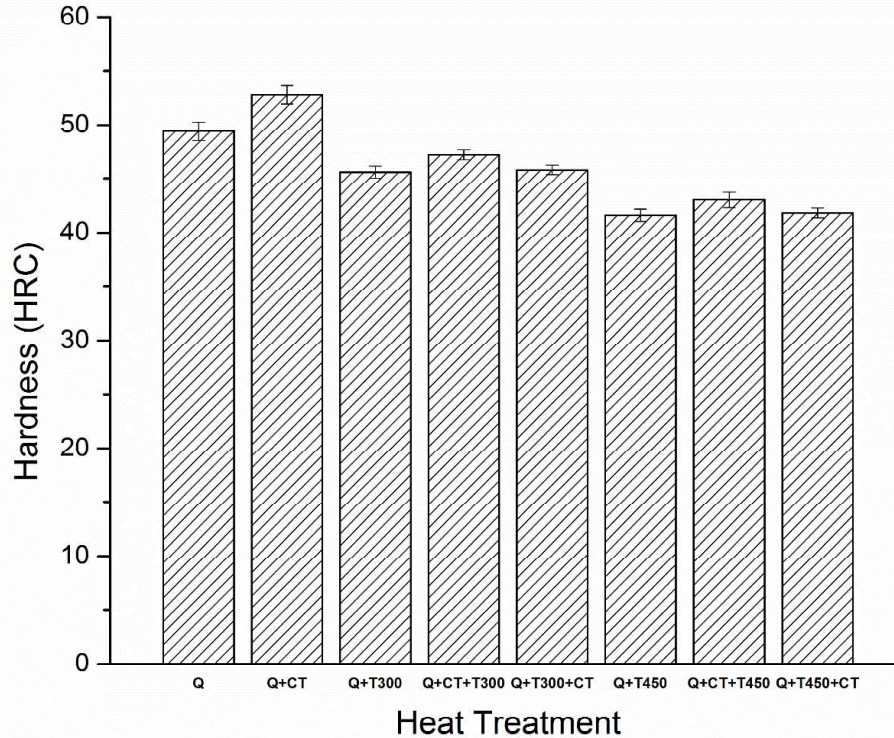
Fig. 6.9 Bar-chart showing hardness variations of EN18 after various heat treatment steps.

6.2.3 Tensile Test

Engineering Stress-Strain curves of EN18 after key heat treatment steps are presented in Fig. 6.10 and critical quantitative data obtained from the tensile tests are summarized in Table 6.5. Figure 6.11 provides the variation in the tensile properties against the heat treatment.

As shown in stress-strain graph, annealed specimens (A) of EN18 possess lowest strength (628 MPa) and highest ductility (20.16%), and that, hardened and tempered (Q+T450) specimens show significantly increased strength and decreased ductility than the annealed specimens. It is observed that Q+CT+T450 specimen shows better strength in comparison to Q+T450 and Q+T450+CT. Increase in strength is attributed to transformation of retained austenite into martensite during cryogenic treatment. However, it is to be noted that

cryogenic treatment followed after conventional heat treatment does not produce any significant amount of increased strength. The changes observed in stress-strain curves of tempered/cryogenic treated specimens of EN18 are quite marginal suggesting that the variation in the strength and ductility of EN18 due to cryogenic treatment is rather subtle.

Table 6.5 Tensile properties of EN18.

Heat treatment	YS (MPa)	UTS (MPa)	Elongation (%)	Reduction (%)	Yield Ratio	Toughness (MJ/m^3)
A	340	628	20.16	16.8	0.54	126.6
Q+T450	1111	1191	9.97	9.06	0.93	118.74
Q + CT + T450	1170	1238	9.5	8.7	0.95	117.61
Q +T450 + CT	1148	1210	9.9	9.0	0.95	119.79
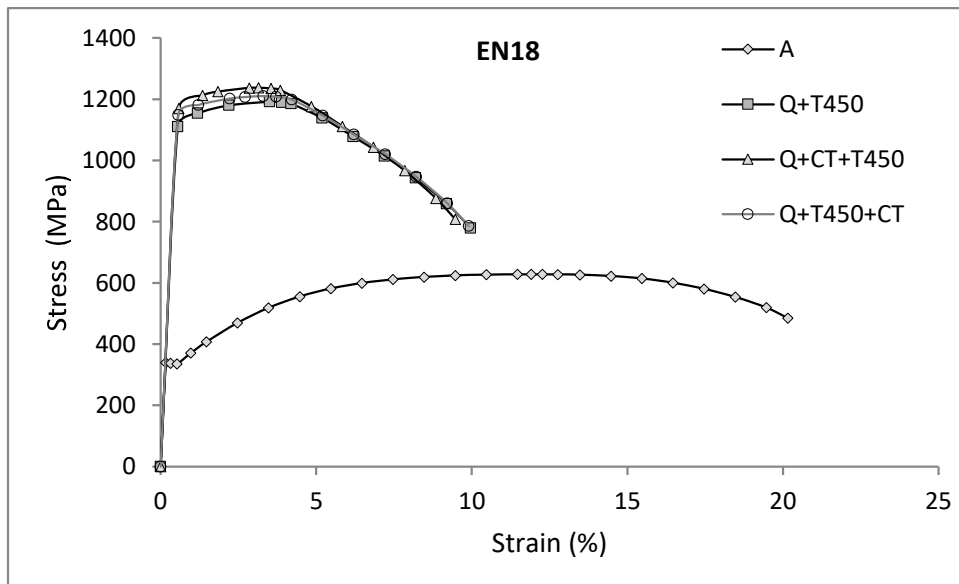
Fig. 6.10. Engineering Stress-Strain curves of EN18 for key heat treatment cycles.

80
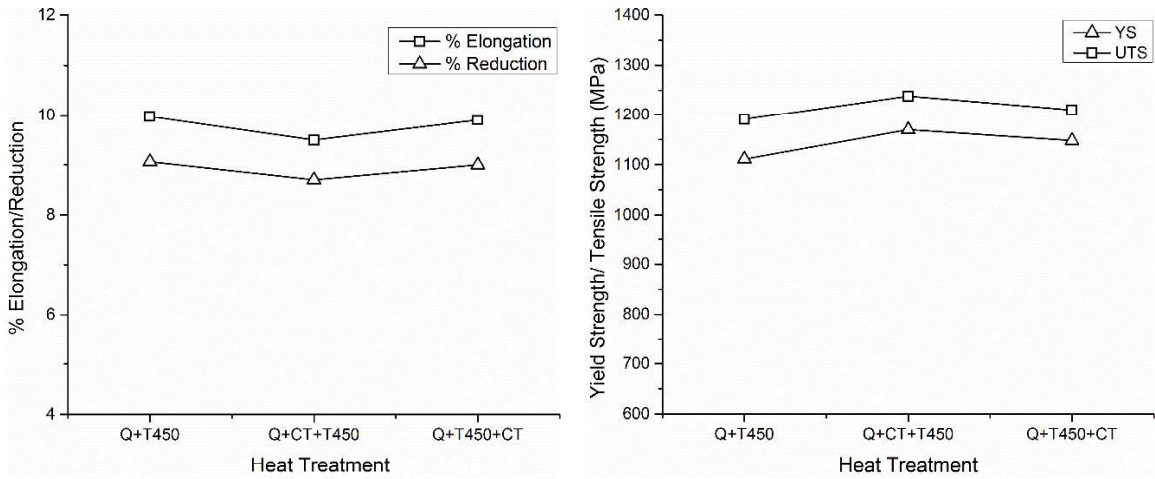
Fig. 6.11 Variation in the key tensile properties of tempered EN18 as a function of heat treatment cycles.

6.2.4 Microstructural Analysis

Figure 6.12 shows the microstructure of EN18 in the annealed condition depicting the pearlite and ferrite phases. Even though the carbon percentage in EN18 is only 0.4, addition of chromium (1%) acts as the carbon equivalent and increases the pearlite percentage in the annealed microstructure.
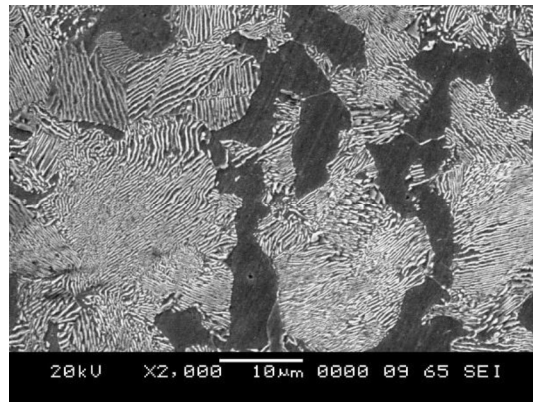
Fig. 6.12. Microstructure of EN18 steel in annealed condition.
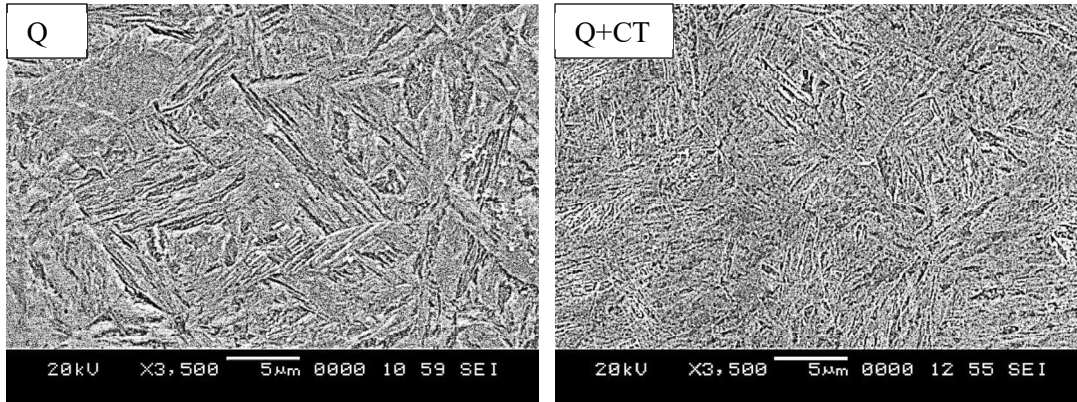
Fig. 6.13. SEM images showing as quenched and cryogenic treated microstructures of EN18.
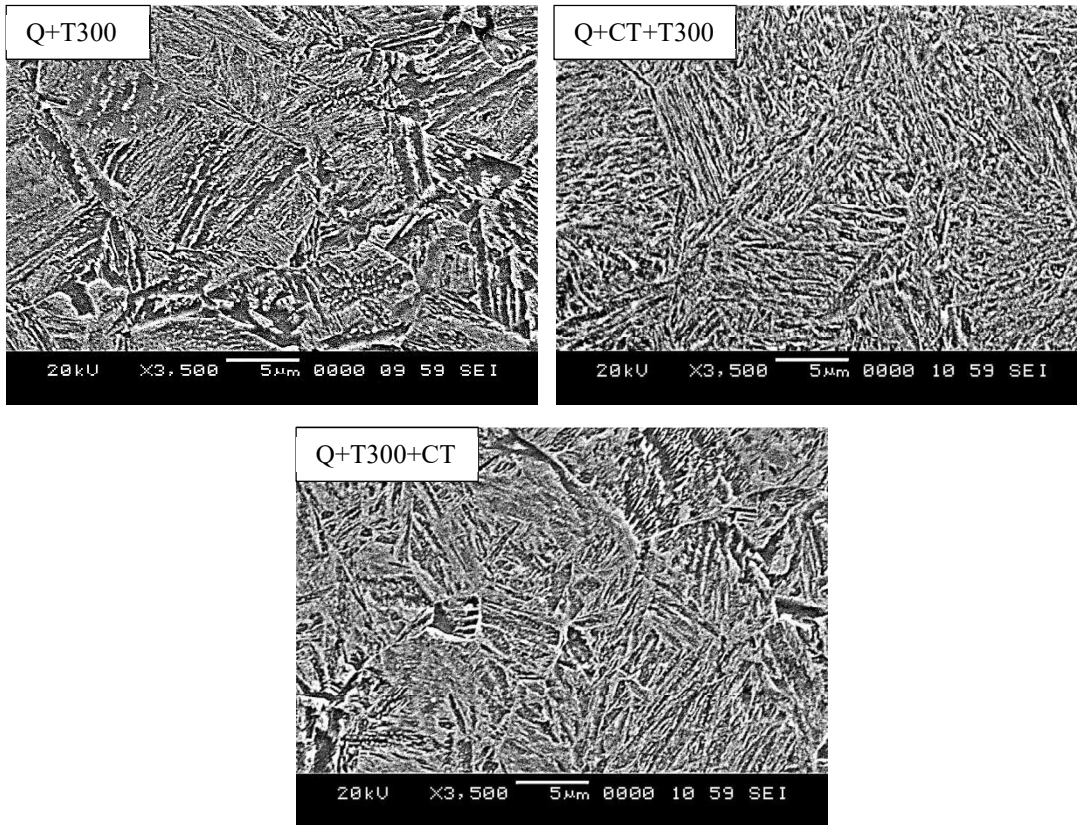
Fig. 6.14. SEM images of 300 °C tempered EN18 specimens.

As shown in Fig. 6.13, as-quenched EN18 specimen (Q) shows coarse Martensite colonies oriented randomly and that it is difficult to discern Martensite and Retained Austenite phases in the microstructure. However, Martensite colonies are dense, fine, and uniformly

distributed in the microstructure of quenched and cryogenic treated specimen (Q+CT). This difference in the microstructures suggests that the retained austenite distributed between the coarse martensitic plates/laths in as-quenched specimen transforms into fine Martensite during the cryogenic treatment. This explains the improvement of mechanical properties of EN18, when subjected to cryogenic treatment.

Formation of coarse Martensite during oil quenching of EN18 is further confirmed from the microstructure of hardened and tempered specimen (Q+T300) when compared to the specimens that are subjected to cryogenic treatment before or after tempering (Q+CT+T300 or Q+T300+CT). Microstructural results of EN18 confirm that cryogenic treatment helps in making the microstructure finer, denser, and more uniform (Fig. 6.14).
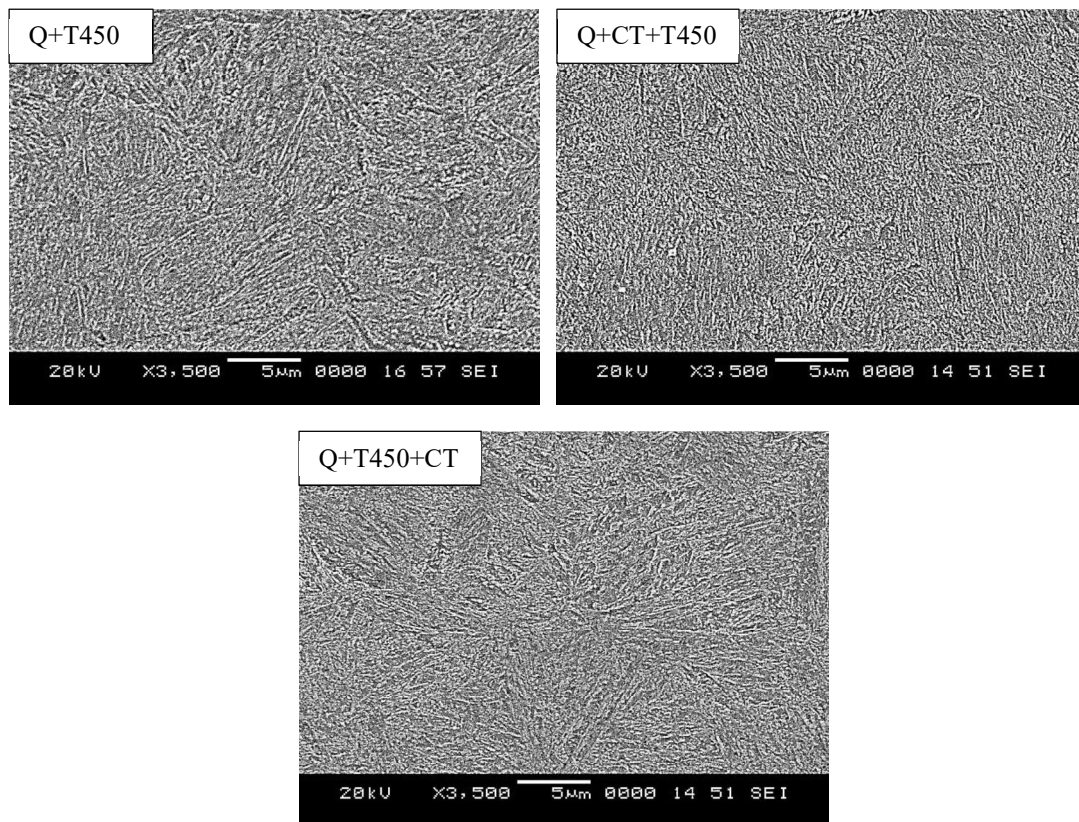
Fig. 6.15. SEM images of 450 °C tempered EN18 specimens.

Compared to heat treatment cycles involving tempering temperature of 300 °C, specimens subjected to tempering temperature of 450 °C show fine, tempered martensitic structure. Tempering at 450 °C helps in attaining the toughness at the expense of drop in hardness. As shown in Fig. 6.15, specimen involving Q+CT+T450 shows more homogeneity and denser martensite in the microstructure, demonstrating conversion of retained austenite into martensite during cryogenic treatment.

6.2.5 Fractography

Fractography images of the tensile specimens subjected to Q+T450, Q+CT+T450 and Q+T450+CT are shown in Fig. 6.16. All the specimens show dimples as the main highlighting feature, indicating ductile mode of fracture. Presence of no cleavages in the Q+CT+T450 indicate that cryogenic treatment is not inducing brittleness with the increase in hardness.
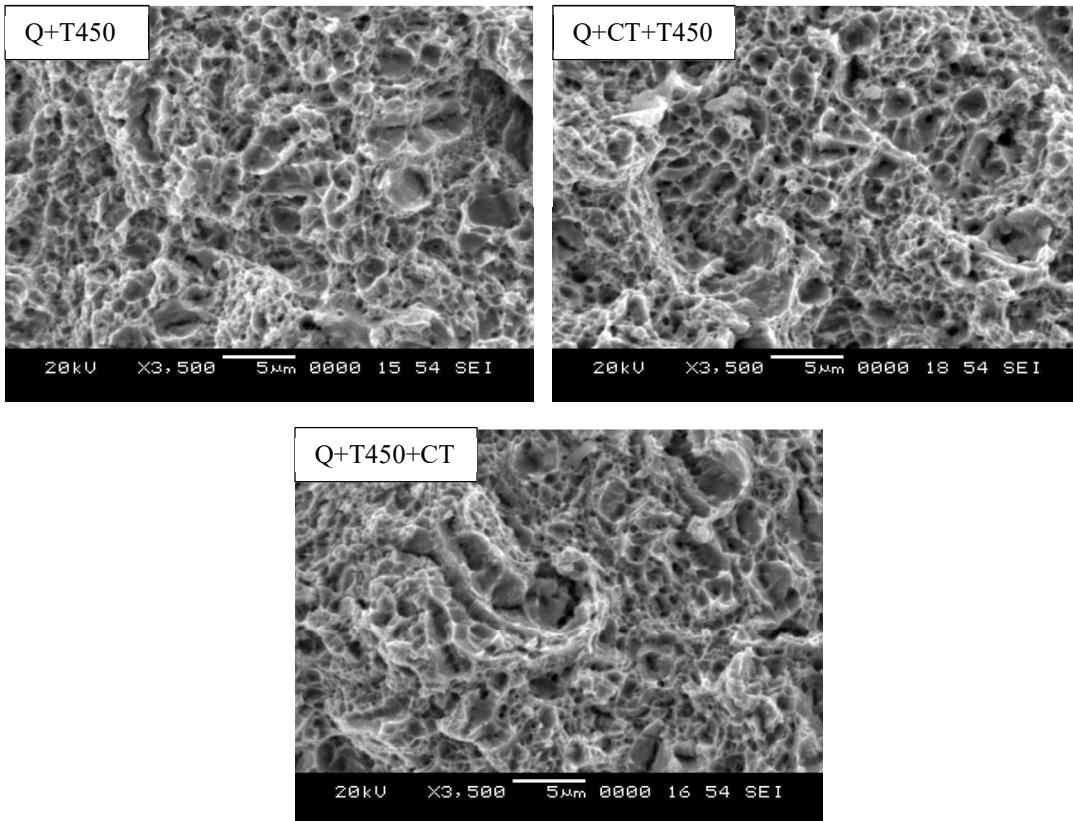
Fig. 6.16. Fractographs of 450 °C tempered tensile specimens of EN18.

6.2.6 Summary

Results of hardness test, tensile test, microstructural analysis and fractography as presented in this section suggest that pre-tempering cryogenic treatment is effective in improving the mechanical properties of EN18 whereas post-tempering cryogenic treatment is not effective.

6.3 Results of EN47 Steel

6.3.1 Chemical Composition

The result of the spark emission spectroscopy for EN47 bars is shown in Table 6.6 against the materials specification. The measured composition of the steel bars conforms to the standard specification confirming that the experimental material used for the heat-treatment experiments is indeed medium carbon steel, EN47.

Table 6.6. Measured chemical composition (wt. %) of steel bars against EN47 specification.

	C	Mn	Si	Ni	Cr	Mo	S	P	Fe
EN47 Spec.	0.45-0.55	0.5-0.8	0.10-0.35	-	0.80-1.20	-	0.04 max	0.04 max	Balance
Measured	0.49	0.65	0.33	-	1.01	-	0.04	0.04	Balance

6.3.2 Hardness Measurement

Fig. 6.17 provides the hardness variations in EN47 steel following various heat treatment steps. With slightly higher carbon percentage and chromium as an additional alloying element, EN47 offers more hardenability as compared to EN18. Having 54 HRC in the as-quenched condition, hardness of EN47 increased to 57 HRC when the as-quenched specimen was subjected to cryogenic treatment. Among 300 °C tempered specimens of EN47, conventionally quenched and tempered (Q+T300) specimen shows lowest hardness, Q+T300+CT specimen shows higher hardness, and Q+CT+T300 specimen shows the highest hardness. This trend is consistent for 450°C-tempered specimens as well. Hardness results of EN47 confirm that cryogenic treatment increases the hardness of both as-

quenched and as-tempered specimens. However, highest hardness is achieved when cryogenic treatment is applied as an intermediate step between quenching and tempering steps.
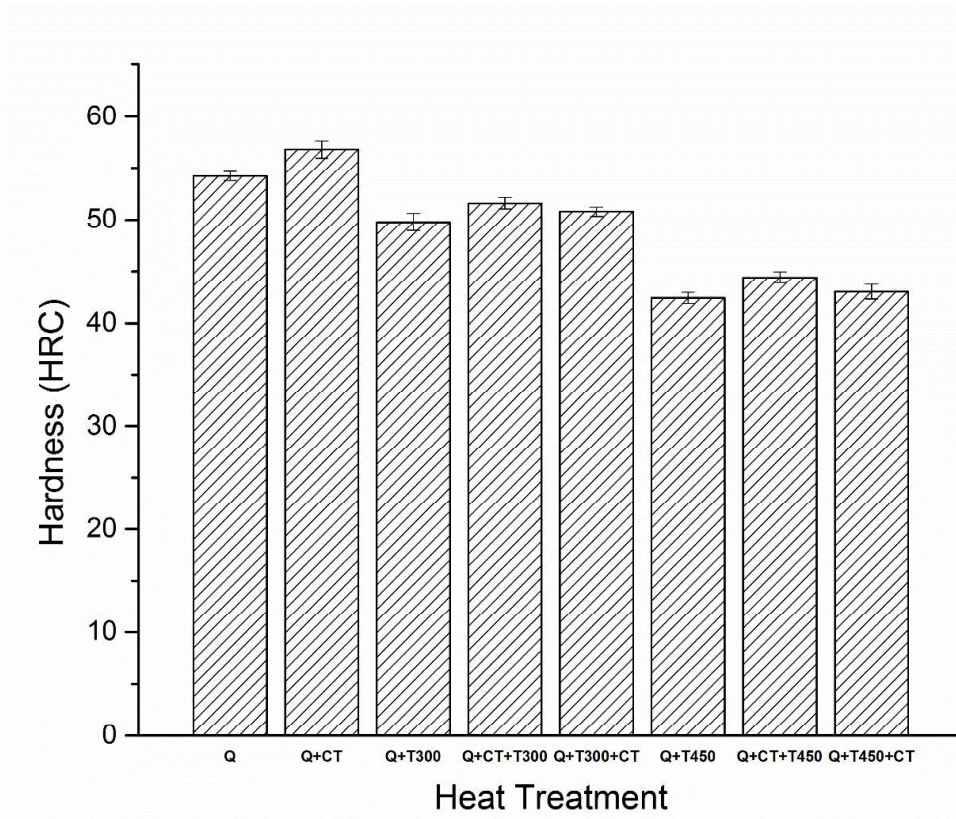
Fig. 6.17. Bar-chart showing hardness variations of EN47 after various heat treatment steps.

6.3.3 Tensile Test

Engineering Stress-Strain curves of EN47 after various heat treatment cycles are shown in Fig. 6.18. Tensile properties of EN47 after the heat treatment cycles are listed quantitatively in Table 6.7. Variations in the strength and ductility of EN47 as a function of heat treatment cycles are shown in Fig. 6.19.

In comparison to EN18, EN47 has slightly higher carbon content and hence the yield strength and tensile strength of the EN47 are slightly higher than the EN18 grade. However, the improvement observed is quite marginal similar to EN18. It is observed that specimen subjected to cryogenic treatment as an intermediate step between quenching and tempering shows slightly higher strength (50 MPa) in comparison to conventional heat treatment (Q+T450). As EN47 does not possess any major allowing additions other than 1 % Chromium, effect of cryogenic treatment is minimal in improving the mechanical properties. However, it can be stated that cryogenic treatment carried out before tempering produces better mechanical properties in comparison to conventional tempering and tempering carried out after cryogenic treatment.
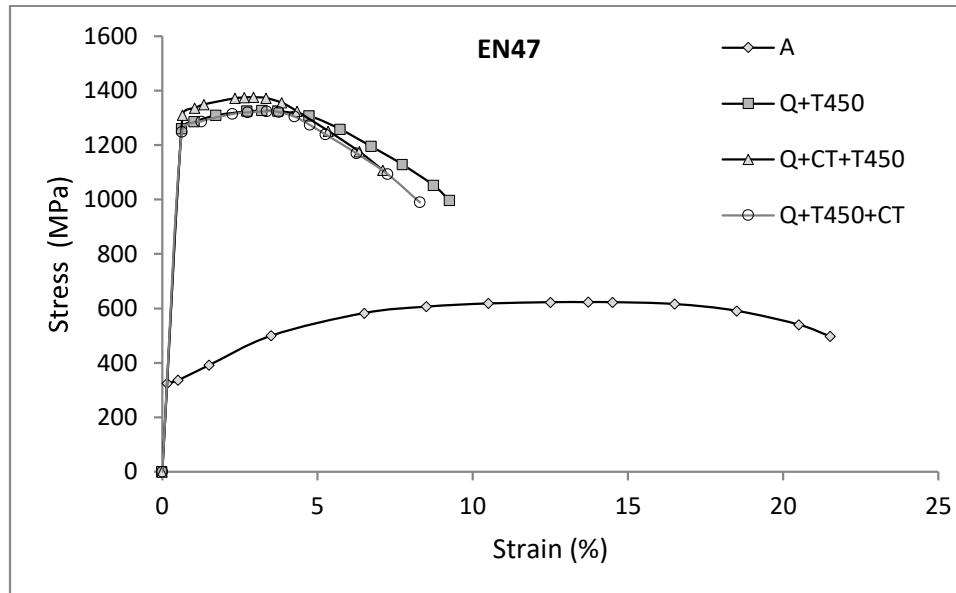
Fig. 6.18. Engineering Stress-Strain curves of EN47 for key heat treatment cycles.
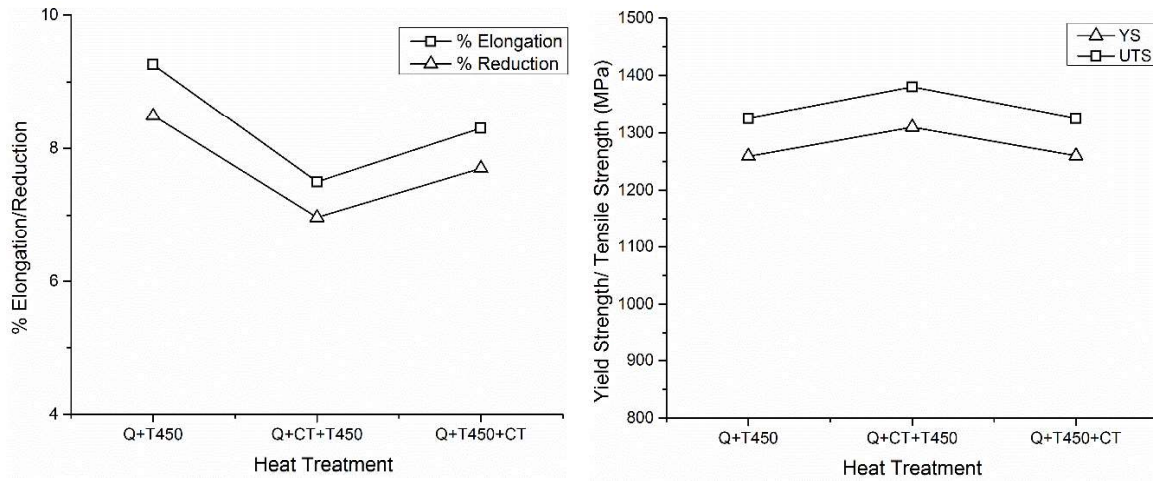
Fig. 6.19 Variation in the key tensile properties of tempered EN47 as a function of heat treatment cycles.

Table 6.7 Tensile properties of EN47.

Heat Treatment	YS (MPa)	UTS (MPa)	Elongation (%)	Reduction (%)	Yield Ratio	Toughness (MJ/m^3)
A	325	623	21.51	17.7	0.52	134.
Q+T450	1259	1325	9.26	8.49	0.95	122.7
Q + CT + T450	1310	1380	7.5	6.97	0.95	103.5
Q +T450 + CT	1260	1325	8.3	7.7	0.95	109.97

6.3.4 Microstructural Analysis

Figure 6.20 shows microstructure of EN47 showing pearlite and ferrite phases, indicating annealed microstructure of EN47. As shown in Fig. 6.21, cryogenic treated sample shows fine and uniform microstructure as compared to the coarse martensitic structure in the as-quenched sample. Along with fine martensitic microstructure, there is also uniform distribution of carbides as compared to the randomly distributed carbides in the as quenched conditions.
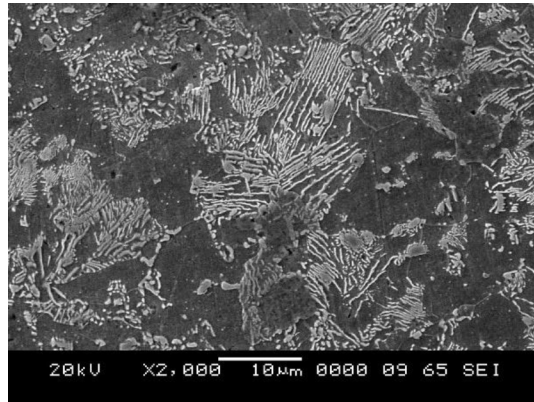
Fig. 6.20. Microstructure of EN47 steel in annealed condition.
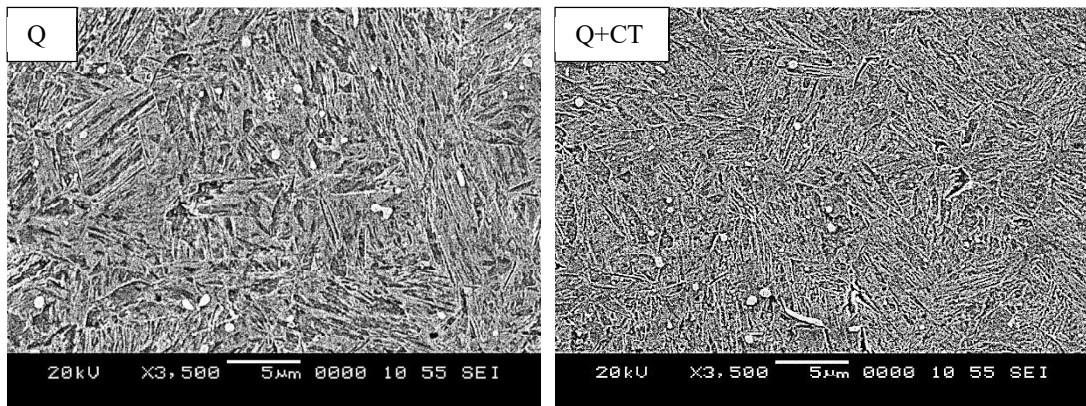
Fig. 6.21. SEM images showing as quenched and cryogenic treated microstructures of EN47.
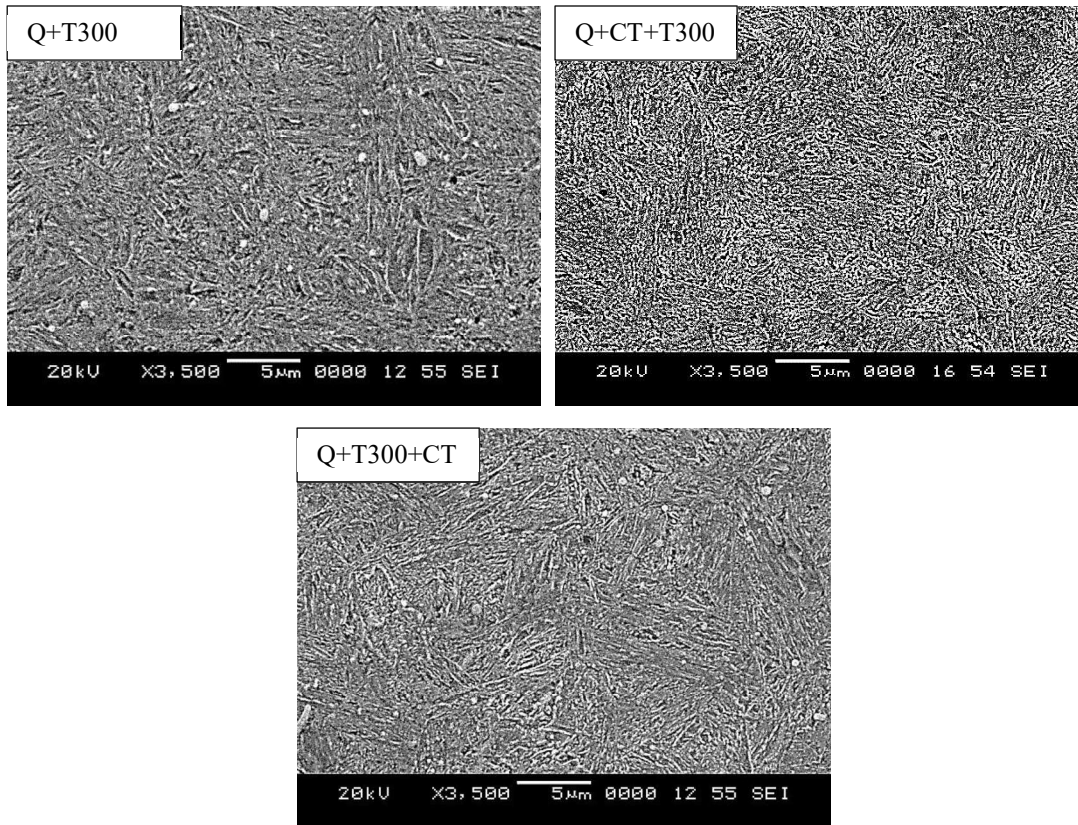
Fig. 6.22. SEM images of 300 °C tempered EN47 specimens.

With tempering temperature of 300 °C, cryogenic treatment carried out in between quenching and tempering produces more uniform martensite as compared to the conventional heat treatment and cryogenic treatment carried out after tempering (Fig. 6.22). Though carbide precipitation is observed in the all heat treatment cycles (Fig. 6.23) invoving tempering temperature of 450 °C, no significant changes are observed in the microstructures. However, incorporation of cryogenic treatment in between quenching and tempering shows homogenized and fine microstructure in comparion to other two heat treatment cycles.
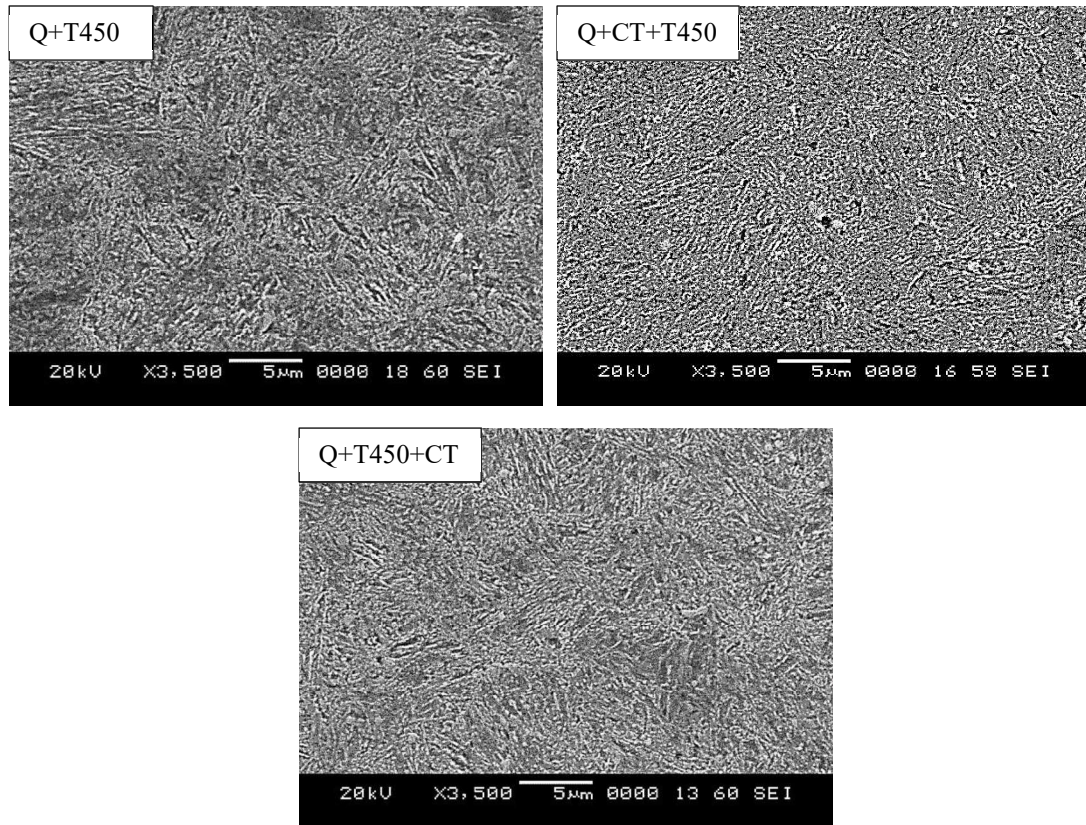
Fig. 6.23. SEM images of 450 °C tempered EN47 specimens.

It is interesting to note that there is a marginal increase (1–2 HRC) in the hardness when conventionally hardened and tempered specimens are subjected to CT. This behavior suggests that there must be some phase transformation happening even when tempered steel is exposed to the cryogenic temperature. It is likely that the retained austenite formed during quenching does not completely transform or decompose during tempering. The residual retained austenite present in the tempered specimen might have transformed into martensite during post-tempering CT.

6.3.5 Fractography

Even though all the fractography images shown in Fig. 6.24 show dimples, indicating ductile mode of fracture, the size and distribution of dimples differentiate the different heat treatments. Both Q+T450 and Q+T450+CT show larger sized dimples as compared to Q+CT+T450. In comparison, Q+T450+CT shows bigger dimples than the conventional

heat treatment. Q+CT+T450, being the optimal heat treatment shows fine and uniform distribution of dimples indicating increased toughness.

6.3.6 Summary

Results of hardness tests, tensile tests, and microstructural analysis confirm that EN47 steel responds positively to the cryogenic treatment. However, the cryogenic treatment applied as an intermediate step between quenching and tempering is more effective than the unusual post-tempering cryogenic treatment.
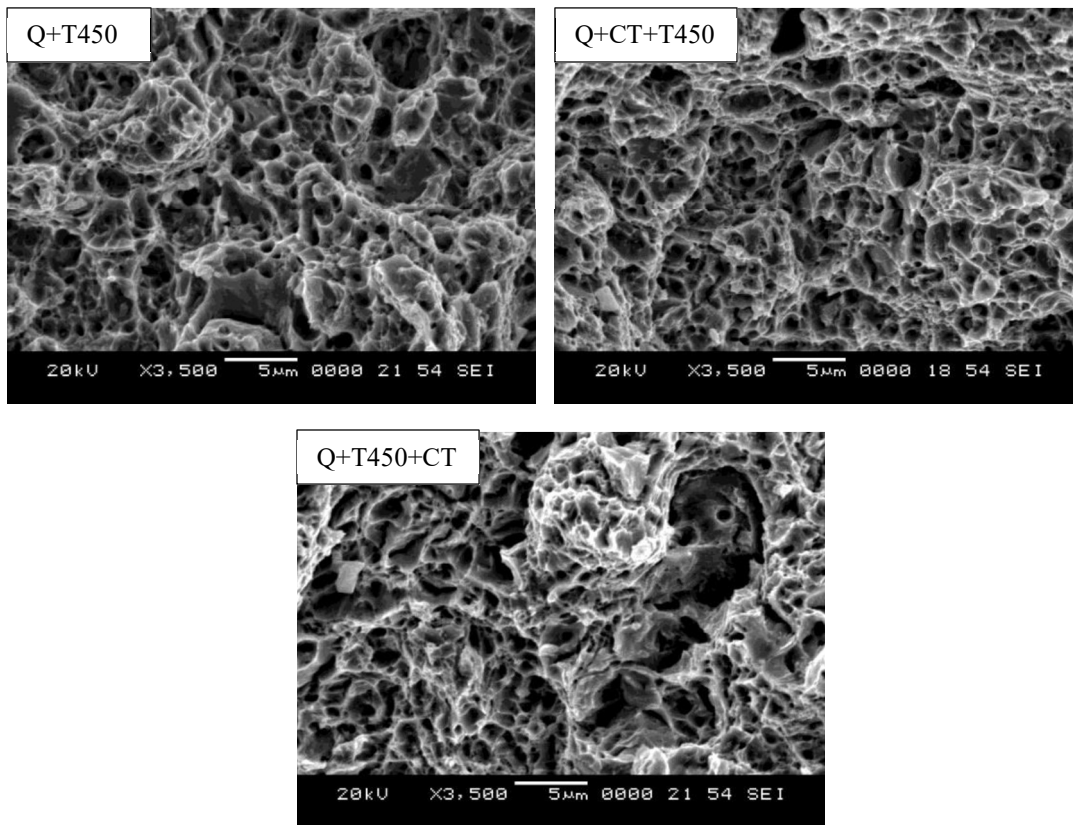
Fig. 6.24. Fractographs of 450 °C tempered tensile specimens of EN47.

6.4 Results of EN24 Steel

6.4.1 Chemical composition

Table 6.8 shows the chemical composition of EN24 steel bars against the standard specifications of EN24 grade. It is observed that the measured chemical composition through spark emission spectroscopy matches well with the standard specifications and the experimental material used for the heat treatment experiments is indeed medium carbon low alloy steel, EN24.

Table 6.8. Measured chemical composition (wt. %) of steel bars against EN24 specification.

	C	Mn	Si	Ni	Cr	Mo	S	P	Fe
EN24 Spec.	0.36-0.44	0.45-0.70	0.10-0.35	1.30-1.70	1.00-1.40	0.20-0.35	0.04 max	0.04 max	Balance
Measured	0.37	0.79	0.32	1.56	1.12	0.20	0.03	0.04	Balance

6.4.2 Hardness Measurement

Figure 6.25 shows the hardness variations of EN24 with respect to various heat treatment cycles in the bar chart form. EN24 specimens achieve the hardness of 50 HRC after subjecting to conventional hardening process. However, the hardness increases from 50 to 54 HRC when as quenched samples are subjected to cryogenic treatment. This proves that EN24 responds very well to the cryogenic treatment. As tempering improves the toughness with a drop in hardness values, it is observed that hardness drops to 44 and 38 HRC after subjecting to conventional tempering of 300 °C and 450 °C, respectively. However, significant gain can be achieved if cryogenic treatment is added as an additional step right after quenching, as the hardness improves by 2 to 3 units for both the tempering cycles. In addition, when cryogenic treatment is carried out after conventional tempering process minor increase in hardness, about 1 unit, is also observed. This indicates that cryogenic treatment carried out before tempering suits well for EN24 in increasing the hardness irrespective of tempering temperature.
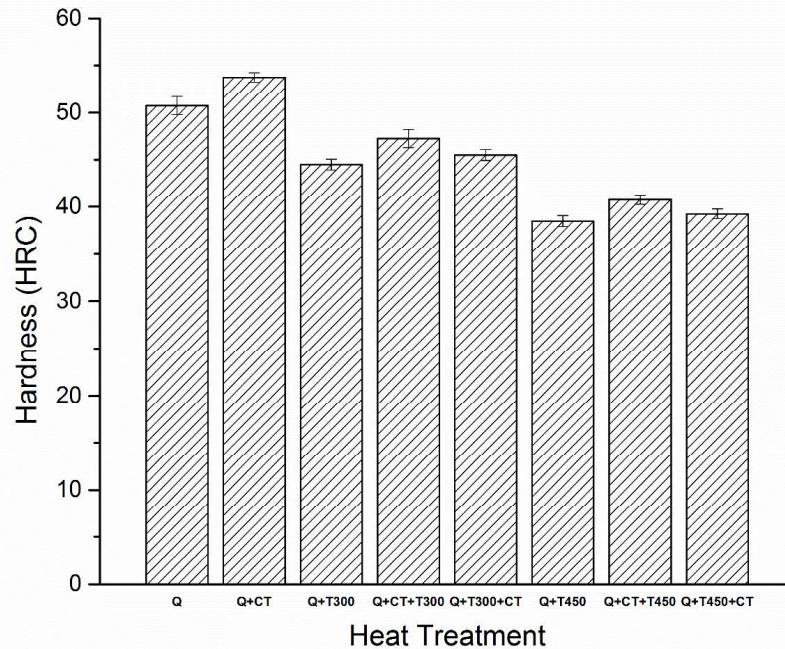
Fig. 6.25. Bar-chart showing hardness variations of EN24 after various heat treatment steps.

6.4.3 Tensile Test

Engineering Stress-Strain curves of EN24 after various heat treatment cycles are shown in Fig. 6.26. Tensile properties of EN24 after the heat treatment cycles are listed quantitatively in Table 6.9 and variations in strength and ductility of EN24 as a function of heat treatment cycles are shown in Fig. 6.27.

The stress-strain curves convincingly show that cryogenic treatment carried out before tempering (Q+CT+T450) imparts superior properties to EN24 as compared to the cryogenic treatment carried out after tempering step (Q+T450+CT). The tensile behaviour also confirms that inclusion of cryogenic exposure provides substantial advantage over traditional hardening and tempering heat treatment process for EN24. It can be stated that mechanical properties of EN24 steel can be significantly improved by applying proper sequence of cryogenic treatment (Q+CT+T). However, it is to be noted that cryogenic treatment carried after tempering results drastic drop in toughness of EN24, indicating that cryogenic treatment should not be carried out after tempering on EN24.

94
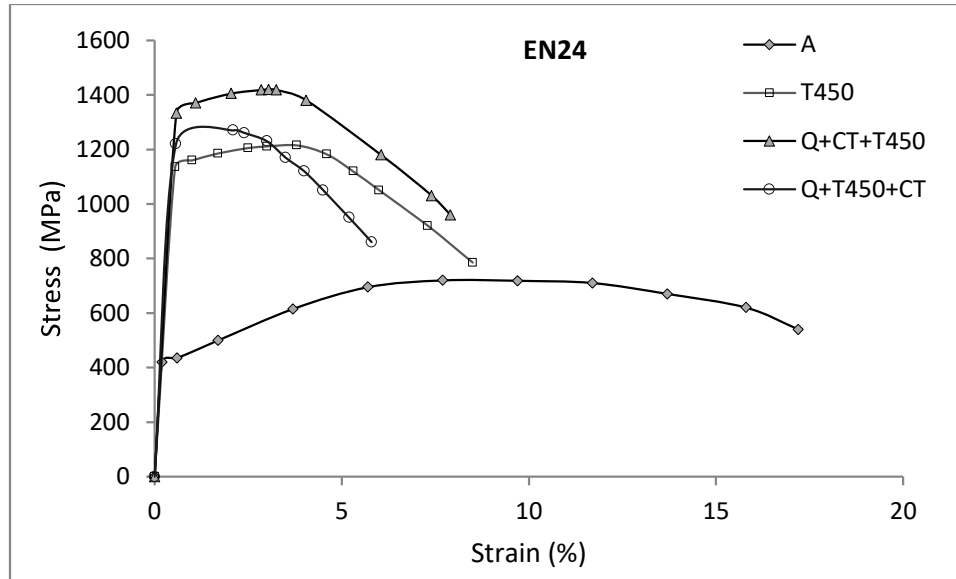
Fig. 6.26 Engineering Stress-Strain curves of EN24 for key heat treatment cycles.

Table 6.9. Tensile properties of EN24.

Heat treatment	YS (MPa)	UTS (MPa)	Elongation (%)	Reduction (%)	Yield Ratio	Toughness (MJ/m^3)
A	410	720	17.2	24.22	0.57	123.84
Q+T450	1135	1215	8.5	7.8	0.93	103.27
Q + CT + T450	1333	1420	7.9	7.3	0.94	112.18
Q +T450 + CT	1220	1270	5.8	5.48	0.96	73.66
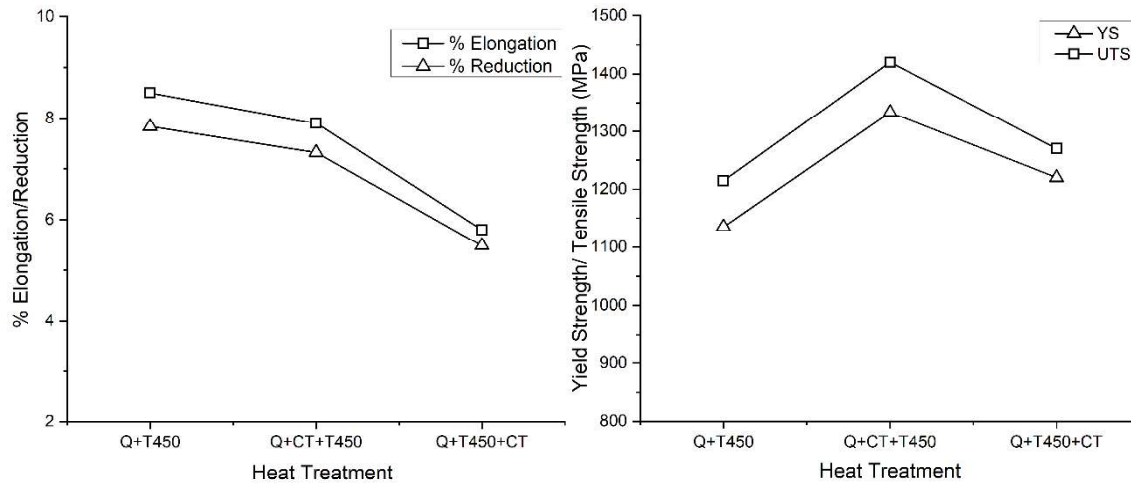
Fig. 6.27 Variation in the key tensile properties of tempered EN24 as a function of heat treatment cycles.

6.4.4   Microstructural Analysis

Figure 6.28 shows the annealed microstructure of EN24 with scattered pearlite and ferrite phases. Microstructures of as-quenched and cryogenic treated specimens are shown in Fig. 6.29. It can be clearly seen that cryogenic treated specimen shows fine martensitic microstructure as compared to the coarse microstructure of as-quenched specimen, confirming the fact that retained austenite transforms into martensite during cryogenic treatment.

Fig. 6.30 shows the microstructures of specimens involving conventional treatment, cryogenic treatment carried out before tempering and cryogenic treatment carried out after tempering, with constant tempering temperature of 300 °C. It is observed from the figure that specimen with cryogenic treatment carried out before tempering shows more uniform and finer martensitic structure as compared to the specimens with conventional treatment and cryogenic treatment carried out after tempering.

Figure 6.31 shows the microstructural changes observed with constant tempering temperature of 450 °C. Since the tempering temperature is high, the microstructures show fine structures in comparison to specimens subjected to 300 °C tempering. The changes observed follow the same trend as of 300 °C, clearly depicting finer and homogenous

microstructure for the cryogenic treated specimen (Q+CT+T450) as compared to the other two heat treatment steps.
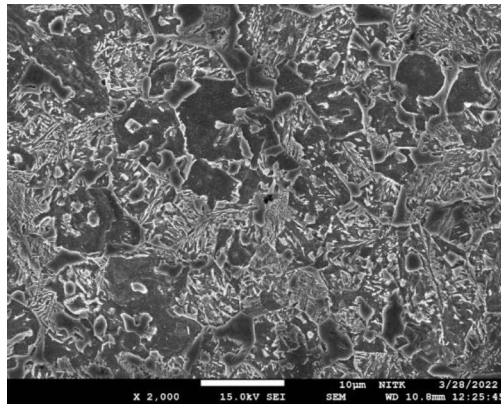
Fig. 6.28 Microstructure of EN24 steel in annealed condition.
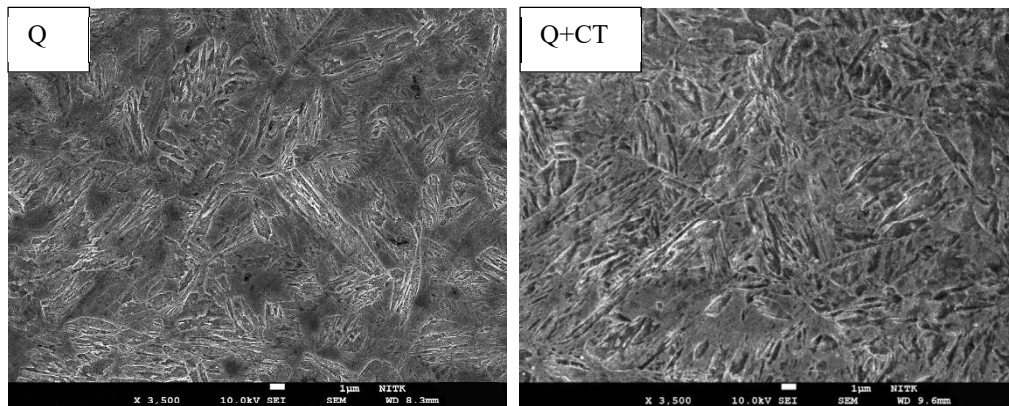
Fig. 6.29 SEM images showing as quenched and cryogenic treated microstructures of EN24.
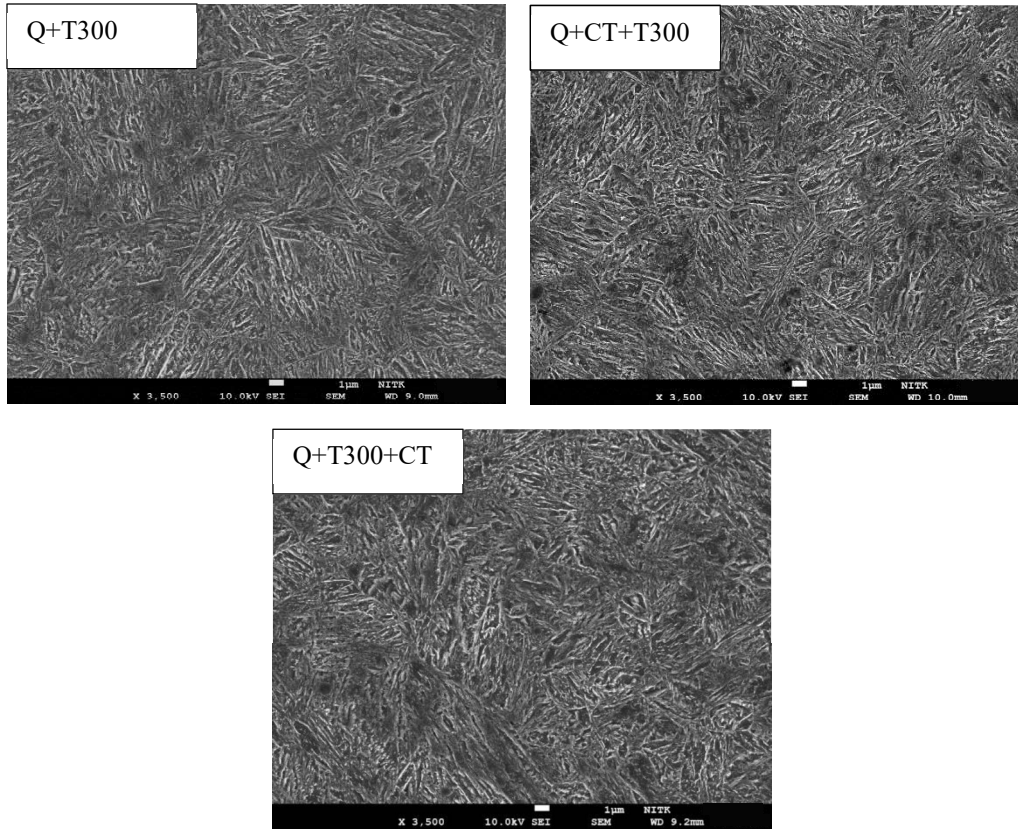
Fig. 6.30 SEM images of 300 °C tempered EN24 specimens.
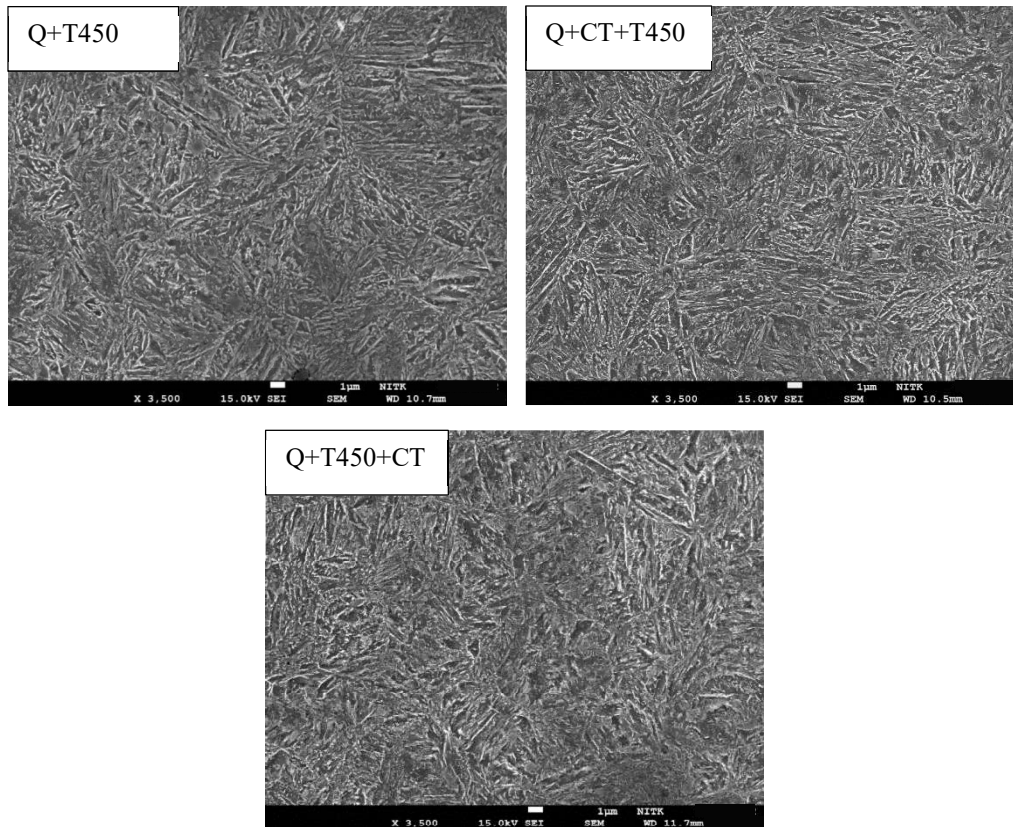
Fig. 6.31 SEM images of 450 °C tempered EN24 specimens.

6.4.5   Fractography

Fractographs of EN24 after tensile test are provided in Fig. 6.32. Fractographic observation of tensile specimen reveals dimples as the main fracture feature indicating that all the specimens failed by ductile fracture. Q+CT+T450 has fine dimples, distributed uniformly, indicating more toughness. Despite the fact that Q+T450 shows fine dimples they are not uniformly distributed when compared with Q+CT+T450. Dimples observed in Q+T450+CT were coarse which meant that specimen subjected to Q+T450+CT failed before Q+T450 and Q+CT+T450.
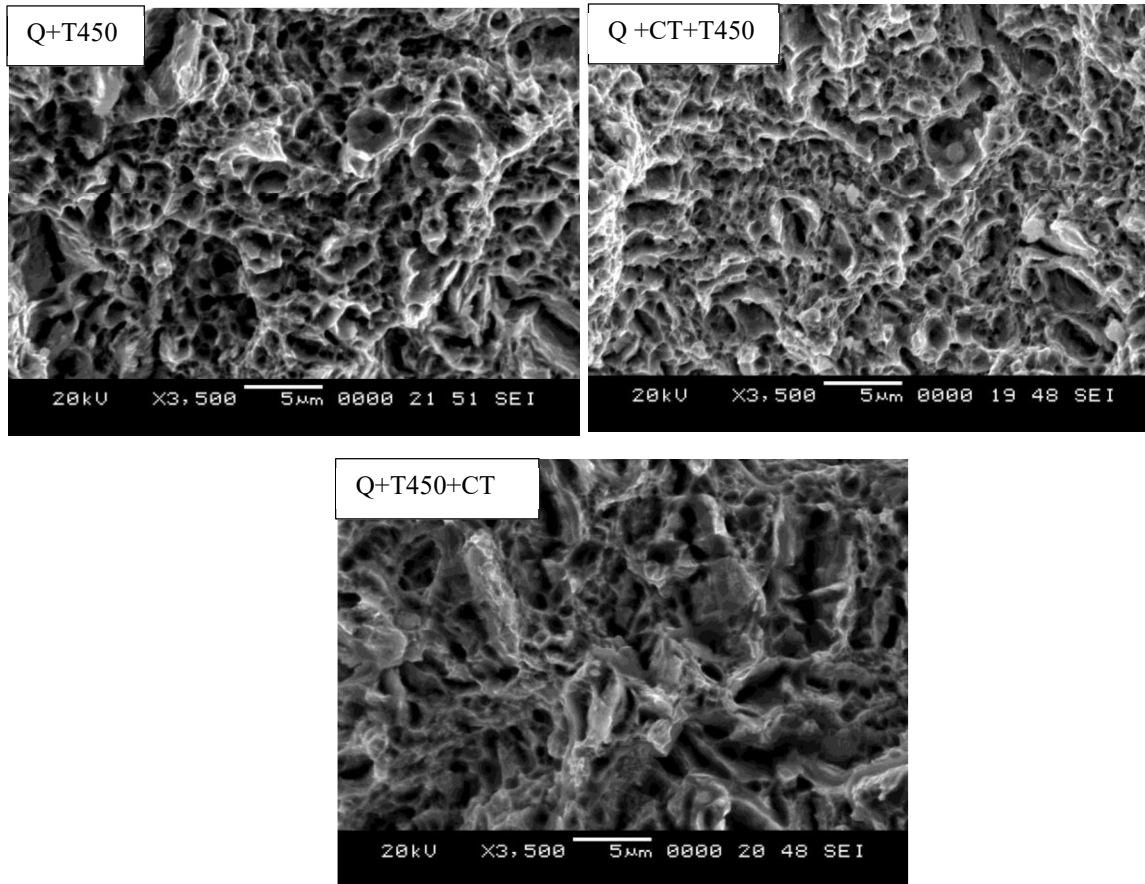
Fig. 6.32 Fractographs of 450 °C tempered tensile specimens of EN24.

6.4.6 Summary

Results of hardness tests, tensile tests, and microstructural analysis confirm that EN24 steel shows better response to the cryogenic treatment. However, the cryogenic treatment applied as an intermediate step between quenching and tempering is more effective than the unusual post-tempering cryogenic treatment. Even though the cryogenic treatment carried out after the conventional tempering process improves the strength marginally, drop in ductility is observed for that heat treatment step.

6.5 Results of EN45 Steel

6.5.1 Chemical composition

The result of the spark emission spectroscopy for EN45 bars is shown in Table 6.10 against the materials specification. The measured composition of the steel bars conforms to the standard specification confirming that the experimental material used for the heat - treatment experiments are indeed medium carbon steel, EN45.

Table 6.10. Measured chemical composition (wt. %) of steel bars against EN45 specification.

	C	Mn	Si	Ni	Cr	Mo	S	P	Fe
EN45 Spec.	0.50-	0.7-	1.50-	-	-	-	0.04	0.04	Balance
	0.60	1.0	2.00				max	max	
Measured	0.60	0.82	1.92	-	-	-	0.04	0.04	Balance

6.5.2 Hardness Measurement

Figure 6.33 presents hardness variations in EN45 steel following various heat treatment steps. The results show that the hardness of as-quenched specimen is 53 HRC and this increases to 58 HRC after the cryogenic treatment. This is a substantial increase in the hardness suggesting that EN45 grade responds very well to the cryogenic treatment. Having high carbon content with additional high silicon, the carbon equivalent of EN45 is significantly high. Hence it is likely that this grade produces significantly high fraction of retained austenite on quenching and transforms the same into martensite during the cryogenic exposure. Thus, EN45 responds very well to cryogenic treatment as compared to EN8, EN18 and EN47. It is important to note that when quenched and cryogenic treated EN45 is tempered at 300 °C the hardness is retained at the as-quenched level. Similar observation can be made when as-quenched and cryogenic exposed specimen is subjected to 450 °C tempering. However, conventional tempering drops the hardness significantly. Cryogenic treatment carried out after conventional heat treatment increases the hardness of about 1 HRC for both the tempering temperatures. However, incorporating cryogenic treatment as an intermediate step, hardness increases by 3 units.
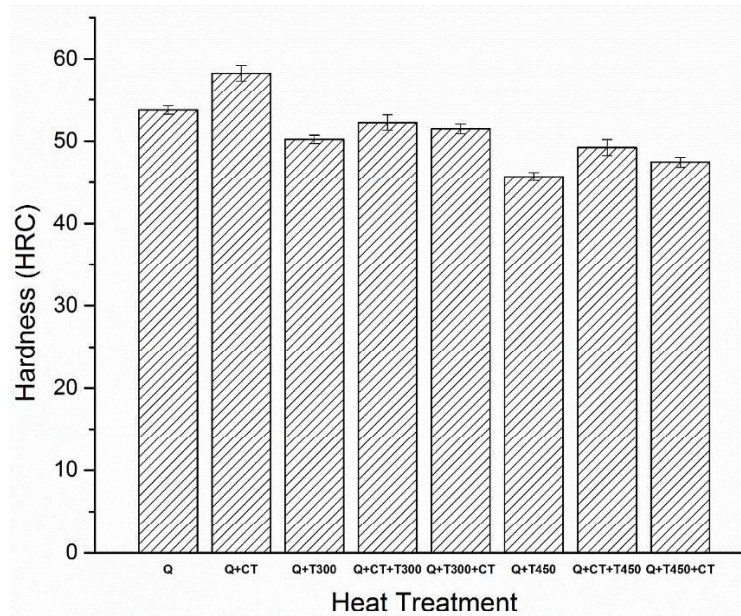
Fig. 6.33. Bar-chart showing hardness variations of EN45 after various heat treatment steps.

6.5.3 Tensile Tests

Engineering Stress-Strain curves of EN45 after various heat treatment cycles are shown in Fig. 6.34. Tensile properties of EN45 after the heat treatment cycles are listed quantitatively in Table 6.11. Variations in the strength and ductility of EN45 as a function of heat treatment cycles are shown in Fig. 6.35. EN45 shows significant change in the stress-strain behavior suggesting that this steel grade responds very well to cryogenic treatment. It is important to recognize here that both the tensile strength and yield strength of EN45 increase significantly due to cryogenic treatment. The heat treatment cycle involving cryogenic treatment as an intermediate step between quenching and tempering shows highest yield strength and tensile strength as compared to conventional heat treatment, and cryogenic treatment carried out after tempering. As Q+CT transforms most of the retained austenite into martensite there will be corresponding increase in the carbide fraction during tempering. Thus, increased carbide fraction in the ferritic matrix should cause increased hardness, increased strength, and marginally reduced ductility of Q+CT+T processed steels.
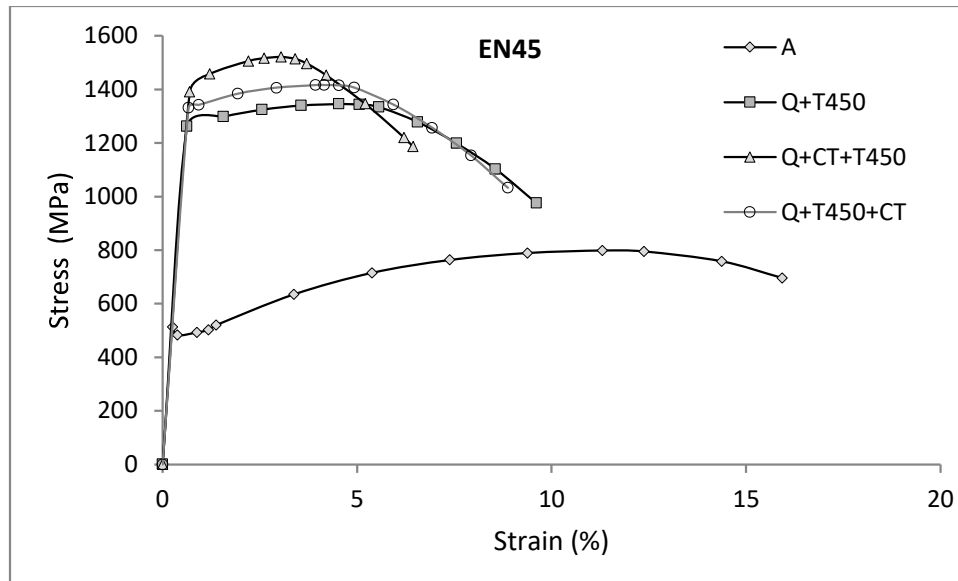
Fig. 6.34. Engineering Stress-Strain curves of EN45 for key heat treatment cycles.

Table 6.11 Tensile properties of EN45.

Heat Treatment	YS MPa	UTS MPa	Elongation (%)	Reduction (%)	Yield Ratio	Resilience (MJ/m^3)	Toughness (MJ/m^3)
A	513	798	15.93	13.74	0.64	1.83	127.121
Q+T450	1261	1344	9.61	8.77	0.94	3.94	129.158
Q + CT + T450	1390	1521	6.44	6.05	0.91	4.82	97.95
Q +T450 + CT	1331	1416	8.87	8.15	0.94	4.43	125.6
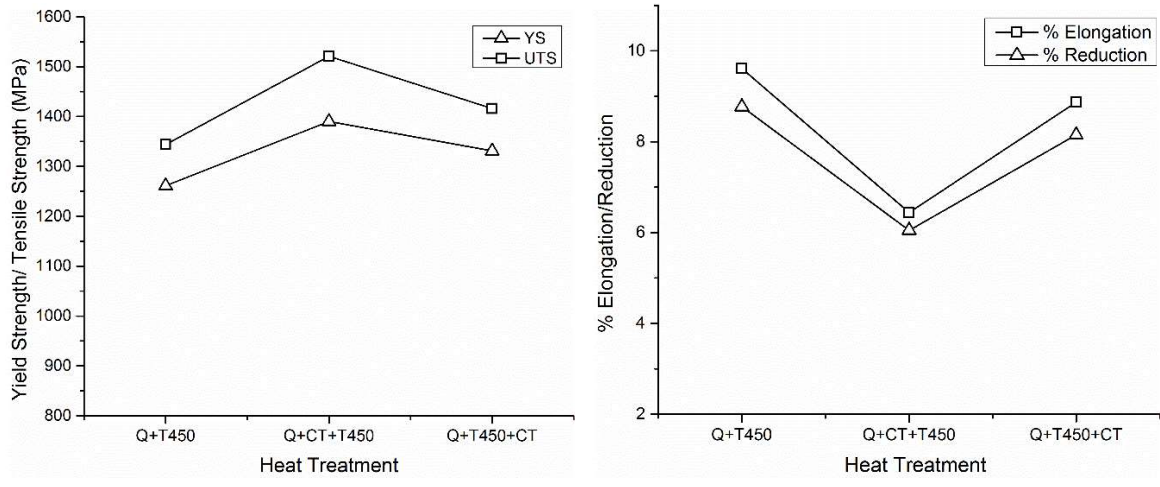
Fig. 6.35 Variation in the key tensile properties of tempered EN45 as a function of heat treatment cycles.
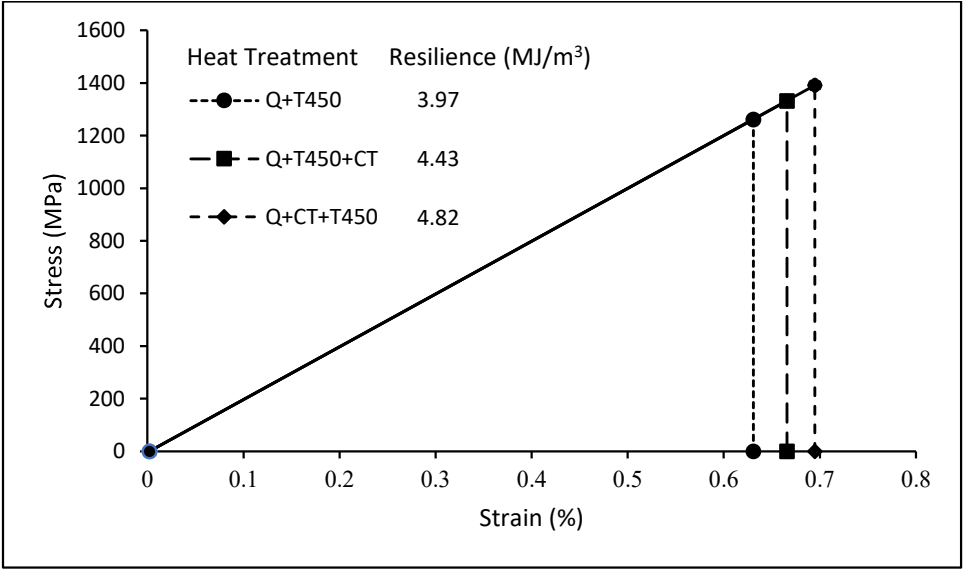
Fig. 6.36 Engineering Stress-strain curve within the elastic limit showing the effect of cryogenic treatment on the resilience of EN45.

EN45 is mostly used in spring steels and yield strength plays a major role as it accounts for the resilience as shown in Fig. 6.36. As compared to conventional heat treatment, cryogenic treatment as an intermediate step, increases the yield strength from 1261 MPa to 1390 MPa and tensile strength from 1344 MPa to 1521 MPa.

Though cryogenic treatment followed after tempering increases the yield strength and tensile strength to 1331 MPa and 1416 MPa, the increment is marginal as compared to the cryogenic treatment carried out before tempering.

Thus, the experimental results confirm that by properly applying deep cryogenic treatment, yield strength, tensile strength and resilience of EN45 can be increased by 10%, 13%, and 21% respectively. The improvement in the strength and resilience is quite significant considering that EN45 is a spring steel that is used for making coil and leaf-springs to store/absorb elastic energy.

It is to be noted that EN45 contains Si as the main alloying element that is known as a strong ferrite strengthener. Thus, high carbon equivalent and silicon strengthening of ferrite matrix could be responsible for improving the strength and hardness of cryogenic treated and tempered EN45. This suggests that other spring steel grades having silicon as the major alloying addition should also respond positively to cryogenic treatment. Thus, potential of spring steels as a material for elastic resilient structure could be fully realized by applying cryogenic treatment as an intermediate step between hardening and tempering step.

6.5.4 Microstructural Analysis

Microstructure of EN45 in annealed condition is shown in Fig. 6.37. The microstructure shows scattered pearlitic and ferritic grains conforming to EN45 grade. Figure 6.38 comparatively presents microstructures of as-quenched, and quenched and cryogenic treated EN45 specimens. Microstructural changes due to various heat-treatment cycles involving tempering at 300 °C and 450 °C are presented in Fig. 6.39, and Fig. 6.40 respectively.
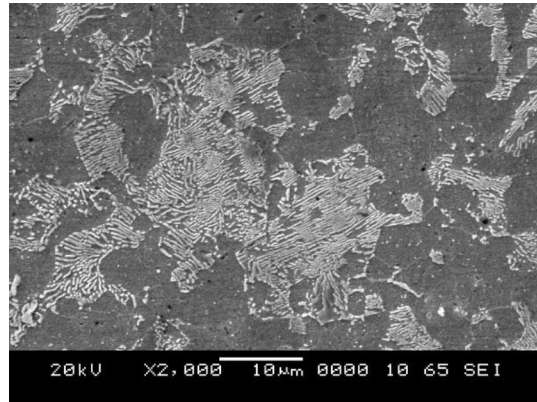
Fig. 6.37. Microstructure of EN45 steel in annealed condition.
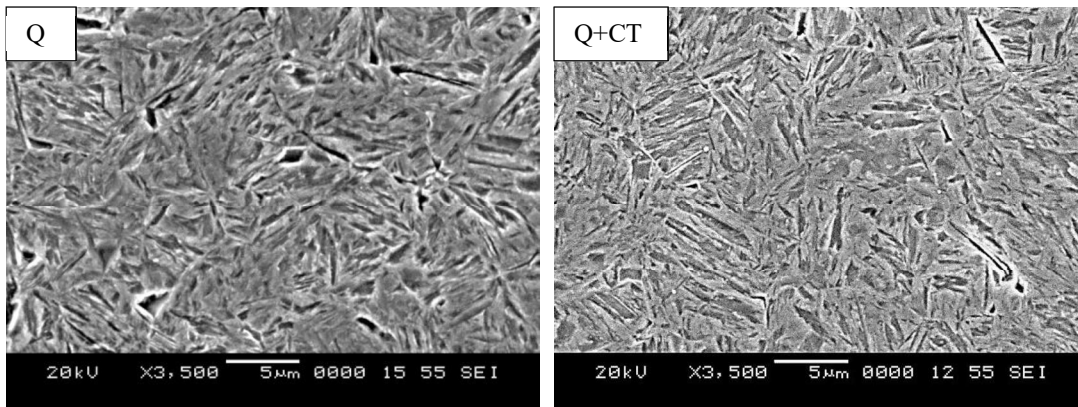
Fig. 6.38. SEM images showing as quenched and cryogenic treated microstructures of EN45.
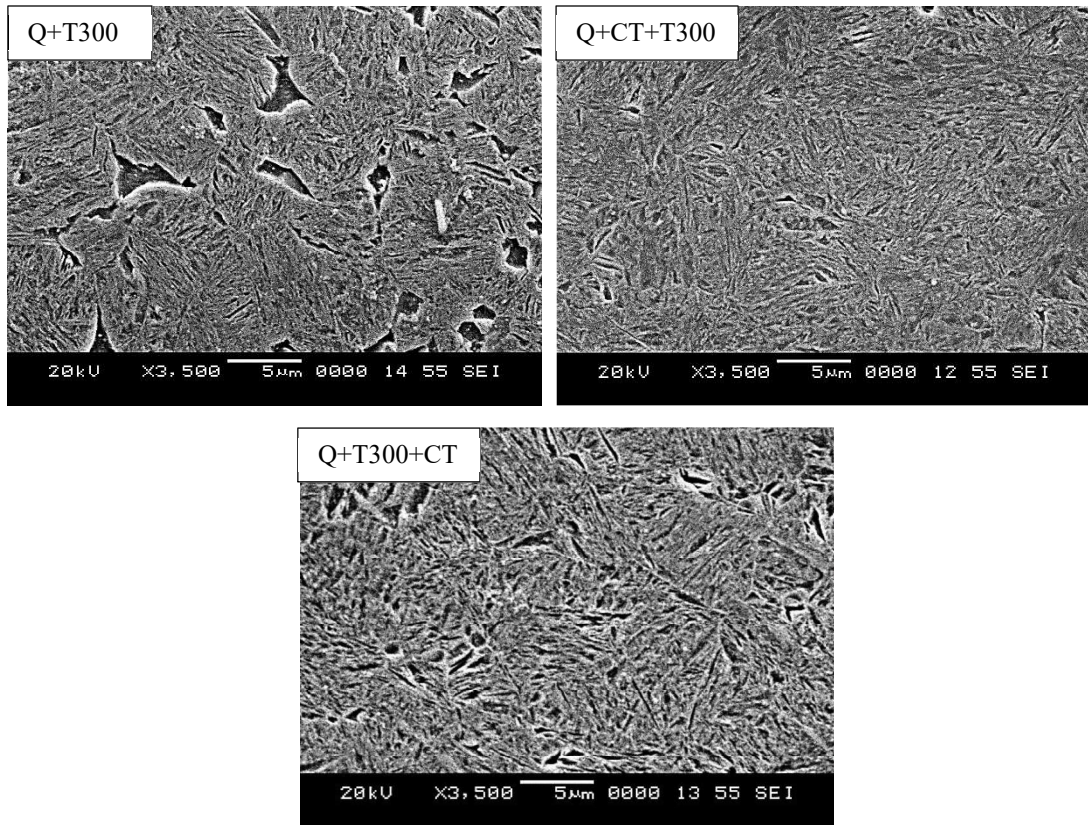
Fig. 6.39. SEM images of 300 °C tempered EN45 specimens.
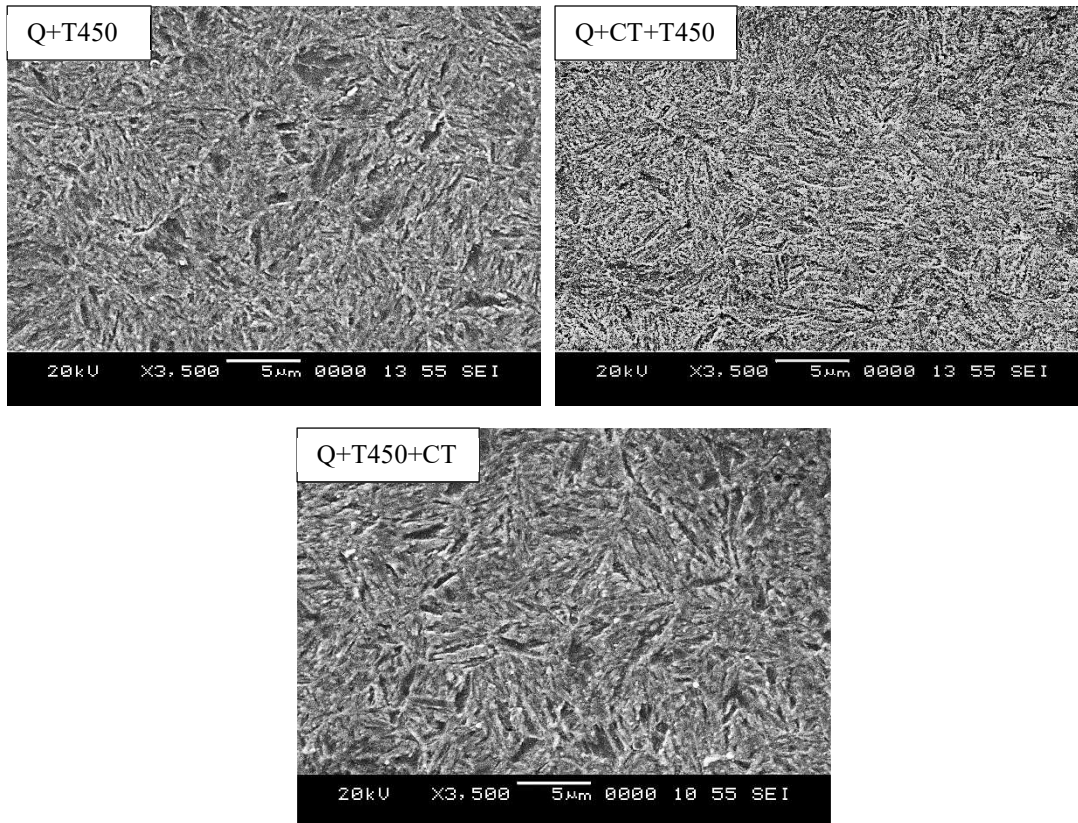
Fig. 6.40. SEM images of 450 °C tempered EN45 specimens.

As-quenched EN45 specimen shows coarse martensite colonies while the quenched and cryogenic treated specimen shows finer, and denser martensitic structure indicating the transformation of retained austenite into martensite during the cryogenic exposure.

The 300 °C tempered specimens show hazy microstructure of tempered martensite. However, by visusal comparison, it is clear that Q+CT+T300 specimen has the finest and most uniform microstructure. This is more pronounced in 450 °C tempered specimens as Q+CT+T450 shows very fine and homogeneous microstructure as compared to Q+T450 and Q+T450+CT. Thus, from the microstructural analysis it is clear that cryogenic treatment when applied as an intermediate step between quenching and tempering yields the ideal microstructure for the strengthening of EN45.

6.5.5 Fractography

The fractographs of all three tempered specimen show dimples suggesting that all three specimens failed by ductile fracture (Fig. 6.41). The difference in the fractographic features of these specimens is rather subtle. However, Q+CT+T450 specimen shows slightly coarser dimples than that of other two specimens. This suggests that Q+CT+T450 specimen is least ductile. The tensile test results confirm the same.

6.5.6 Summary

Results of hardness tests, tensile tests, and microstructural analysis confirm that EN45 steel responds quite positively to the cryogenic treatment. However, the cryogenic treatment applied as an intermediate step between quenching and tempering is more effective than the unusual post-tempering cryogenic treatment. The tensile test results demonstrate that the regular cryogenic treatment not only improves the tensile strength and hardness, but also improves the yield strength and the resilience of EN45. However, this substantial increase in the strength due to the cryogenic exposure, brings about slightly reduced ductility in EN45 steel.
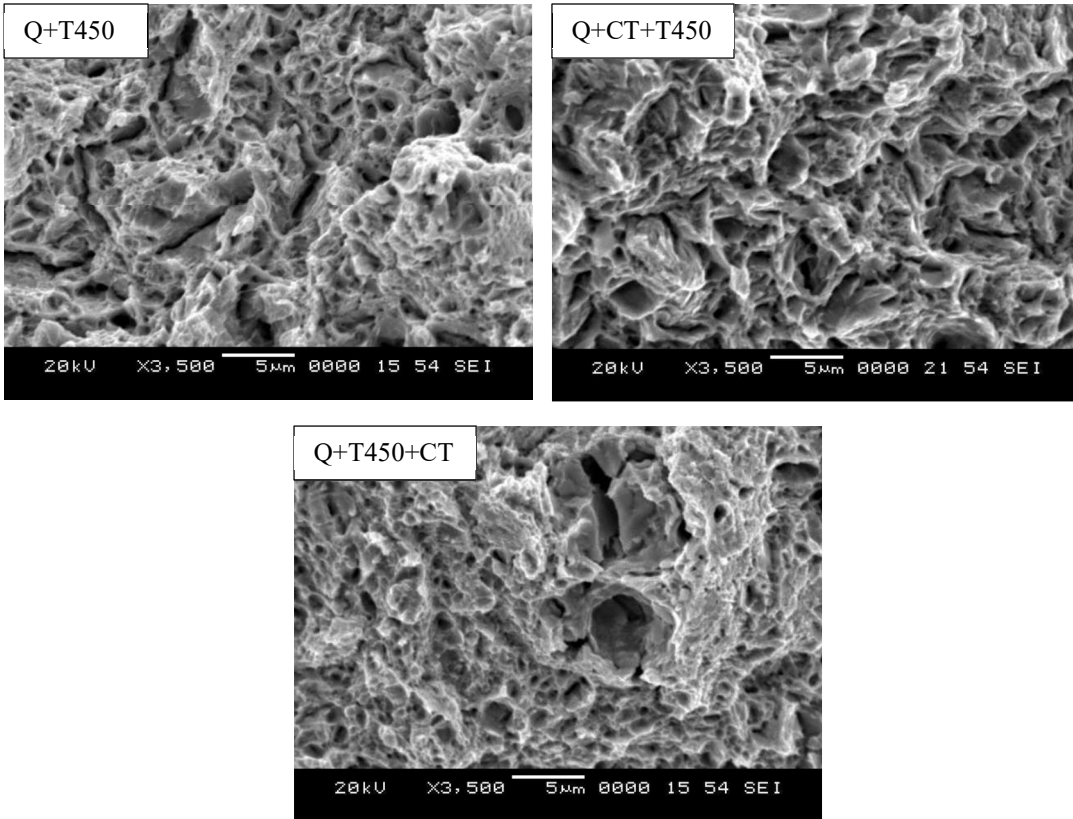
Fig. 6.41. Fractographs of 450 °C tempered tensile specimens of EN45.

6.6 Wear Study

6.6.1 Wear test results

The wear behaviour of materials is a complex function of the test conditions apart from the mechanical properties of the test specimen and the counter body. The degree of improvement in wear resistance by cryogenic treatment is thus strongly dependent on the experimental conditions that determine whether the operative mode and mechanism of wear for the QT and the QCT specimens would be similar or dissimilar (Das et al. 2009b).

Figure 6.42 and Fig. 6.43 show the effect of various heat treatment steps on the wear rate for different loads for the EN24 material. Figure 6.42a shows the results of wear rate for different heat treatment steps for a tempering temperature of 300 °C and 4000 m as sliding distance. For the applied load of 39.24 N, conventionally heat treated specimens show 24% higher wear rate (WR) than the specimens subjected to cryogenic treatment as an intermediate step between quenching and tempering. However, the magnitude becomes lesser when compared to the specimens subjected to cryogenic treatment after conventional heat treatment (9% higher). This shows that specimens subjected to cryogenic treatment as an intermediate step show better wear resistance in comparison to conventionally heat treated specimens and specimens subjected to cryogenic treatment carried out after conventional heat treatment. Similar observation was made for the applied load of 58.86 N. However, magnitude of the wear rate observed was much higher for the applied load of 58.86 N. For the applied load of 58.86 N, specimens subjected to cryogenic treatment as an intermediate step showed 27% and 18% lesser wear rate than the specimens subjected to conventional heat treatment and cryogenic treatment after conventional heat treatment respectively. Considering both the applied load and different heat treatments specimen subjected to conventional heat treatment for the applied load of 58.86 N showed highest wear rate and the specimens subjected to cryogenic treatment as an intermediate step with applied load of 39. 4 N showed lowest wear rate.

Figure 6.42(b) shows the results of wear rate for different heat treatment steps for a tempering temperature of 300 °C and 8000 m as sliding distance. Similar trend was

followed for 8000 m sliding distance as the specimens subjected to cryogenic treatment as an intermediate step showed 26% and 17% lower wear rate than conventional heat treatment and cryogenic treatment after tempering, respectively, for the applied load of 39.24 N. The magnitude of the wear rate increased with the increase in the applied load and in the case of 58.86 N, specimens subjected to cryogenic treatment as an intermediate step showed 37% and 21% lower wear rate than conventional heat treatment and cryogenic treatment after tempering, respectively. Considering both the applied load and different heat treatments specimen subjected to conventional heat treatment for the applied load of 58.86 N showed highest wear rate and the specimens subjected to cryogenic treatment as an intermediate step with applied load of 39.4 N showed lowest wear rate.

Figure 6.43a and Fig. 6.43b show the graphs of wear rate against various heat treatment steps for a tempering temperature of 450 °C and sliding distance of 4000 m and 8000 m respectively. For a sliding distance of 4000 m and 39.4 N applied load, Q+CT+T450 specimens showed 25% and 14% lesser wear rate than the Q+T450 and Q+T450+CT specimens respectively. Whereas, for 58.86 N Q+CT+T450 specimens showed 27% and 16% lesser wear rate than the Q+T450 and Q+T450+CT specimens respectively. Considering both the loading conditions, specimens subjected to Q+T450 with 58.86 N show highest wear rate in comparison to specimens subjected to Q+CT+T450 with 39.24 N. Similarly, for 8000 m and 39.4 N applied load, Q+CT+T450 specimens showed 26% and 16% lesser wear rate than the Q+T450 and Q+T450+CT specimens respectively. With the increase in load (58.81 N), Q+CT+T450 specimens showed 33% and 19% lesser wear rate than the Q+T450 and Q+T450+CT specimens respectively. Considering both the loading conditions, specimens subjected to Q+T450 with 58.81 N show highest wear rate in comparison to specimens subjected to Q+CT+T450 with 39.4 N.

Fig. 6.42 Graphs showing wear rate vs different heat treatment cycles of EN24 for tempering temperature of 300 °C: (a) for sliding distance of 4000 m (b) for sliding distance of 8000 m.

Fig. 6.43 Graphs showing wear rate vs different heat treatment cycles of EN24 for tempering temperature of 450 °C: (a) for sliding distance of 4000 m (b) for sliding distance of 8000 m.

Figure 6.44 and Fig. 6.45 show the results of wear rate of EN45 steel against the various heat treatment steps for different loads. The wear results obtained for EN45 are similar to the results obtained for EN24. As shown in Fig. 6.44a, for 4000 m sliding distance and 39.24 N load, specimens subjected to cryogenic treatment as an intermediate step for a tempering temperature of 300 °C showed 24% and 16% better wear rate than conventional heat treatment and cryogenic treatment respectively. Similarly, the specimens subjected to Q+CT+T300 for the increased load of 58.81 N showed 37% and 19% better wear rate over Q+T300 and Q+T300+CT respectively. It can be also seen from the graph that Q+T300 specimens tested for 58.81 N load showed highest wear rate and Q+CT+T300 specimens subjected to 39.4 N applied load show lowest wear rate. Figure 6.44b shows the wear results for different loads against various heat treatment for the sliding distance of 8000 m. It can be seen that for 39.4 N, Q+CT+T300 specimens showed 36% and 17% lower wear rate than Q+T300 and Q+T300+CT respectively. As the magnitude of the wear rate increased with the increase in wear rate; for 58.81 N, Q+CT+T300 specimens showed 43% and 18% lower wear rate than Q+T300 and Q+T300+CT respectively. As shown in the figure, Q+T300 specimens tested for 58.81 N load showed highest wear rate and Q+CT+T300 specimens subjected to 39.4 N applied load showed lowest wear rate.

Figure 6.45a and Fig.6.45b show the wear results for different loads against different heat treatment steps with constant tempering temperature of 450 °C, for a sliding distance of 4000 m and 8000 m respectively. With 39.4 N as the applied load and 4000 m as the sliding distance, specimens subjected to Q+CT+T450 showed 25% and 16% lesser wear rate than Q+T450 and Q+T450+CT respectively. Whereas, for 58.81N Q+CT+T450 samples showed 37% and 19% lesser wear rate than Q+T450 and Q+T450+CT specimens respectively. Specimens subjected to Q+T450 for an applied load of 58.81 N showed highest wear rate whereas Q+CT+T450 specimens tested at 39.4 applied load showed least wear rate. Similarly, for the testing conditions of 8000 m as sliding distance and 39.4 N as applied load, specimens subjected to Q+CT+T450 showed 31% and 17% lesser wear rate than Q+T450 and Q+T450+CT respectively. Whereas, for an applied load of 58.81 N Q+CT+T450 samples showed 140% and 18% lesser wear rate than Q+T450 and

Q+T450+CT specimens respectively. As observed, specimens subjected to Q+T450 for an applied load of 58.81 showed highest wear rate whereas Q+CT+T450 specimens tested under applied load of 39.4 N showed lowest wear rate.

This shows that for the identical wear test conditions cryogenic treatment carried out as an intermediate step shows better wear resistance. However, irrespective of the heat treatment step/sequence, specimen subjected to higher applied load show higher wear rate, indicating that applied load plays a major role in determining the wear rate.
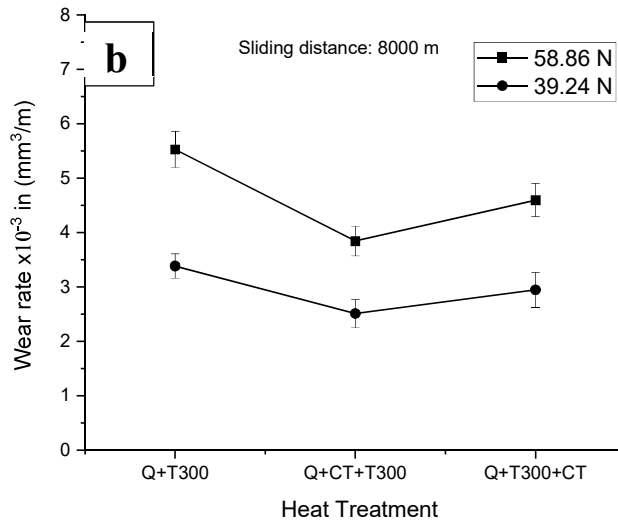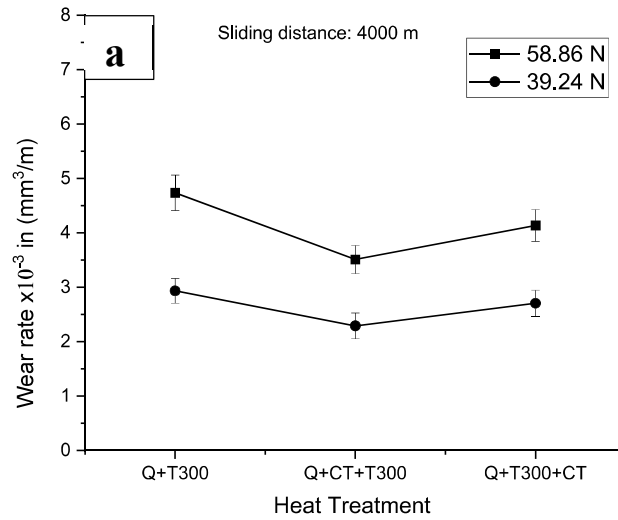
Fig. 6.44 Graphs showing wear rate vs different heat treatment cycles of EN45 for tempering temperature of 300 °C: (a) for sliding distance of 4000 m (b) for sliding distance of 8000 m.
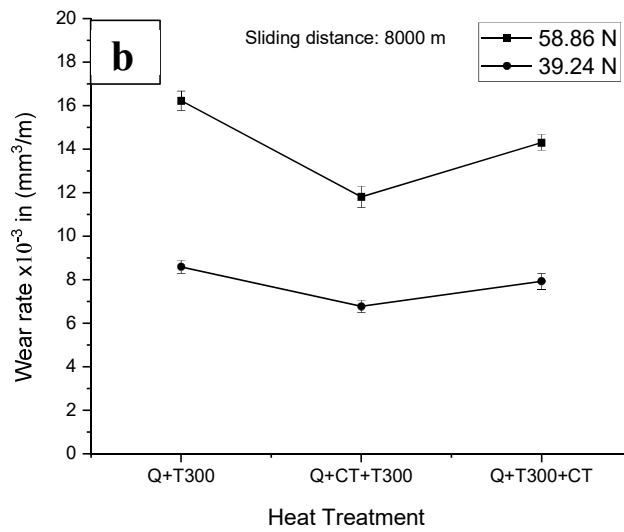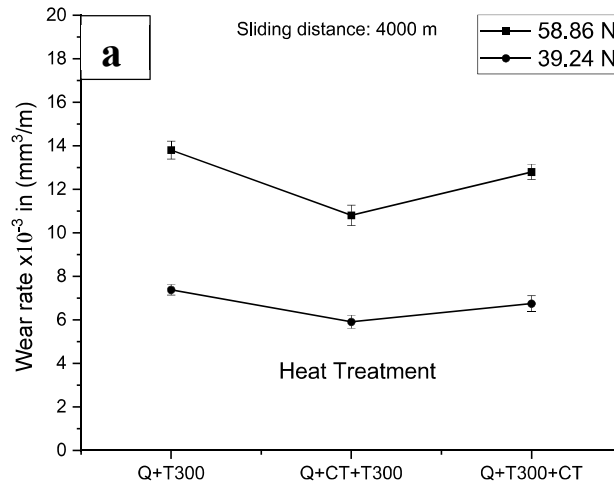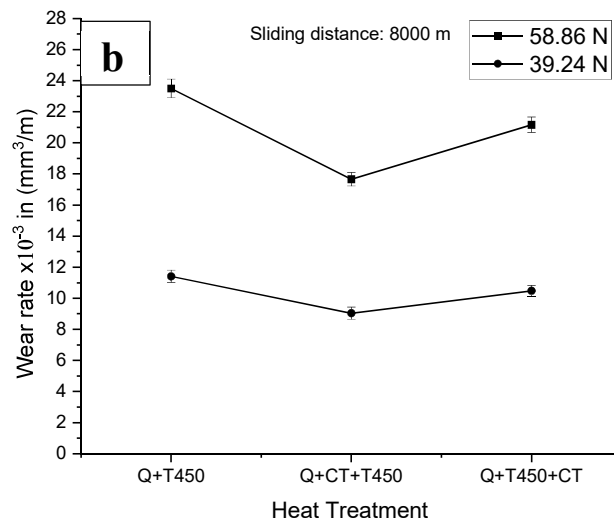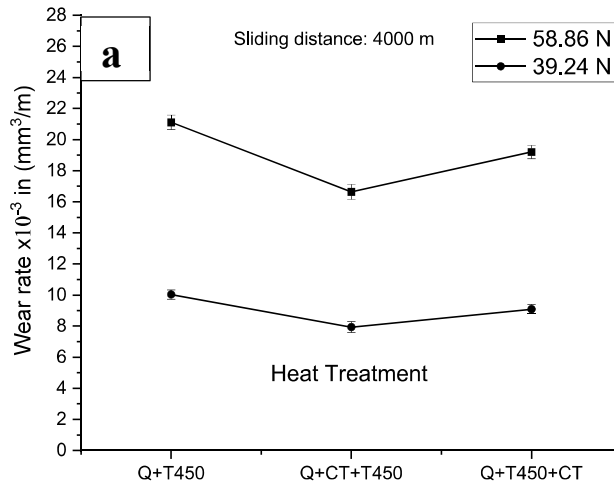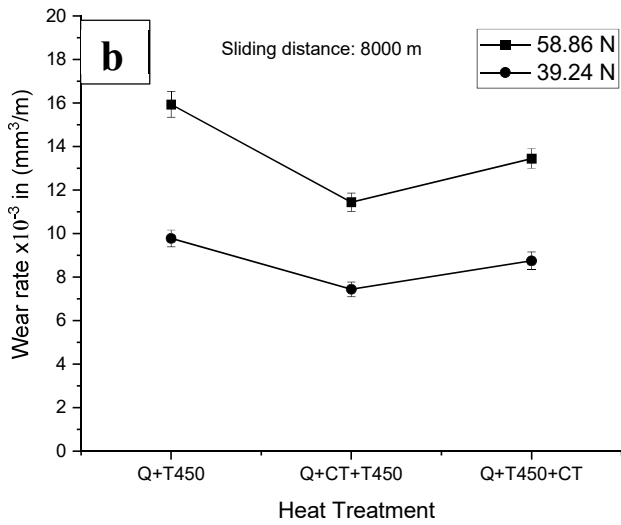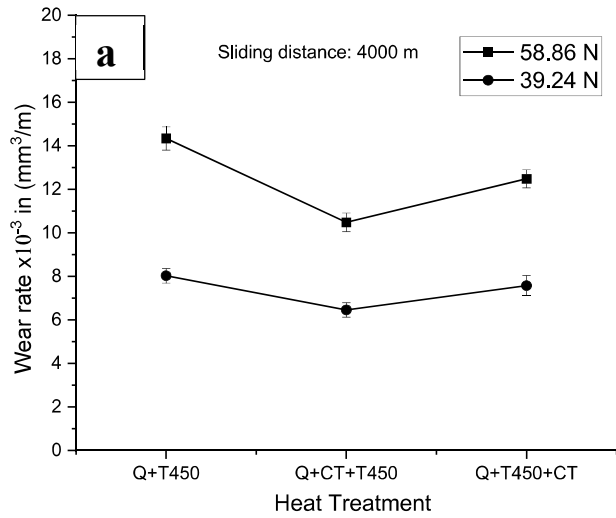
Fig. 6.45 Graphs showing wear rate vs different heat treatment cycles of EN45 for tempering temperature of 450 °C: (a) for sliding distance of 4000 m (b) for sliding distance of 8000 m.

6.6.2 Wear Morphology

The alterations in the morphology of wear for EN24 and EN45 for different loads and various heat treatments are shown in Fig. 6.46-6.49. Irrespective of the heat treatment and load applied, the worn surfaces appear rough but shiny and are metallic in nature. Under the identical wear test conditions, worn surfaces of Q+CT+T specimens appear much smoother than the Q+T and Q+T+CT samples for both the tempering temperatures (300 °C and 450 °C). The wear surfaces of the Q+T and Q+T+CT samples exhibit severe deformation bands/grooves stretched parallel to the sliding direction in comparison to Q+CT+T specimens. The grooves are associated with sub surface cracking and fracture ridges. These wedge-like patterns indicate that the contact surface of the specimens has undergone extensive plastic flow and associated shear fracture (Das et al. 2009a) (Grimanelis and Eyre 2006). Increase in load makes the worn surfaces more uneven and produces large fracture adhesive junction (e.g Q+T300 of 58.8 N). These observations infer that increased load results in increased plastic deformation and extrusion of the contact surface and subsurface of the pin specimen during wear test (Wilson and Alpas 1998).

It is well known that resistance to plastic deformation enhances with the reduction of retained austenite content and modifications in the precipitation behavior of secondary carbides (Roberts et al. 1998). Soft retained austenite in the conventional sample causes severe plastic deformation, which is markedly absent in the cryotreated samples. Thus, severe plastic deformation associated with delamination is considered to be the active wear mechanism in the conventionally-treated specimens and cryotreated samples (Das et al. 2007) (Das and Ray 2015). The process of delamination wear consists of subsurface plastic deformation, crack initiation and crack propagation. Cracks around the inclusions nucleate below a certain depth from the surface owing to large hydrostatic pressure near the asperity contact above certain depth owing to stress and deformation with distance from the contact (Suh 1977)(Fleming and Suh 1977). Increase in load increases the hydrostatic pressure and hence more will be the wear rate. In other words, material with less resistance to plastic deformation accumulate more subsurface plastic deformation leading to faster crack

initiation consequently leading to higher wear rate. This explains the observed variation of wear behavior of various heat-treatment conditions.
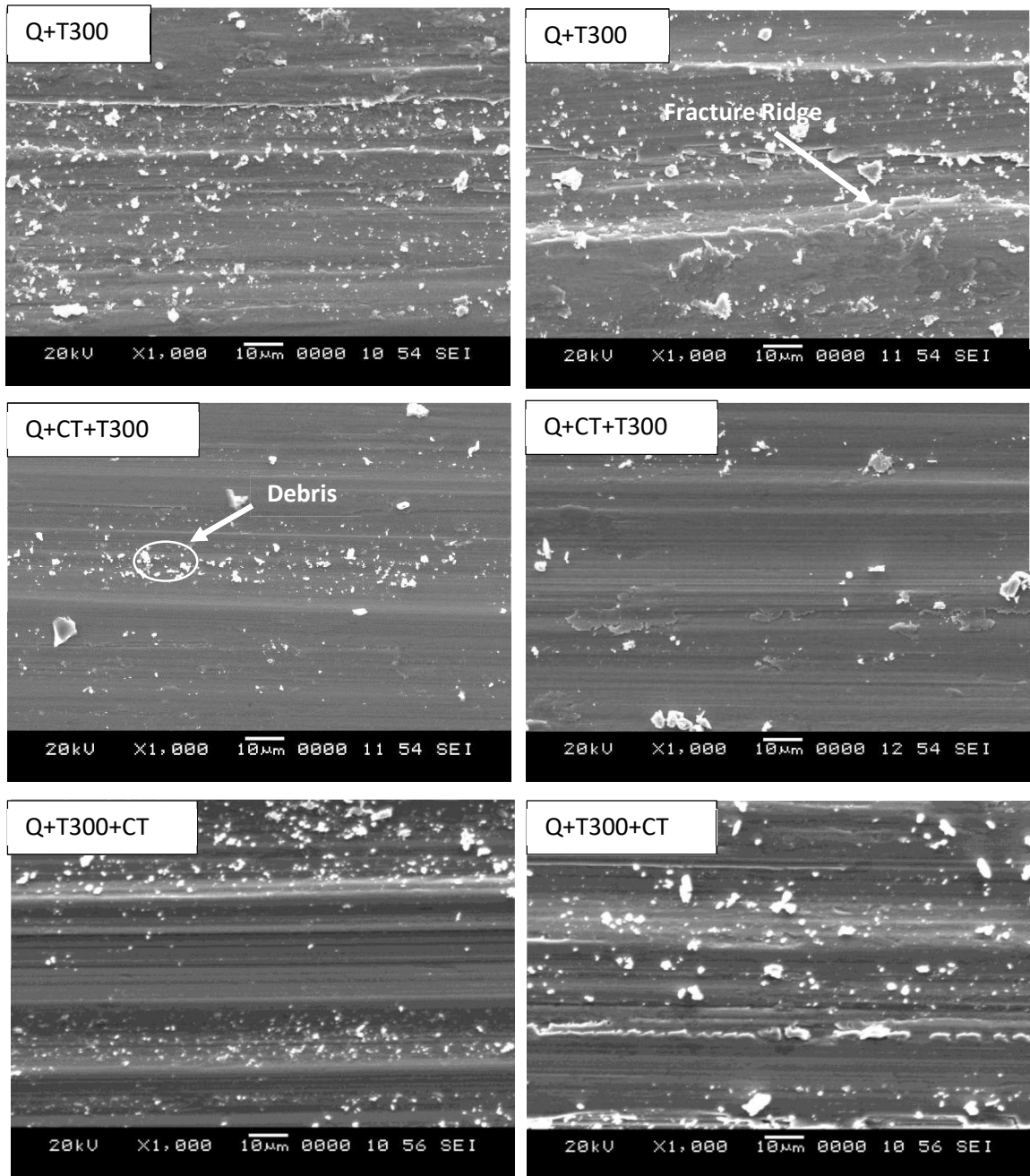
Fig. 6.46 Wear morphology of EN24 after different heat treatment cycles with tempering temperature of 300 °C. Left-side images show wear morphology for the parameter 39.24 N load and 4000 m sliding distance and right-side images show wear morphology for the parameter 59.86 N load and 8000 m sliding distance.
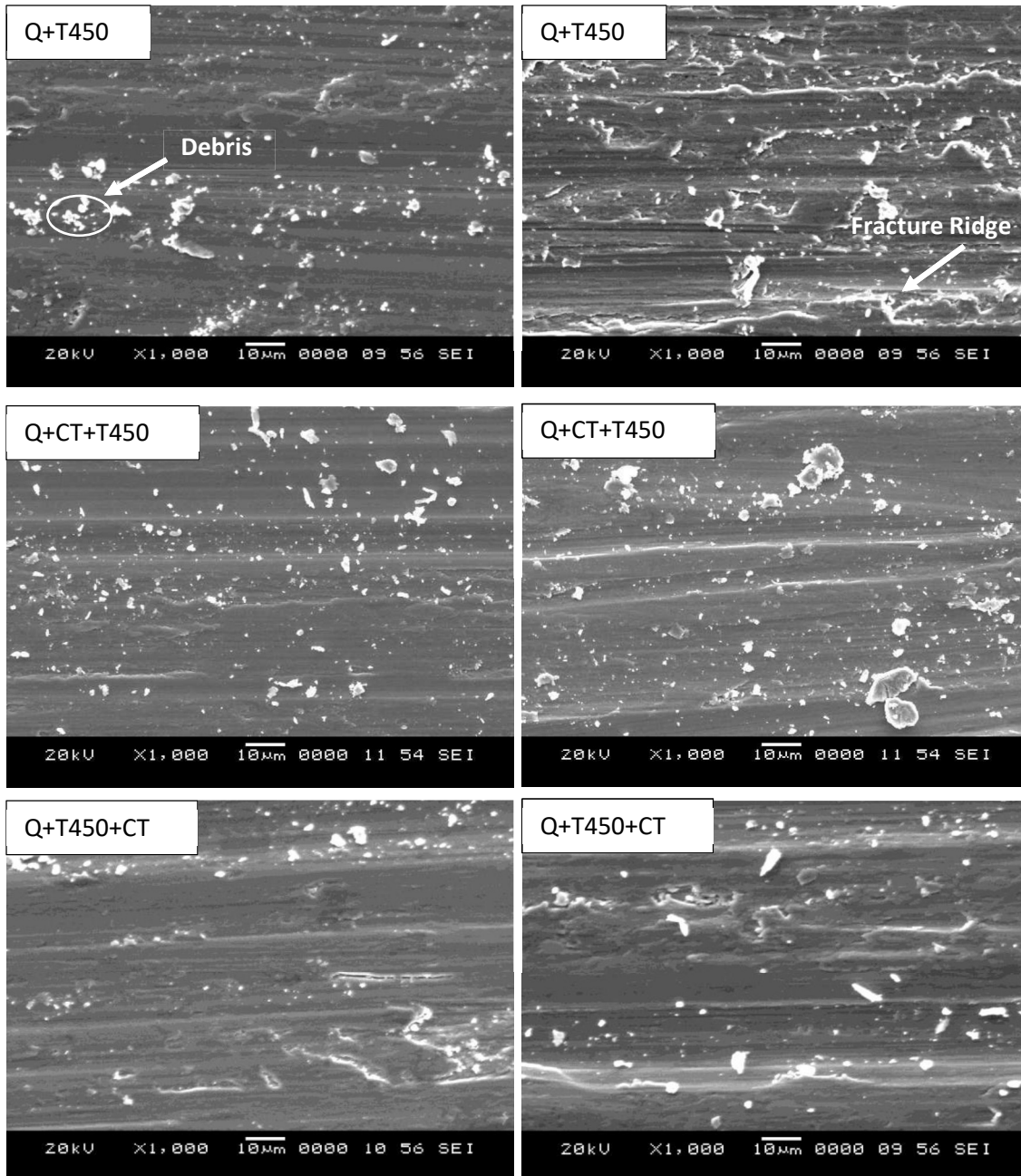
Fig. 6.47 Wear morphology of EN24 after different heat treatment cycles with tempering temperature of 450 °C. Left-side images show wear morphology for the parameter 39.24 N load and 4000 m sliding distance and right-side images show wear morphology for the parameter 59.86 N load and 8000 m sliding distance.
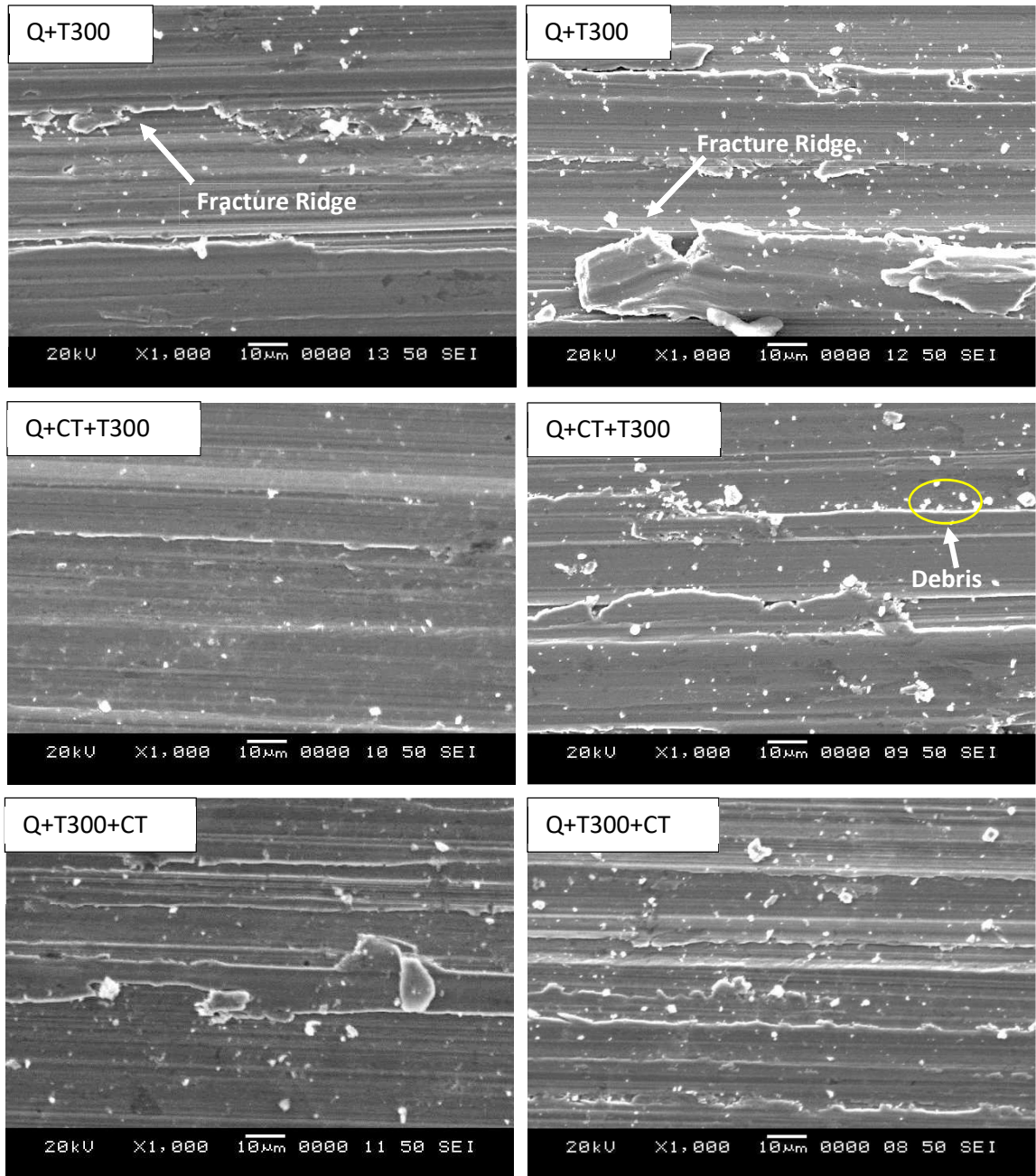
Fig. 6.48 Wear morphology of EN45 after different heat treatment cycles with tempering temperature of 300 °C. Left-side images show wear morphology for the parameter 39.24 N load and 4000 m sliding distance and right-side images show wear morphology for the parameter 59.86 N load and 8000 m sliding distance.
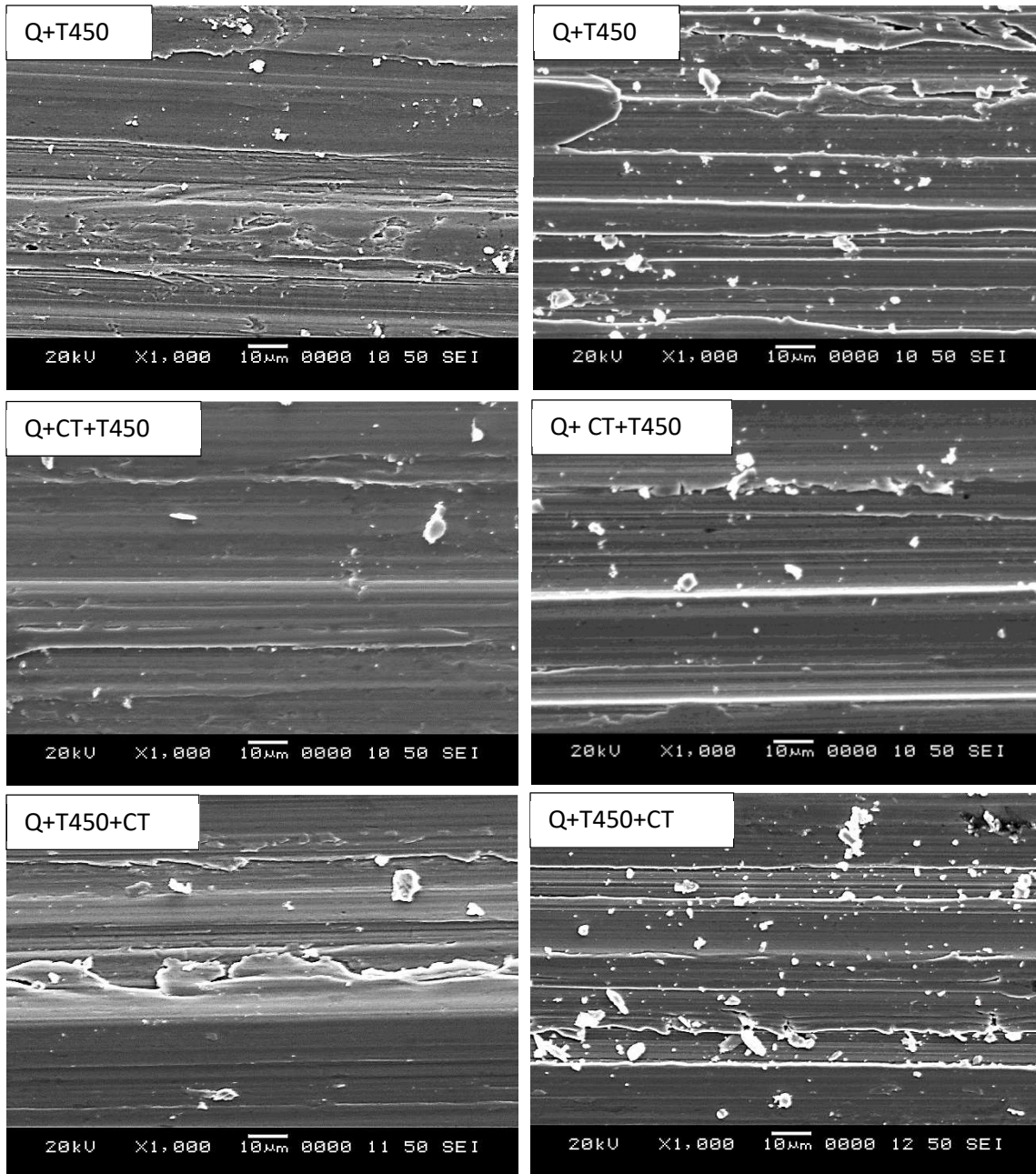
Fig. 6.49 Wear morphology of EN45 after different heat treatment cycles with tempering temperature of 450 °C. Left-side images show wear morphology for the parameter 39.24 N load and 4000 m sliding distance and right-side images show wear morphology for the parameter 59.86 N load and 8000 m sliding distance.

6.7 Discussion

The aim of this research work is to generalize the influence of deep cryogenic treatment in the heat-treatment cycles of structural low-alloy steels. To achieve this, a wide range of experimental materials are used in the work including: low-carbon (EN36), medium-carbon (EN18, EN18, EN47, EN24), and high-carbon (EN45) steel grades. With varying carbon content and alloying additions, the hardenability and corresponding mechanical properties of these grades should vary accordingly. Therefore, it is important to consider both the carbon content and other alloying additions to compute the carbon equivalent (CE) of each experimental material. Thus, influence of hardening, tempering, and cryogenic exposure can be expressed as a function of the carbon equivalent of the experimental materials. This way, a general trend in the mechanical properties of low-alloy steel grades and response to the hardening/tempering/cryogenic treatment can be obtained. The following are the reliable empirical formulae for computing the carbon equivalent of low-alloy steels (Bhadeshia and Honeycombe 2006).

For steels having; C < 0.18 %,
$$CE = C + \frac{Si}{30} + \frac{Mn + Cu + Cr}{20} + \frac{Ni}{60} + \frac{Mo}{15} + \frac{V}{10} + 5B \ldots \ldots \ldots (1)$$

For steels having C > 0.18 %,
$$CE = C + \frac{Mn + Si}{6} + \frac{Cr + Mo + V}{5} + \frac{Ni + Cu}{15} \ldots \ldots \ldots \ldots \ldots \ldots (2)$$

By using the nominal compositions in the above equations, carbon equivalent of the experimental materials is obtained and presented in Table 6.12.

Table 6.12 Carbon content, total alloying additions, and carbon equivalent of steel grades.

	EN36 (Bulk)	EN8	EN18	EN47	EN24	EN45	EN36 (Case)
Carbon %	0.16	0.4	0.4	0.5	0.4	0.6	0.8
Total Alloying Additions %	5.1	1.1	2	1.92	3.81	2.6	5.1
Carbon Equivalent %	0.3	0.58	0.63	0.7	0.93	1.03	1.35

Results of the hardness test from both the heat-treatment experiments and the case-study is comprehensively presented in Table 6.13. The results from the case-study provides the hardness variation of carburized EN36 steel. Since hardness values of both the core and carburized-case are tracked as a function of heat-treatment steps, effects of cryogenic treatment on the bulk and carburized EN36 are obtained from the case-study.

Additionally, to simulate the industrial heat-treatment practice, the tempering temperature used in the case-study is 200 °C. However, in the heat-treatment experiments, EN8, EN18, EN47, EN45, and EN24 specimens are tempered at much higher temperatures, 300 °C and 450 °C. Thus, a perspective on the effects of cryogenic treatment on six important low alloy steel grades having isothermally tempered over a wide temperature range (200 °C - 450 °C) can be obtained from Table 6.13. Thus, the effects of cryogenic exposure on low-carbon, medium-carbon, and high carbon alloy steels can be generalized.

Table 6.13. Hardness test results.

Heat-Treatment	EN36 (Bulk)	EN8	EN18	EN47	EN24	EN45	EN36 (Carburized)
Q	44	45	50	54	50	53	60
Q+CT	47	48	53	57	54	58	65
Q+T200	42	-	-	-	-	-	58
Q+T200+CT	43	-	-	-	-	-	60
Q+CT+T200	44	-	-	-	-	-	61
Q+T300	-	38	46	50	44	50	-
Q+T300+CT	-	38	46	51	45	51	-
Q+CT+T300	-	40	47	52	47	53	-
Q+T450	-	31	42	42	38	46	-
Q+T450+CT	-	31	42	43	39	47	-
Q+CT+T450	-	32	43	44	40	48	-

It is clear from the first two rows of Table 6.13 that all steel grades respond positively when as-quenched specimens are subjected to cryogenic treatment. Depending on the carbon content and alloying additions, as-quenched bulk hardness of these steel grades varies from 44 HRC to 54 HRC. On cryogenic exposure, there is a substantial increase in the bulk hardness of these steels in the range, 47 HRC to 58 HRC. Thus, gain in the bulk-hardness of the as-quenched low-alloy steels due to cryogenic exposure is in the range, 3-5 HRC. The higher the carbon equivalent, the better is the response to the cryogenic exposure, and the higher is the gain in the hardness.

Now, it is important to consider that EN36 is a low-carbon low-alloy steel. On cryogenic exposure, the bulk hardness of this grade is increased only by 3 HRC. However, hardness

of the carburized-case of this grade is increased by 5 HRC. This difference is quite significant from the application point-of-view. Case-hardened steel components are known to possess good wear-resistance and fatigue properties due to high hardness and presence of compressive residual stresses at the surface and sub-surface respectively. Since the carburized case of EN36, gained significantly higher hardness than the core, wear resistance and service life of cryogenic treated EN36 components should improve significantly.

Reduction in the hardness after tempering at, 200 °C, 300 °C and 450 °C is by 2 HRC, 3-7 HRC and 7-13 HRC respectively. Thus, the higher the tempering temperature, the greater is the softening of the as-quenched steels. When the tempering temperature is 300 °C and above, there is a substantial reduction in the hardness of these steel grades. However, quenched and cryogenic exposed EN36, after tempering at 200 °C retains the hardness of both the core and the case at least at the as-quenched level. This is again an important result as the case-hardened steel components are generally tempered at relative low temperatures, 150 °C - 250 °C. Thus, a great surface property can be achieved if cryogenic treatment is suitably applied to case-carburized steel components. As the EN36 having low carbon equivalent is showing a positive response to the cryogenic treatment, the other low-alloy steel grades having higher carbon equivalent are expected respond very well to the cryogenic exposure. From the results of hardness measurement, response to cryogenic treatment of low-alloy steels can be generalized as follows. Low-alloy steels respond well to the cryogenic treatment. The higher the carbon equivalent, the better is the response. However, the cryogenic treatment applied to as-quenched steels show much better results than that applied after the tempering step.

Now, the results of hardness measurement should be corroborated with the results of tensile and wear tests. A summary of the tensile, hardness, and wear test results is presented in Table 6.14. It is important to notice that the table essentially compares the effects of regular cryogenic treatment (Q+CT+T) with the results of unusual cryogenic treatment (Q+T+CT).

Table 6.14 Summary of experimental results.

Property	Heat-Treatment Cycle	Improvement over Conventional Heat-treatment (Q+T)				
		EN8	EN18	EN47	EN24	EN45
Tensile Strength	Q+T450+CT	0 %	1.6 %	0 %	4.5 %	5.4 %
	Q+CT+T450	5.7	3.9 %	4.2 %	16.8 %	13.2 %
Yield Strength	Q+T450+CT	0 %	3.3 %	0 %	7.5 %	5.6 %
	Q+CT+T450	6.5 %	5.3 %	4 %	17.4 %	10 %
Resilience	Q+T450+CT	0 %	5.3 %	0 %	11 %	10.8 %
	Q+CT+T450	11.7 %	11.2 %	9 %	24 %	21 %
Hardness	Q+T450/T300+CT	0 HRC	0 HRC	1 HRC	1 HRC	1 HRC
	Q+CT+T450/T300	1 HRC	1 HRC	2 HRC	2-3 HRC	2-3 HRC
Wear Resistance	Q+T450/T300+CT	-	-	-	14-21 %	16-18 %
	Q+CT+T450/T300	-	-	-	25-36 %	24-42 %

It is clear from the table that irrespective of the tempering temperature, the heat treatment cycle having cryogenic treatment as an intermediate step between quench-hardening and tempering (Q+CT+T) yields much better properties to low-alloy steels when compared to unusual heat treatment cycles having cryogenic treatment as the final step after quench-hardening and tempering (Q+T+CT). The comprehensive experimental results shown in the table, in general, indicate that the higher the carbon equivalent the better is the improvement in the mechanical properties of the steels due to the application of the regular cryogenic treatment. The unusual cryogenic treatment either shows no improvement or very little improvement over conventional hardening and tempering heat-treatments (Q+T).

The table shows that when the cryogenic treatment is suitably applied to low-alloy steels improvements in the hardness, tensile strength, yield strength, resilience and wear resistance are possible up to, 3 HRC, 16.8 %, 17.4%, 24%, and 42% respectively. However, interestingly enough, the unusual cryogenic treatment can also improve these properties, but to a lesser extent. Thus, to realize the full potential of low-alloy steel grades as the structural materials, cryogenic treatment should be applied in the as-quenched condition and that one round of low temperature tempering should be followed.

When the experimental results are correlated with the microstructural features, it appears that the retained austenite in the as-quenched steels, when exposed to cryogenic temperature, transforms isothermally into martensite in most parts and thus increases the martensite fraction. These dense martensite colonies, during tempering, precipitate fine carbides densely and uniformly throughout the ferritic matrix. This tempered configuration should be responsible for the superior properties and performance of the steel grades that are subjected to the regular cryogenic heat-treatment cycle.

When the quenched-hardened steels are tempered, a fraction of the retained austenite may transform into various phases including ferrite, bainite, etc (Bhadeshia and Honeycombe 2006). A fraction of retained austenite may stabilize due to the diffusion of carbon atoms (Mohanty 1995). Thus, only a small fraction of the retained austenite would be transformed into Martensite when the tempered steels are exposed to cryogenic temperature. Therefore, the resulting microstructure would be less homogenous causing only marginal improvements in the mechanical properties of the steels.

More rigorous microstructural characterization and accurate phase fraction analysis is needed to confirm the above theory and that becomes the future work of this thesis. However, the experimental results and quantification of the wear performance presented in this work convincingly demonstrate the positive effects of the deep cryogenic treatment on low-alloy steel grades. Thus, the industrial heat-treaters can confidently apply cryogenic or sub-zero treatments for improving the performance of the low-alloy steel components.

7. SUMMARY AND CONCLUSIONS

7.1   Summary

In the present work, effect of cryogenic treatment has been studied by carrying out detailed experiments involving hardness test, tensile test, wear test and microstructural study on meticulously chosen five grades of steel.

The aim and objectives of the work were designed based on the case study where failure analysis of hydraulic lathe chuck assembly was carried out. Plunger and Jaw carrier were the two components that failed during the operation and both were made of EN36 steel grade. Detailed analysis revealed that one of main reasons of failure of the chuck components was improper sequence of subzero treatment. After successfully carrying out the proper sequence of cryogenic treatment on EN36 steel grade, it was proved that proper sequence of cryogenic treatment (Q+CT+T) can lead to better mechanical and microstructural properties in comparison to improper sequence of cryogenic treatment (Q+T+CT).

Considering the well-established theory and experimental work conducted on EN36 the work was extended by carrying out detailed experiments on five steel grades namely EN8, EN18, EN47, EN24 and EN45. Results of hardness test, tensile test, microstructural analysis revealed that there was subtle improvement for EN8, EN18 and EN47 after carrying out proper sequence of cryogenic treatment. Both EN24 and EN45 showed positive response to the cryogenic treatment that was carried out before tempering (Q+CT+T). Hence, wear test was carried out on these two materials and as expected wear behavior was found to follow the trend of hardness results. Even though the cryogenic treatment carried out after the conventional tempering process improved the mechanical properties of EN24 and EN45 marginally, drop in ductility was observed for EN24 material.

Through well-established scientific theory and detailed experimental work, present research work provides a clear guideline on carrying out cryogenic treatment on low alloy steel grades.

7.2 Conclusions

Influence of deep cryogenic treatment on the mechanical properties and wear performance of low-alloy structural steels is studied in this thesis. Based on the detailed experimental work involving, a case study, heat-treatment experiments, hardness tests, tensile tests, wear tests and microstructural analysis, the thesis arrives at the following conclusions.

1. Effects of cryogenic treatment in improving the mechanical properties depends on the carbon content and alloying additions. Both plain-carbon and low-alloy structural steels having more than 0.3 % carbon equivalent respond quite positively to the cryogenic treatment. The higher the carbon equivalent, the better is the response to the cryogenic exposure, and the higher will be the gain in the mechanical properties.

2. Chromium as the key alloying addition in steels (as in EN18 and EN47) is found to be less-effective in terms of the response to the cryogenic treatment, while addition of nickel (as in EN24) and silicon (as in EN45) show much better response, especially when cryogenic treatment is suitably applied in the heat-treatment cycle.

3. Irrespective of the tempering temperature, the heat treatment cycle having cryogenic treatment as an intermediate step between quench-hardening and tempering (Q+CT+T) yields much better properties when compared to the unusual heat treatment cycle having cryogenic treatment as the final step after tempering (Q+T+CT).

4. Microstructural analysis confirms that sparse and coarse martensitic colonies of as-quenched steels, on cryogenic exposure, transform into fine and uniform martensitic microstructure suggesting that retained austenite transforms into fine martensite.

5. The quenched and cryogenic treated steels, on tempering (Q+CT+T), produce finer and more uniform microstructure as compared to the microstructures produced by

conventional tempering (Q+T), and conventional tempering followed by cryogenic treatment (Q+T+CT).

6. Considering the identical wear test conditions, quenched, cryogenic treated and tempered specimens display the best wear resistance. Microscopic examination of worn-out specimens reveals fine deformation bands and grooves stretched parallel to the sliding direction. This suggests that severe plastic deformation and associated delamination is the active wear mechanism of low-alloy steels irrespective of the heat treatment cycles.

7. Improvements in the hardness, tensile strength, yield strength, resilience and wear resistance are possible up to, 3 HRC, 16.8%, 17.4%, 24%, and 42% respectively when the cryogenic treatment is suitably applied to low-alloy steels. Interestingly enough, the unusual cryogenic treatment can also improve these properties, but to a lesser extent.

8. For realizing the best combination of microstructure, mechanical properties, and performance, as-quenched low-alloy steels should be subjected to cryogenic treatment followed by low-temperature tempering.

7.3 Scope for future work

The present work reveals that nickel (EN24) and silicon (EN45) bearing steels respond very well to cryogenic exposure and produce suitable microstructural features and superior mechanical properties in general and excellent resilience in particular. Thus, application of cryogenic treatment to these alloys is a great value addition in making industrial springs. Therefore, this research work can be extended to other Ni or Si containing commercial steels including, EN26 (2.5% nickel), EN51 (3% nickel), EN37 (4.8 % nickel), and EN52 (3.25 % Si). This work may also be extended to carburizing steel grades such as, 16MnCr5, 20MnCr5, 14NiCrMo13-4, etc. More rigorous microstructural characterization and accurate phase fraction analysis can be carried out on these materials to confirm the phase-

transformation involved and understand the theory behind the improvements in the microstructure and mechanical properties.

REFERENCES

Akhbarizadeh, A., Amini, K., and Javadpour, S. (2012). "Effects of applying an external magnetic field during the deep cryogenic heat treatment on the corrosion resistance and wear behavior of 1.2080 tool steel." *Materials and Design*, 41, 114–123.

Akhbarizadeh, A., Shafyei, A., and Golozar, M. A. (2009). "Effects of cryogenic treatment on wear behavior of D6 tool steel." *Materials and Design*, 30(8), 3259–3264.

Amini, K., Akhbarizadeh, A., and Javadpour, S. (2012a). "Effect of deep cryogenic treatment on the formation of nano-sized carbides and the wear behavior of D2 tool steel." *International Journal of Minerals, Metallurgy and Materials*, 19(9), 795–799.

Amini, K., Akhbarizadeh, A., and Javadpour, S. (2012b). "Investigating the effect of holding duration on the microstructure of 1.2080 tool steel during the deep cryogenic heat treatment." *Vacuum*, 86(10), 1534–1540.

Amini, K., Akhbarizadeh, A., and Javadpour, S. (2013). "Investigating the effect of the quench environment on the final microstructure and wear behavior of 1.2080 tool steel after deep cryogenic heat treatment." *Materials and Design*, 45, 316–322.

Arun, M., Arunkumar, N., Vijayaraj, R., and Ramesh, B. (2018). "Investigation on the performance of deep and shallow cryogenic treated tungsten carbide drills in austenitic stainless steel." *Measurement: Journal of the International Measurement Confederation*, 125, 687–693.

Bain, E. C., and Paxton, H. W. (1966). "Alloying elements in steel." *291 P.* American Society For Metals, Metals Park, Ohio.

Baldissera, P. (2009). "Fatigue scatter reduction through deep cryogenic treatment on the 18NiCrMo5 carburized steel." *Materials and Design*, 30(9), 3636–3642.

Baldissera, P., and Delprete, C. (2009). "Effects of deep cryogenic treatment on static mechanical properties of 18NiCrMo5 carburized steel." *Materials and Design*, 30(5), 1435–1440.

Bannister, A. C., Ocejo], J. [Ruiz, and Gutierrez-Solana, F. (2000). "Implications of the yield stress/tensile stress ratio to the SINTAP failure assessment diagrams for homogeneous materials." *Engineering Fracture Mechanics*, 67(6), 547–562.

Basavaraja, J. S., and Mujawar, S. M. S. (2014). "Modelling, Simulation and Analysis of Gripping Force Loss in High Speed Power Chuck." *Procedia Materials Science*, 5, 1417–1423.

Bensely, A., Senthilkumar, D., Mohan Lal, D., Nagarajan, G., and Rajadurai, A. (2007). "Effect of cryogenic treatment on tensile behavior of case carburized steel-815M17." *Materials Characterization*, 58(5), 485–491.

Bensely, A., Venkatesh, S., Mohan Lal, D., Nagarajan, G., Rajadurai, A., and Junik, K. (2008). "Effect of cryogenic treatment on distribution of residual stress in case carburized En 353 steel." *Materials Science and Engineering A*, 479(1–2), 229–235.

Bhadeshia, H., and Honeycombe, R. (2006). *Steels: Microstructure and Properties*. *Steels: Microstructure and Properties*, Burlinton, USA.

Boniardi, M., D'Errico, F., and Tagliabue, C. (2006). "Influence of carburizing and nitriding on failure of gears - A case study." *Engineering Failure Analysis*, 13(3 SPEC. ISS.), 312–339.

Bramfitt, B. L., and Benscoter, A. O. (2002). *Metallographer's Guide: Practices and Procedures for Irons and Steels - Common Etchants for Iron and Steel*. ASM International, Materials Park, OH, USA.

Cajner, F., Landek, D., Rafael, H., Šolić, S., and Kovačić, S. (2012). "Effect of deep cryogenic treatment on dilatometric curve and tribological properties of high speed steel." *International Heat Treatment and Surface Engineering*, 6(2), 67–71.

Cameron, T. B., Diesburg, D. E., and Kim, C. (1983). "Fatigue and Overload Fracture of Carburized Steels." *JOM: Journal of The Minerals, Metals & Materials Society*, 35(7), 37–41.

Çiçek, A., Kara, F., Kıvak, T., Ekici, E., and Uygur, İ. (2015). "Effects of Deep Cryogenic Treatment on the Wear Resistance and Mechanical Properties of AISI H13 Hot-Work Tool Steel." *Journal of Materials Engineering and Performance*, 24(11), 4431–4439.

Cohen, R. E., Matlock, D. K., and Krauss, G. (1992). "Specimen edge effects on bending fatigue of carburized steel." *Journal of Materials Engineering and Performance*, 1(5), 695–703.

Cui, J., and Chen, L. (2017). "Microstructure and abrasive wear resistance of an alloyed ductile iron subjected to deep cryogenic and austempering treatments." *Journal of Materials Science and Technology*, 33(12), 1549–1554.

Das, D., Dutta, A. K., and Ray, K. K. (2009a). "Correlation of microstructure with wear behaviour of deep cryogenically treated AISI D2 steel." *Wear*, 267(9–10), 1371–1380.

Das, D., Dutta, A. K., and Ray, K. K. (2009b). "Inconsistent wear behaviour of cryotreated tool steels: role of mode and mechanism." *Materials Science and Technology*, 25(10), 1249–1257.

Das, D., Dutta, A. K., and Ray, K. K. (2010a). "Sub-zero treatments of AISI D2 steel: Part II. Wear behavior." *Materials Science and Engineering A*, 527(9), 2194–2206.

Das, D., Dutta, A. K., and Ray, K. K. (2010b). "Sub-zero treatments of AISI D2 steel: Part I. Microstructure and hardness." *Materials Science and Engineering A*, 527(9), 2182–2193.

Das, D., Dutta, A. K., and Ray, K. K. (2010c). "Sub-zero treatments of AISI D2 steel: Part II. Wear behavior." *Materials Science and Engineering: A*, 527(9), 2194–2206.

Das, D., Dutta, A. K., Toppo, V., and Ray, K. K. (2007). "Effect of deep cryogenic treatment on the carbide precipitation and tribological behavior of D2 steel." *Materials and Manufacturing Processes*, 22(4), 474–480.

Das, D., and Ray, K. K. (2012a). "Structure-property correlation of sub-zero treated AISI D2 steel." *Materials Science and Engineering A*, 541, 45–60.

Das, D., and Ray, K. K. (2012b). "On the mechanism of wear resistance enhancement of

tool steels by deep cryogenic treatment." *Philosophical Magazine Letters*, 92(6), 295–303.

Das, D., and Ray, K. K. (2015). "Cryogenic processing to improve tribological performance of die steels." *International Journal of Surface Science and Engineering*, 9(2–3), 124–144.

Dhokey, N. B., and Hake, A. R. (2013). "Instability in wear mechanism and its relevance to microstructural features in cryotreated T42." *Tribology - Materials, Surfaces and Interfaces*, 7(4), 193–200.

Dhokey, N. B., and Lalge, P. K. (2018). "Influence of cryosoaking period on wear characteristics and surface topography of M35 tool steel." *Tribology - Materials, Surfaces and Interfaces*, 12(3), 170–175.

Farina, P. F. S., Farina, A. B., Barbosa, C. A., Goldenstein, H., Silva, P. F., Farina, A. B., Barbosa, C. A., Farina, P. F. S., Farina, A. B., Barbosa, C. A., and Goldenstein, H. (2013). "International Heat Treatment and Surface Engineering Effects of cryogenic and stress relief treatments on temper carbide precipitation in AISI D2 tool steel Effects of cryogenic and stress relief treatments on temper carbide precipitation in AISI D2 tool." *International Heat Treatment and Surface Engineering*, 7(3), 120–124.

Feng, P. F., Yu, D. W., Wu, Z. J., and Uhlmann, E. (2008). "Jaw-chuck stiffness and its influence on dynamic clamping force during high-speed turning." *International Journal of Machine Tools and Manufacture*, 48(11), 1268–1275.

Feng, W., Feng, Z., and Mao, L. (2020). "Failure analysis of a secondary driving helical gear in transmission of electric vehicle." *Engineering Failure Analysis*, 117, 104934.

Firouzdor, V., Nejati, E., and Khomamizadeh, F. (2008a). "Effect of deep cryogenic treatment on wear resistance and tool life of M2 HSS drill." *Journal of Materials Processing Technology*, 206(1), 467–472.

Firouzdor, V., Nejati, E., and Khomamizadeh, F. (2008b). "Effect of deep cryogenic treatment on wear resistance and tool life of M2 HSS drill." *Journal of Materials*

Processing Technology, 206(1–3), 467–472.

Fleming, J. R., and Suh, N. P. (1977). "Mechanics of crack propagation in delamination wear." *Wear*, 44(1), 39–56.

Gavriljuk, V. G., Sirosh, V. A., Petrov, Y. N., Tyshchenko, A. I., Theisen, W., and Kortmann, A. (2014). "Carbide precipitation during tempering of a tool steel subjected to deep cryogenic treatment." *Metallurgical and Materials Transactions A: Physical Metallurgy and Materials Science*, 45(5), 2453–2465.

Gavriljuk, V. G., Theisen, W., Sirosh, V. V., Polshin, E. V., Kortmann, A., Mogilny, G. S., Petrov, Y. N., and Tarusin, Y. V. (2013). "Low-temperature martensitic transformation in tool steels in relation to their deep cryogenic treatment." *Acta Materialia*, 61(5), 1705–1715.

Ghasemi-Nanesa, H., and Jahazi, M. (2014). "Simultaneous enhancement of strength and ductility in cryogenically treated AISI D2 tool steel." *Materials Science and Engineering A*, 598, 413–419.

Ghosh, P., and Dhokey, N. B. (2017). "Optimization of Cryosoaking Period and Microstructural Transformation on Wear Mechanism of SAE 8620 Gear Steel." *Tribology Transactions*, 60(6), 1070–1077.

Gill, S. S., Singh, J., Singh, R., and Singh, H. (2012). "Effect of cryogenic treatment on AISI M2 high speed steel: Metallurgical and mechanical characterization." *Journal of Materials Engineering and Performance*, 21(7), 1320–1326.

Grimanelis, D., and Eyre, T. S. (2006). "Sliding wear mapping of an ion nitrocarburized low alloy sintered steel." *Surface and Coatings Technology*, 201(6), 3260–3268.

Gu, K., Zhang, H., Zhao, B., Wang, J., Zhou, Y., and Li, Z. (2013). "Effect of cryogenic treatment and aging treatment on the tensile properties and microstructure of Ti-6Al-4V alloy." *Materials Science and Engineering A*, 584, 170–176.

Gunes, I., Cicek, A., Aslantas, K., and Kara, F. (2014). "Effect of deep cryogenic treatment

on wear resistance of AISI 52100 bearing steel." *Transactions of the Indian Institute of Metals*, 67, 909–917.

Jaswin, M. A., and Lal, D. M. (2011). "Effect of cryogenic treatment on the tensile behaviour of En 52 and 21-4N valve steels at room and elevated temperatures." *Materials and Design*, 32(4), 2429–2437.

Jurči, P., Donánková, M., Čaplovič, ¸ubomír, Ptačinová, J., Sobotová, J., Salabová, P., Prikner, O., Šuštaršič, B., and Jenko, D. (2015). "Microstructure and hardness of sub-zero treated and no tempered P/M Vanadis 6 ledeburitic tool steel." *Vacuum*, 111, 92–101.

Jurči, P., Donánková, M., Hudáková, M., Ptačinová, J., Pašák, M., and Palček, P. (2017). "Characterization of microstructure and tempering response of conventionally quenched, short- and long-time sub-zero treated PM Vanadis 6 ledeburitic tool steel." *Materials Characterization*, 134, 398–415.

Karthik, K. S., Taj, A. P., and Chandramouli, S. R. (2020). "FEM Approach to Predict Three Jaw Chuck Stiffness and Its Effect on Gripping Force for High Speed Turning and Experimental Verification." *Advances in Simulation, Product Design and Development, Lecture Notes on Multidisciplinary Industrial Engineering,* 203–214.

Khun, N. W., Liu, E., Tan, A. W. Y., Senthilkumar, D., Albert, B., and Mohan Lal, D. (2015). "Effects of deep cryogenic treatment on mechanical and tribological properties of AISI D3 tool steel." *Friction*, 3(3), 234–242.

Kokosza, A., and Pacyna, J. (2005). "Evaluation of retained austenite stability in heat treated cold work tool steel." *Journal of Materials Processing Technology*, 162–163(SPEC. ISS.), 327–331.

Kosmowski, W. B. (1985). "Hydraulic Chuck." United States.

Leskovšek, V., and Podgornik, B. (2012a). "Vacuum heat treatment, deep cryogenic treatment and simultaneous pulse plasma nitriding and tempering of P/M S390MC steel." *Materials Science and Engineering A*, 531, 119–129.

Leskovšek, V., and Podgornik, B. (2012b). "Vacuum heat treatment, deep cryogenic treatment and simultaneous pulse plasma nitriding and tempering of P/M S390MC steel." *Materials Science and Engineering A*, 531, 119–129.

Leskovšek, V., and Podgornik, B. (2013). "Simultaneous ion nitriding and tempering after deep cryogenic treatment of PM S390MC HSS." *International Heat Treatment and Surface Engineering*, 7(3), 115–119.

Li, H., Tong, W., Cui, J., Zhang, H., Chen, L., and Zuo, L. (2016). "The influence of deep cryogenic treatment on the properties of high-vanadium alloy steel." *Materials Science and Engineering A*, 662, 356–362.

Li, J., Feng, Y., Tang, L., and Wu, X. (2013a). "FEM prediction of retained austenite evolution in cold work die steel during deep cryogenic treatment." *Materials Letters*, 100, 274–277.

Li, S., Min, N., Deng, L., Wu, X., Min, Y., and Wang, H. (2011). "Influence of deep cryogenic treatment on internal friction behavior in the process of tempering." *Materials Science and Engineering A*, 528(3), 1247–1250.

Li, S., Min, N., Li, J., and Wu, X. (2013b). "Internal friction measurements of phase transformations during the process of deep cryogenic treatment of a tool steel." *Cryogenics*, 57, 1–5.

Li, S., Min, N., Li, J., Wu, X., Li, C., and Tang, L. (2013c). "Experimental verification of segregation of carbon and precipitation of carbides due to deep cryogenic treatment for tool steel by internal friction method." *Materials Science and Engineering A*, 575, 51–60.

Liu, Y., Lin, J., Min, J., Ma, Z., and Wu, B. (2018). "Effect of Deep Cryogenic Treatment on Mechanical Properties and Microstructure of the Tool Steel CR7V for Hot Stamping." *Journal of Materials Engineering and Performance*, 27(9), 4382–4391.

Lyman, T. (1973). *Metals handbook.* American Society for Metals, Metals Park (Ohio).

Mahmudi, R., Ghasemi, H. M., and Faradji, H. R. (2008). "Classic contributions: cryogenic

treatment Effects of cryogenic treatments on mechanical properties and wear behaviour of high-speed steel M2." *International Heat Treatment and Surface Engineering*, 2(3–4), 162–166.

Mebraki, N., Lamesle, P., Delanges, D., Delmas, F., and Levaillant, C. (2002). *Proceedings of the 6th International Tooling Conference, The Use of Tool Steels: Experience and Research*. Karlstad University.

El Mehtedi, M., Ricci, P., Drudi, L., El Mohtadi, S., Cabibbo, M., and Spigarelli, S. (2012). "Analysis of the effect of Deep Cryogenic Treatment on the hardness and microstructure of X30 CrMoN 15 1 steel." *Materials and Design*, 33(1), 136–144.

Meng, F., Tagashira, K., and Sohma, H. (1994). "Wear resistance and microstructure of cryogenic treated Fe-1.4Cr-1C bearing steel." *Scripta Metallurgica et Materiala*, 31(7), 865–868.

Mohan Lal, D., Renganarayanan, S., and Kalanidhi, A. (2001). "Cryogenic treatment to augment wear resistance of tool and die steels." *Cryogenics*, 41(3), 149–155.

Mohanty, O. N. (1995). "On the stabilization of retained austenite: mechanism and kinetics." *Materials Science and Engineering B*, 32(3), 267–278.

Mokarian, B., Amini, K., Ghayour, H., and Gharavi, F. (2019). "The combined effect of cryogenic and boronising treatments on the wear behaviour and microstructure of DIN 1.2344 steel." *Transactions of the Institute of Metal Finishing*, 97(3), 121–128.

Molinari, A., Pellizzari, M., Gialanella, S., Straffelini, G., and Stiasny, K. H. (2001). "Effect of deep cryogenic treatment on the mechanical properties of tool steels." *Journal of Materials Processing Technology*, 118(1–3), 350–355.

Niaki, K. S., and Vahdat, S. E. (2015a). "Optimization of Tensile Properties of AISI S1 Tool Steel." *Transactions of the Indian Institute of Metals*, 68(5), 777–781.

Niaki, K. S., and Vahdat, S. E. (2015b). "Optimization of Tensile Properties of AISI S1 Tool Steel." *Transactions of the Indian Institute of Metals*, 68(5), 777–781.

Oila, A., Lung, C., and Bull, S. (2014). "Elastic properties of eta carbide (η-Fe2C) from ab initio calculations: Application to cryogenically treated gear steel." *Journal of Materials Science*, 49(5), 2383–2390.

Oppenkowski, A., Weber, S., and Theisen, W. (2010). "Evaluation of factors influencing deep cryogenic treatment that affect the properties of tool steels." *Journal of Materials Processing Technology*, 210(14), 1949–1955.

Pacheco, J. L., and Krauss, G. (1989). "Microstructure and high bending fatigue strength in carburized steel." *Journal of Heat Treating*, 7(2), 77–86.

Pérez, M., and Belzunce, F. J. (2015). "The effect of deep cryogenic treatments on the mechanical properties of an AISI H13 steel." *Materials Science and Engineering A*, 624, 32–40.

Podgornik, B., Majdic, F., Leskovsek, V., and Vizintin, J. (2012). "Improving tribological properties of tool steels through combination of deep-cryogenic treatment and plasma nitriding." *Wear*, 288, 88–93.

Podgornik, B., Paulin, I., Zajec, B., Jacobson, S., and Leskovšek, V. (2016). "Deep cryogenic treatment of tool steels." *Journal of Materials Processing Technology*, 229, 398–406.

Preciado, M., Bravo, P. M., and Alegre, J. M. (2006). "Effect of low temperature tempering prior cryogenic treatment on carburized steels." *Journal of Materials Processing Technology*, 176(1–3), 41–44.

Roberts, G. A., Kennedy, R., and Krauss, G. (1998). *Tool Steels, 5th Edition*. EngineeringPro collection, ASM International. Matrrials Park, OH.

Senthilkumar, D., Rajendran, I., and Pellizzari, M. (2011). "Effect of cryogenic treatment on the hardness and tensile behaviour of AISI 4140 steel." *International Journal of Microstructure and Materials Properties*, 6(5), 366.

Shunmugam, M. S., and Kanthababu, M. (2018). *Advances in Simulation, Product Design*

and Development. Proceedings of AIMTDR, *Lecture Notes on Multidisciplinary Industrial Engineering*.

SreeramaReddy, T. V., Sornakumar, T., VenkataramaReddy, M., and Venkatram, R. (2009). "Machinability of C45 steel with deep cryogenic treated tungsten carbide cutting tool inserts." *International Journal of Refractory Metals and Hard Materials*, 27(1), 181–185.

Sri Siva, R., Mohan Lal, D., and Arockia Jaswin, M. (2012). "Optimization of deep cryogenic treatment process for 100Cr6 bearing steel using the Grey-Taguchi method." *Tribology Transactions*, 55(6), 854–862.

Straffelini, G., and Versari, L. (2009). "Brittle intergranular fracture of a thread: The role of a carburizing treatment." *Engineering Failure Analysis*, 16(5), 1448–1453.

Stratton, P. F. (2007). "Optimising nano-carbide precipitation in tool steels." *Materials Science and Engineering A*, 449–451(August 2005), 809–812.

Suh, N. P. (1977). "An overview of the delamination theory of wear." *Wear*, 44(1), 1–16.

Thelning, K. E. (1986). *Steel and its heat treatment*. Butterworths Heinemann, Jordan Hill, Oxford.

Thornton, R., Slatter, T., and Ghadbeigi, H. (2013). "Effects of deep cryogenic treatment on the dry sliding wear performance of ferrous alloys." *Wear*, 305(1–2), 177–191.

Thornton, R., Slatter, T., and Lewis, R. (2014). "Effects of deep cryogenic treatment on the wear development of H13A tungsten carbide inserts when machining AISI 1045 steel." *Production Engineering*, 8(3), 355–364.

Tyshchenko, A. I., Theisen, W., Oppenkowski, A., Siebert, S., Razumov, O. N., Skoblik, A. P., Sirosh, V. A., Petrov, Y. N., and Gavriljuk, V. G. (2010). "Low-temperature martensitic transformation and deep cryogenic treatment of a tool steel." *Materials Science and Engineering A*, 527(26), 7027–7039.

Vahdat, S. E., Nategh, S., and Mirdamadi, S. (2013). "Microstructure and tensile properties

of 45WCrV7 tool steel after deep cryogenic treatment." *Materials Science and Engineering A*, Elsevier, 585, 444–454.

Vimal, A. J., Bensely, A., Lal, D. M., and Srinivasan, K. (2008). "Deep cryogenic treatment improves wear resistance of en 31 steel." *Materials and Manufacturing Processes*, 23(4), 369–376.

Vander Voort, G. F. (1991). *Atlas of Time-Temperature Diagrams for Irons and Steels. ASM International*, USA.

Widmark, M., and Melander, A. (1999). "Effect of material, heat treatment, grinding and shot peening on contact fatigue life of carburized steels." *International Journal of Fatigue*, 21(4), 309–327.

Wierszyllowski, I., Samolczyk, J., Wieczorek, S., Andrzejewska, E., and Marcinkowska, A. (2008). "The influence of deep cryogenic treatment on transformation during tempering of quenched D2 steel. Studies of XRD, structures, DSC, dilatometry, hardness and impact energy." *Diffusion in Solids and Liquids*, 273–276, 731–739.

Wilson, S., and Alpas, A. T. (1998). "TiN coating wear mechanisms in dry sliding contact against high speed steel." *Surface and Coatings Technology*, 108–109(1–3), 369–376.

Xu, N., Cavallaro, G. P., and Gerson, A. R. (2010). "Synchrotron micro-diffraction analysis of the microstructure of cryogenically treated high performance tool steels prior to and after tempering." *Materials Science and Engineering A*, 527(26), 6822–6830.

Xu, X. L., and Yu, Z. W. (2012). "Brittle cracking of flanks of a big gear." *Journal of Failure Analysis and Prevention*, 12(6), 689–696.

Yu, Z. wei, Xu, X. lei, Yang, Z., and Li, Y. yuan. (2012). "Case internal oxidation and intergranular fracture of carburized splined-shaft." *Engineering Failure Analysis*, 22, 141–151.

Yun, D., Xiaoping, L., and Hongshen, X. (2008). "Classic contributions: cryogenic treatment Deep cryogenic treatment of high speed steel: microstructure and mechanism."

International Heat Treatment and Surface Engineering, 2(2), 80–84.

Zare, A., and Hosseini, S. R. (2016). "Influence of soaking time in deep cryogenic treatment on the microstructure and mechanical properties of low-alloy medium-carbon HY-TUF steel." *International Journal of Minerals, Metallurgy and Materials*, 23(6), 658–666.

Zare, A., Mansouri, H., and Hosseini, S. R. (2015). "Effect of Deep Cryogenic Treatment on the Microstructure and Mechanical Properties of HY-TUF Steel." *Metallography, Microstructure, and Analysis*, 4(3), 169–177.

Zhang, H., Chen, L., Sun, J., Wang, W., and Wang, Q. (2014). "Influence of deep cryogenic treatment on microstructures and mechanical properties of an ultrafine-grained WC-12Co cemented carbide." *Acta Metallurgica Sinica (English Letters)*, 27(5), 894–900.

Zhirafar, S., Rezaeian, A., and Pugh, M. (2007). "Effect of cryogenic treatment on the mechanical properties of 4340 steel." *Journal of Materials Processing Technology*, 186(1–3), 298–303.

Zhou, C., Yang, H., Yang, L., and Qing, R. (2011). "Piecewise model and experiment of power chuck's gripping force loss during high speed turning." *Science China Technological Sciences*, 54(4), 972–982.

Zhu, Y. Z., Yin, Z. M., Zhou, Y., Lei, Q. F., and Fang, W. S. (2008). "Effects of cryogenic treatment on mechanical properties and microstructure of Fe-Cr-Mo-Ni-C-Co alloy." *Journal of Central South University of Technology (English Edition)*, 15(4), 454–458.

Zinchenko, V. M., Georgievskaya, B. V., and Olovyanishnikov, V. A. (1987). "Effect of residual austenite on the mechanical properties of carburized steels." *Metal Science and Heat Treatment*, 29(12), 919–925.

PUBLICATIONS

1. **Pavankumar R. Sondar** and Subray R. Hegde, "Deep Cryogenic Treatment of Plain-Carbon and Low-Alloy Steels," *Materials Performance and Characterization* 9, no. 1 (2020): 346–356. https://doi.org/10.1520/MPC20200026

2. **Pavankumar R Sondar**, Gurudath, B., Ahirwar, V., & Hegde, S. R. (2021). Failure of Hydraulic Lathe Chuck Assembly. Engineering Failure Analysis, 106001. https://doi.org/10.1016/j.engfailanal.2021.106001

Under review/submitted

1. **Pavankumar R. Sondar** and Subray R. Hegde "Effect of Deep Cryogenic Treatment on EN45 Spring Steel" *International Journal of Minerals, Metallurgy and Materials* (under review)

2. **Pavankumar R. Sondar** and Subray R. Hegde "Influence of Cryogenic Treatment on Low Alloy Steels After Tempering", submitted to *Journal of Materials Performance and Engineering*

Other Publications

1. **Pavankumar R. Sondar**, JK Rakshan Kumar, Sanjay Chawla, Preetish C. Dsilva, and Subray R. Hegde. "Failure of a Cooling Water Pump Shaft." *Journal of Failure Analysis and Prevention* (2020): 1-11. https://doi.org/10.1007/s11668-020-01043-0

2. Padasale Basavaraj, JK Rakshan Kumar, **Pavankumar R. Sondar**, Sumanth Govindarajan, and Subray R. Hegde. "Failure Analysis of Cooling Tower Fan-Arm." *Journal of Failure Analysis and Prevention* 20, no. 4 (2020): 1417-1425. https://doi.org/10.1007/s11668-020-00947-1

3. Basavaraj, **Pavankumar R. Sondar**, and Subray R. Hegde "Effect of spheroidization of cementite in ductile cast iron", *International Journal of*

Minerals, Metallurgy and Materials (2020), https://doi.org/10.1007/s12613-020-2041-0

4. B. Gurudath, Kamal Kishore Kumawat, Vijinigiri Tejaswi, **Pavankumar R. Sondar**, J. K. Rakshan Kumar & Subray R. Hegde "Failure Analysis of Bucket Elevator Shaft." *Journal of Failure Analysis and Prevention* (2021): https://doi.org/10.1007/s11668-020-01101-7

5. Subray R. Hegde, JK Rakshan Kumar, **Pavankumar R. Sondar**, Preetish C. Dsilva, "Catastrophic Failure of Urea Prill-Tower Fan", *Engineering Failure Analysis* (2021), https://doi.org/10.1016/j.engfailanal.2020.105207

6. Preetish C. Dsilva , Preeti Shetty, **Pavankumar R. Sondar**, B. Ganesh Kumar & Subray R. Hegde "Failure Analysis of Reciprocating CO_2 Compressor" *Journal of Failure Analysis and Prevention* (2021), https://doi.org/10.1007/s11668-020-01109-z

7. Preethi Shetty, Preetish Dsilva, **Pavankumar Sondar**, Kumar B. Ganesh, and Subray Hegde. "Biodegradation of PEEK Piston Rings." *Polymer Degradation and Stability* (2021): 109666.
    https://doi.org/10.1016/j.polymdegradstab.2021.109666

Conferences

1. Lightweighting for Defence and Transportation: Trends, New Paradigms and Strategies, BITS, Pilani-K K Birla Goa, NMD ATM 2017, Presented Topic: *"Cryogenic Treatment of Low alloy Steels Before and After Tempering"*

2. International Symposium on Advanced Materials for Industrial and Societal Application, Trivandrum, 13 Nov 2019, NMD ATM-2019, Presented Topic: "*Effect of Cryogenic Treatment on Plain Carbon and Low Alloy Steels"*

3. International Conference on Processing and Characterization of Metals, NIT-Rourkela, 12 Dec 2019, Presented Topic: "*Deep Cryogenic Treatment of Plain Carbon and Low Alloy Steels"*

Biodata

Name: Pavankumar R Sondar

Father's name: Ramappa

Mothers name: Shantamma

Nationality: Indian

Contact details:
Mobile: +91 7795415789
Email id: pavansondar1@gmail.com

Permanent Address:
Pavankumar R Sondar
s/o Ramappa Sondar
Sadhanakeri Heblikar Compound
Dharwad, Karnataka, India
58008

Present Address
Pavankumar R Sondar
Research Scholar
Dept. of Metallurgical and Materials
Engg.
National Institute of Technology
Karnataka Surathkal, Mangaluru,
Karnataka, India
575025

Educational Qualification:

Course	Institute	University	Year
M.Tech (Materials Engineering)	National Institute of Technology Karnataka	National Institute of Technology Karnataka	2014-2016
B.E (Industrial and Production Engineering)	Gogte Institute of Technology	Visvesvaraya Technological University	2010-2014